



Loma Linda University Electronic Theses, Dissertations & Projects

6-1983

Mathematical Evaluation of Steady, Laminar Flow by the use of Continuous-Wave (CW) Doppler and Pitot Tube System

Malek Mansoor Sharif

Follow this and additional works at: <https://scholarsrepository.llu.edu/etd>



Part of the [Applied Mathematics Commons](#)

Recommended Citation

Sharif, Malek Mansoor, "Mathematical Evaluation of Steady, Laminar Flow by the use of Continuous-Wave (CW) Doppler and Pitot Tube System" (1983). *Loma Linda University Electronic Theses, Dissertations & Projects*. 1348.

<https://scholarsrepository.llu.edu/etd/1348>

This Dissertation is brought to you for free and open access by TheScholarsRepository@LLU: Digital Archive of Research, Scholarship & Creative Works. It has been accepted for inclusion in Loma Linda University Electronic Theses, Dissertations & Projects by an authorized administrator of TheScholarsRepository@LLU: Digital Archive of Research, Scholarship & Creative Works. For more information, please contact scholarsrepository@llu.edu.

Abstract

MATHEMATICAL EVALUATION OF STEADY, LAMINAR FLOW BY THE USE OF CONTINUOUS-WAVE (CW) DOPPLER AND PITOT TUBE SYSTEM

by

Malek Mansoor Sharif

Investigation, as to the usefulness of spectral analysis of the acoustical signal from the Doppler ultrasonic flowmeter, is being conducted. The purpose was to determine some of the hemodynamic influences on the spectrum. The hypothesis was that both hematocrit and pressure head influence the amplitude of the spectrum. Experiments were designed to: a) evaluate their roles on amplitude; b) derive the associated functional relationship.

Preliminary experiments revealed that: a) the accuracy of our Doppler flowmeter was satisfactory, since a very good linear relation was found between electromagnetically and Doppler derived flow; b) the relative weight of the hematocrit parameter on flow velocity was twice that of the pressure.

Experiments were carried out to determine the distribution of velocities and the particle profile within the tube prior to investigation of functional dependence of Doppler amplitude on hematocrit and pressure head. A pitot tube system whose bent tube

component was capable of radial movement was developed to measure the instantaneous blood (or particle) velocity. The bent tube was moved across the lumen of the vessel in steps of 0.1 mm., and particle velocity was measured at each sampling point. The distribution of velocity was parabolic and the agreement between experimental data and the 2nd degree polynomial least squares fitting was good ($\xi = .94$). An array of small bent tubes, each placed successively deeper within the lumen of the rubber tubing and connected to a small syringe, was constructed to measure the distribution of red cells. Small uniform samples were taken from the flowing stream. The particle profile was parabolic and the hematocrit, as a function of radius, was expressible in terms of a 2nd degree polynomial. A mapping of particle velocities onto the set of hematocrit values is also parabolic.

To determine the dependency of ultrasonic energy backscattering on hematocrit, Doppler signals were recorded, digitized, and frequency resolved via the fast Fourier transform, for hematocrits ranging from 4.5% to 46.5%. The mean amplitude corresponding to each given hematocrit was calculated by evaluating the area under the curve fitted to the transformed data. The Doppler amplitude was found to be a linear function of hematocrit for all cases of applied pressure heads. A generalized Doppler amplitude function of double variables was also derived in terms of hematocrit and pressure head.

It was hypothesized that blood viscosity (μ) is an exponential function of hematocrit (\hat{H}), that is, $\mu = A \exp(B \hat{H})$. Experimental results using a Falling ball type viscosimeter supported the theory with a high correlation between the data and the fitted curve ($\xi=.99$).

The constant A has the dimensions of viscosity and is dependent on temperature, whereas, B is dimensionless and a linear function of hematocrit. A consequence of this hypothesis is that flow velocity decreases exponentially as a function of hematocrit. It can be hypothesized that viscosity influences the power content of the Doppler signal, which requires further work and research.

UNIVERSITY LIBRARY
LOMA LINDA, CALIFORNIA

LOMA LINDA UNIVERSITY
Graduate School

MATHEMATICAL EVALUATION OF STEADY, LAMINAR FLOW
BY THE USE OF CONTINUOUS-WAVE (CW) DOPPLER
AND PITOT TUBE SYSTEM

by

Malek Mansoor Sharif

A Dissertation in Partial Fulfillment
of the Requirements for the Degree Doctor of Philosophy
in Mathematical Science

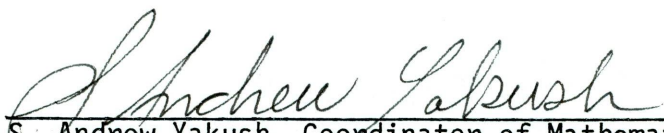
June 1983

© 1983

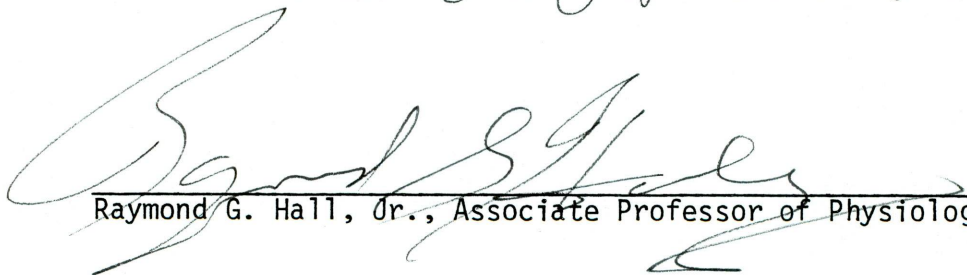
Malek M. Sharif

All Rights Reserved


Each person whose signature appears below certifies that this dissertation in his opinion is adequate, in scope and quality, as a dissertation for the degree Doctor of Philosophy.


_____, Chairman
S. Andrew Yakush, Coordinator of Mathematical Sciences and
Assistant Research Professor of Physiology

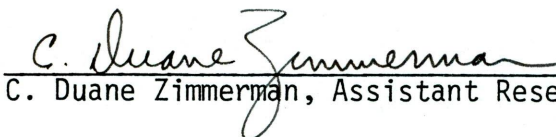

_____, Co-Chairman
Ramon R. Gonzalez, Jr., Assistant Professor of Physiology



Raymond G. Hall, Jr., Associate Professor of Physiology



George Maeda, Assistant Professor of Physiology



C. Duane Zimmerman, Assistant Research Professor of Physiology

ACKNOWLEDGMENTS

I am grateful to my thesis supervisor, Dr. Ramon R. Gonzalez, Jr. for his guidance, patience, criticisms, and encouragement throughout my research and in the preparation of this manuscript.

I would like to thank Drs. Yakush, Zimmerman, Maeda, and Hall who as members of my committee made valuable suggestions and gave their continued moral support during my course of study.

I am indebted to the staff of the Departments of Mathematical Sciences and Physiology for their direction and assistance.

I also wish to thank Dr. Gonzalez for making available machine language routines for processing of my data, Edward Duke for helping with experimental procedures, and Linda Hamm for typing this manuscript.

I extend my appreciation to Dr. Ian Fraser, Chairman of the Department of Physiology and Pharmacology for providing me with financial assistance at a crucial period of time required to complete this project.

I extend a special thanks to my wife Alice and our children, Shirzad and Samira, for their tolerance, understanding, and encouragement through it all.

Finally, I especially dedicate this work to the memory of my father whose inspiration made it all possible.

TABLE OF CONTENTS

	Page
INTRODUCTION	1
Historical Perspective	1
General Introduction	6
Statement of the Hypotheses	16
MATERIALS AND METHODS	19
General	19
Fluids	19
Measurement Techniques of Blood Flow	19
Steady Flow Procedure	20
Series of Experimental Stages	22
The Experiments	22
Signal Processing	25
Determination of Blood Viscosity and Density	27
RESULTS	28
Functional Relationship of Doppler Flow and Electromagnetic Flow	28
The Experimental Results	28
Statistical Analysis	28
A Quantitative Study of Simultaneous Influence of Head Pressure and Hematocrit Upon Velocity of Blood Flow	34
Determination of Instantaneous and Spatial Velocity of Blood Flow by Pitot Tube Complex and Doppler Flowmeter, and Hematocrit Measurement	36
Distribution of Particle Velocity by Pitot Tube Complex	36
Measurement of Blood Hematocrit	42
Calculation of Mean Doppler Amplitude	51
Functional Relationship of Blood Viscosity and Blood Hematocrit	70
DISCUSSION	83
A Functional Relationship of Doppler Flow and Electromagnetic Flow	83
A Quantitative Study of Simultaneous Influence of Pressure Head and Hematocrit Upon Velocity of Blood Flow	85
Velocity-Hematocrit Correlation	86
Distribution of Particle Velocity	86
Measurement of Blood Hematocrit	91
Calculation of the Mean Doppler Amplitude	96
Functional Relationship of Blood Viscosity and Hematocrit.	104
SUMMARY AND CONCLUSIONS	111

	Page
LITERATURE CITED	116
APPENDIX A: DERIVATION OF FORMULAS AND THEORIES	123
A1. Principles of Operation of Electromagnetic Flowmeter	124
A2. Principles of Operation of Continuous-Wave (CW) Doppler Flowmeter	125
A3. Descarte's Rule of Signs	126
A4. Consequence of Mean Value Theorem	127
A5. Equation of the Velocity Profile for Steady, Laminar Flow	128
APPENDIX B: LISTING OF PROGRAMS	130

LIST OF TABLES

		Page
Table 3.1	Measurement of electromagnetic and Doppler flow for various rates of flow	29
Table 3.2	Doppler flow as a linear function of electromagnetic flow	30
Table 3.3	Measurement of average velocity for various hematocrits under a given pressure head	35
Table 3.4	Measurement of instantaneous velocity across lumen of the vessel	37
Table 3.5	Measurement of blood hematocrit across lumen of the vessel	43
Table 3.6	Hematocrit as a function of radius as described by polynomials of 2nd, 3rd, and 4th degrees for total hematocrit of 10% and pressure head of 177 cm.	44
Table 3.7	Hematocrit as a function of radius as described by polynomials of 2nd, 3rd, 4th, and 5th degrees for total hematocrits of 10% and 7%, and pressure head of 131 cm.	52
Table 3.8	Calculated values of mean Doppler amplitude for blood hematocrits of 4.5% to 46.5% and pressure heads of 60 cm. to 100 cm.	57
Table 3.9	Doppler amplitude as a function of blood hematocrit as described by linear functions and polynomials of 2nd degree	58

Table 3.10	Measured values of descent time, blood density and viscosity for hematocrits in the range 7.0% to 29.7%	79
Table 3.11	Blood viscosity as a function of hematocrit as described by exponential, geometric, and 2nd degree polynomials	80

LIST OF FIGURES

		Page
Figure 1.	The experimental set-up	21
Figure 2.	Blood sampling method	23
Figure 3.	Functional relationship of Doppler flow and electromagnetic flow	33
Figure 4.	Polygraph recording of axial and pitot deflections	39
Figure 5.	Distribution of velocities across the lumen of the vessel	41
Figure 6.	Blood particle profile as described by a 2nd degree polynomial for a hematocrit of 10%	46
Figure 7.	Blood particle profile as described by a 3rd degree polynomial for a hematocrit of 10%	48
Figure 8.	Blood particle profile as described by a 4th degree polynomial for a hematocrit of 10%	50
Figure 9.	Blood particle profile as described by 2nd and 3rd degree polynomials for a hematocrit of 7%	54
Figure 10.	Blood particle profile as described by 4th and 5th degree polynomials for a hematocrit of 7%	56
Figure 11.	Doppler amplitude as a function of hematocrit as described by a linear regression curve and a polynomial of 2nd degree for a pressure head of 60 cm.	60

	Page
Figure 12. Doppler amplitude as a function of hematocrit as described by a linear regression curve and a polynomial of 2nd degree for a pressure head of 70 cm.	62
Figure 13. Doppler amplitude as a function of hematocrit as described by a linear regression curve and a polynomial of 2nd degree for a pressure head of 80 cm.	64
Figure 14. Doppler amplitude as a function of hematocrit as described by a linear regression curve and a polynomial of 2nd degree for a pressure head of 90 cm.	66
Figure 15. Doppler amplitude as a function of hematocrit as described by a linear regression curve and a polynomial of 2nd degree for a pressure head of 100 cm.	68
Figure 16. Time-domain representation of Fourier transformed data for hematocrits in the range 24-46.5%	72
Figure 17. Time domain representation of Fourier transformed data for hematocrits in the range 4.5-19.5% . . .	74
Figure 18. Frequency-domain representation of Fourier transformed data for a hematocrit of 40%	76
Figure 19. Frequency-domain representation of Fourier transformed data for a hematocrit of 4.5%	78
Figure 20. Viscosity as an exponential function of blood hematocrit	82

CHAPTER 1

INTRODUCTION

This investigation deals primarily with steady, laminar flow conditions of human blood. My three-fold objective here is to introduce the concepts to be discussed in the following chapters.

In the first section, I will sketch the historical events which lead to quantitative measurement of blood flow by means of the Doppler ultrasonic flowmeter. In this respect, the events leading to the fast Fourier transformation of the digitized Doppler signals will be traced.

In section B, the relevant terms and concepts involved will be defined and discussed. For example, because the experiments are conducted within the boundaries of steady, laminar flow, it would be necessary to define and discuss the significance of Reynolds number. Both the Newtonian and non-Newtonian properties of blood will also be discussed. Because the Doppler flowmeter is the principle equipment used in my experiments, time sampling, Fourier analysis, and Fourier transformation will also be explained.

Finally, in the section entitled "Statement of the Hypothesis," the objectives will be outlined and the underlying purpose will be stated

Historical Perspective

Leeuwenhoek in 1668 reported seeing individual red blood cells flowing in clear plasma in the tail of a live tadpole. Landin in 1964 gives this summary: ". . . He could distinguish single globules following each other, compressed and in single file, through the narrowest channels. Sometimes the corpuscles change into long ovals

as the vessel narrowed. Both the narrowness and the number of these parallel pathways arrested his attention."

The physiological events which led to the invention of square-wave electromagnetic flowmeter in 1953 for measurement of blood flow and the new non-invasive Doppler flowmeter in 1961 for detection of flow velocity were at best semiquantitative in nature.

Stephen Hales in 1733 estimated the force driving the flow in a capillary as the product of the cross-sectional area and the difference of arterial and venous pressure which he measured as 80 inches of blood.

Young in 1808 derived empirical formulas for the pressure drop in pipes, realizing that in small tubes the pressure drop was proportional to the velocity. Precise measurement of the pressure drop in fine glass capillary tubes were made by Poiseuille in 1840 for water, alcohol, and mercury. He expressed his results by the empirical equation $\dot{Q} = K(1+AT+BT^2) (P/L) D^4$, where P is the pressure drop over the length L of the tube, D is the diameter of the tube, T is the temperature, and K , A , and B are empirical constants based on the type of fluid. The analytical result (usually called Poiseuille's law) $\dot{Q} = K(P/L)D^4$ was not derived until 1858 and then independently by Franz Neumann and Edward Hagenbach (50). Poiseuille flow is applied when there is a fully developed laminar flow in a cylindrical tube (44). Rouse and Ince in 1957 pointed out that the tests of Poiseuille were preceded by similar but less accurate tests of Hagen in 1839.

Eular in 1775, convinced that ventricular contraction set up a wave propagated through the arteries with a finite velocity, related particle velocity as a function of time (t) to pressure difference

between different locations by:

$$\vec{dv}/dt = \vec{K} - 1/\rho \text{ grad } P$$

where P is the pressure, v is the particle velocity of blood density ρ , and \vec{K} the external force per mass (52).

Auguste Chauveau in 1860 invented the hemodromograph which permitted recording the details of the velocity pulse and it foreshadowed the details of quantitative records taken by modern electronic instruments (30). Carl Friedric Ludwig and Jan Dogiel in 1867 invented the stromuhr, the first instrument for measurement of volume flow.

Fourier in 1822 showed how a mathematical series of sine and cosine terms can be used to analyze heat conduction in solid bodies. The series that Fourier proposed is of the form:

$$y = 1/2a_0 + \sum_{n=1}^{\infty} (a_n \cos nx + b_n \sin nx).$$

The Fourier series was probably the first systematic application of a trigonometric series to a problem solution. Fourier spent the rest of his life working on his concept and expanded it to include the Fourier integral before his death in 1830. Both the Fourier series and the Fourier integral allow transformation of physically realizable time-domain waveforms to the frequency domain and vice versa. They are mathematical tools for Fourier analysis (54). Porje in 1957, 1960, and 1961 transformed pressure tracings into Fourier series, and discovered that for lower harmonics, the wave velocity was a function of frequency.

The dependence of wave velocity on frequency has been confirmed by McDonald and Taylor in 1957 and by Harding in 1962.

C. Runge in 1903 described the technique that later became known as the fast Fourier transform (FFT). In 1942, a more generalized approach was advanced by Danielson and Lanczas. By recognizing certain symmetries and periodicities, they reduced the evaluation of the discrete Fourier transform (DFT) which is the finite, discrete version of the Fourier transform, a mathematical operation, from about N^2 to about $(N \log_2 N)/2$, where N is the number of sample points in the series to be transformed (7,9,18,20,25,69). In the early 1960's, R. L. Garwin was studying solid helium and had a great need for Fourier techniques. He contacted J. W. Tukey who supplied him with the essence of the FFT. Garwin then approached the director of Mathematical Sciences at IBM with the problem of programming the algorithm, as a result of which J. W. Cooley became involved. Cooley and Tukey in 1965 authored the Cooley-Tukey algorithm for evaluating the DFT in Mathematics of Computation (9,56).

Christian Doppler in 1843 described a change in the perceived frequency of the energy wave emitted from a moving sound source. This change in frequency is related to the velocity of the moving source and is known as the Doppler effect.

Satomura in 1959 and Franklin in 1961 described instruments identifying blood flow by using Doppler-shifted ultrasound signals, and since then it has been used as a non-invasive tool to investigate aspects of flow in cardiovascular system(27). In the first devices of

this kind, only the amplitude, but not the direction of the flow velocity within the vessel could be detected. McLeod in 1967 and Pourcelot in 1971 designed directional systems which processed the backscattered ultrasonic signal in 2 separate channels, in which the respective Doppler shift signals are distinguished by a phase shift of 90° . This separation is the prerequisite for the identification of forward and backward flow (5).

Kolin in 1936 and Wetterer in 1937 independently applied the principle of electromagnetic induction to the blood flow problem. The square-wave electromagnetic flowmeter in 1953 was the first practical instrument for measurement of blood flow in intact arteries and veins. The form of magnetic fields distinguishes it into three types; namely, DC type with constant flux, sine-wave type with alternating flux, and the square-wave type with constant flux periodically alternating (66,67).

Investigators, such as Young, Poiseuille, Weber, and Korteweg, brought their insight and knowledge in other disciplines to the study of circulation. Their influence stimulated the development of quantitative considerations pertaining to events in the systemic arterial segment. Thus, researchers of various backgrounds now work together on the circulation, and we can look forward to the use of more sophisticated mathematics, computers, and animal experiments; all designed to develop and test new theories covering the movement of blood in the larger parts of the circulatory system itself and eventually the control of this movement.

General Introduction

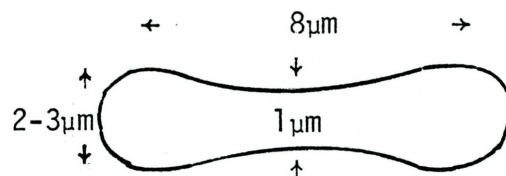
Terms pertinent to understanding the characteristics of this investigation are defined below.

A fluid is a substance that deforms continuously under the application of a shearing or tangential stress. Fluids are treated virtually as an infinitely divisible substance, as a continuum; one does not concern himself with the behavior of individual molecules. Fluids may be broadly classified according to the relation between the applied shear stress and the rate of deformation of the fluid. In Newtonian fluids, the shear stress is directly proportional to the rate of deformation. If the shear stress is not directly proportional to the rate of deformation, then the fluid is non-Newtonian (34).

Blood is a suspension of the various blood cells, called formed elements, and chylomicrons or liquid particles in aqueous solution, the plasma. In the normal physiologic range of flow rates, blood behaves as a Newtonian fluid. However, there is a great difference in the viscosity of blood in normal motion compared to its viscosity at very low flow rates or at rest. In these situations, blood exhibits non-Newtonian properties (45). Plasma, the aqueous constituent of blood, contains numerous low molecular weight organic and inorganic materials in low concentration, and proteins which comprise about 7% by weight (15).

The erythrocytes are the only cells which significantly influence the mechanical properties of blood, because of their high concentration of about 5 million per cubic millimeter. When erythrocytes, or red

cells, are suspended unstressed in plasma, they are highly flexible biconcave discs whose horizontal diameter is $8\ \mu\text{m}$, whereas the vertical diameter ranges from $1\ \mu\text{m}$ to $3\ \mu\text{m}$ as shown in the diagram below:



The red cells are highly deformable due to their shape, properties of the membrane, and to the liquid interior. The bi-concave red cell can deform into an infinite number of shapes without any alteration in its volume or surface area. The sphered red cells cannot deform to the same extent as the normal ones because a given sphere contains the maximum volume for a given surface area. Charged groups on the surface of the cells make them attract one another and cause the red cells to aggregate.

The Hematocrit, the percentage of the total volume of human blood occupied by the cells, is about 45% to 50% in the human and represents a very close packing of the erythrocytes (12). Electronic methods for counting particles, such as the Coulter Counter or the Celloscope Counter, can measure the number of red cells per cubic millimeter of blood.

The Absolute or the Dynamic Viscosity is the constant of proportionality μ given in Newton's law of viscosity by $\tau = \mu du/dy$, where du/dy is the velocity gradient and τ the shear stress. du/dy may be visualized as the rate at which one layer moves relative to an adjacent layer. If the velocity u varies uniformly from 0 to U , then

τ can also be expressed as $\tau = \mu U/D$ where D is the fixed distance over which the change occurs. The ratio U/D is the rate of angular deformation of the fluid.

Since $\tau = \text{Force/Area}$, has the dimension FL^{-2} , u has the dimension LT^{-1} and y has the dimension L , dimensions of viscosity are expressed as $ML^{-1}T^{-1}$. The English unit of viscosity is 1 slug/ft-sec or 1 lb-sec/ft² and the cgs unit of viscosity is called the poise which is 1 gm/cm-sec or 1 dyne-sec/cm². The centipoise (c.p.) is 1/100 of a poise (70) and is the unit in common usage.

Kinematic Viscosity, the ratio of absolute viscosity to mass density (μ/ρ), appears in many applications and is denoted by ν . The dimensions of ν are L^2T^{-1} . The English unit is 1 ft²/sec and the cgs unit is called stokes which is 1 cm²/sec (70).

Compressible and Incompressible Flows. If the variation in density is insignificant, then the flow is considered to be incompressible, whereas if density variations play a dominant role, as in high speed gas flows, the flow is compressible. Most liquid flows are incompressible.

Steady Flow. If the condition at any point in the fluid does not change with time, then the flow is steady, and velocity remains constant indefinitely, with no change in density (ρ), pressure (P), or temperature (T), at any point.

Thus,

$$\frac{\partial \vec{v}}{\partial t} = 0, \quad \frac{\partial \rho}{\partial t} = 0, \quad \frac{\partial P}{\partial t} = 0, \quad \text{and} \quad \frac{\partial T}{\partial t} = 0$$

Laminar and Turbulent Flows and Reynolds Number. In laminar flow, fluid particles move along smooth paths in layers or laminae with one layer sliding over an adjacent layer. When the flow structure is characterized by random, three dimensional motion of fluid particles superimposed on the mean motion, it is considered as turbulent. The classification of flow as laminar or turbulent is identified by Reynolds Number (Re).

Reynolds Number, a dimensionless number calculated on the basis of the characteristic velocity and dimensions of the system, is the ratio of inertial forces to viscous forces. The magnitude of the viscous force is proportional to the product of viscosity and velocity gradient.

Similarly, the inertial force is proportional to the kinetic energy per unit volume of the flow. Hence, Re, is the relative importance of these two quantities, that is, $Re = vD/\nu$.

Starting with turbulent flow in a glass tube, flow always becomes laminar when the velocity is reduced to make $Re < 2000$. The value 2000 is of practical importance and is referred to as Reynolds lower critical number for pipe flow. If flow is carefully controlled from an undisturbed reservoir into the tube, then laminar flow can be maintained with Reynolds number of 12,000 or more. The standard Reynolds number of 2000 is obtained when there are disturbed conditions in the container (50).

Flow and Velocity. For a volume flow rate \dot{Q} throughout an artery of uniform cross-sectional area A, the average velocity is described by \dot{Q}/A . Average velocity is time dependent and similar to flow rate. It has an identical waveform to flow rate but is scaled by a factor $1/A$.

The velocity within the vessel is not uniform across the cross-section.

Velocity Profiles in Large Arteries. In large arteries laminar flow velocity profiles are very blunt ranging from zero at the wall to twice the cross-sectional average velocity at the axis of the vessel (50). The electromagnetic method of measuring blood velocity in arteries, however, only determines a spatially averaged velocity. The ultrasonic constant wave Doppler gives the mean velocity distribution within a vessel. The pulsed Doppler technique can be used to describe the velocity at any point within a vessel.

Frequency Distribution of Particle Velocity. Laminar flow may be steady or unsteady, and because of the presence of vortices or secondary motions may have a complicated structure. Disturbances within laminar flow die out because of viscous action. Disturbances within a turbulent flow, on the other hand, are random in amplitude, frequency, and direction and do not die out. The eddies representing turbulence in a flow are random in size and velocity, producing fluctuating velocity components superimposed upon the bulk flow velocity. Eddies, widely ranging in size, are carried with the flow, and the velocity seen by a stationary probe contains fluctuating components resulting in a broad frequency distribution. The frequency distribution may be characterized by a Fourier analysis and expressed as a graph of velocity against frequency. The spectrum is usually centered on some center frequency f_0 , whose value is determined by the size of the largest eddies, which depend on the geometry of the flow. If the frequency becomes very large or very small as compared to f_0 , then the velocities diminish. In a rigid pipe, if the flow velocity is u , and the largest eddy

diameter is comparable to pipe diameter D , then $f_0 \cong u/D$. The precise point in the spectrum where the maximum amplitude of velocity occurs is dictated by fluid viscosity as well as local and upstream geometry.

Flow and Volume. If \dot{Q} denoted the flow and V the volume, the flow is the rate of change of volume, that is, $\dot{Q} = dV/dt$. But differentiation and integration are the inverse of one another, and thus we have

$$\dot{Q} = dV/dt \rightarrow V = \int_0^t \dot{Q} d\tau$$

Fourier Analysis. The basic principle of Fourier analysis is that of decomposing any complicated periodic wave-form such as Doppler backscatters, into a set of sinusoidal functions. Each of these sinusoidal waves have different amplitudes and different frequencies, and may be out of phase with each other. It is relatively easy to perform mathematical calculations using individual sine and cosine waves, whereas the composite wave is unwieldy. As an example, one can calculate the corresponding sine wave of the flow-rate in an artery from a single sine wave of pressure, and then the composite flow rate waveform can be constructed by adding together all the different flow-rate sine waves, with their different frequencies, amplitudes, and phases. Generally speaking, a recording of blood velocity at a fixed point in an artery may have a complicated shape. This may be expressed as a sum of various sinusoidal oscillations differing in phase, amplitude, and frequency. If T is the overall period of oscillation, then the fundamental frequency is given by $\omega_0 = 2\pi/T$ and frequency of oscillation is a multiple of ω_0 . The different frequency components that make up the complete wave are called the harmonics of the fundamental frequency

(28). The number of harmonics may be large or small depending on the fidelity of representation of the complete oscillation.

Time Sampling. For purposes of computerized analysis, a continuous signal $x(t)$ is sampled at a fixed rate and converted to a digital signal via an analog-to-digital converter. Generally speaking, the digital signal is the product of the original continuous signal and a train of delta functions defined by (78):

$$f(t) = \sum_{n=-\alpha}^{\alpha} \delta(t-n\Delta t) \quad (1.1)$$

where $\Delta t = 1/(\text{sampling rate})$. Hence, one gets an impulse-modulated signal $x_i(t)$, where $x_i(t) = x(t)f(t)$. Moreover, the sampling rate has to be at least twice the highest frequency component of the signal being digitized to avoid aliasing.

The Fourier Transform. Physically, the Fourier transform $X(f)$ represents the distribution of signal strength with frequency, that is to say, $X(f)$ is a density function. If $x(t)$ is the time function or the input data, f the continuous frequency, ω the angular frequency, $i = \sqrt{-1}$, and $F[\omega]$ or $F[f]$ the Fourier transform of $x(t)$, then

$$F[\omega] = X(\omega) = \int_{-\infty}^{\infty} x(t)e^{-i\omega t} dt \quad (1.2)$$

or equivalently

$$F[f] = X(f) = \int_{-\infty}^{\infty} x(t)e^{-i2\pi ft} dt \quad (1.3)$$

For limited duration signals $x(t)$ is zero outside the range $[T_1, T_2]$, thus reducing the range of integration to T_1 to T_2 (82):

$$X(f) = \int_{T_1}^{T_2} x(t)e^{-i2\pi ft} dt$$

Since the waveform $X(f)$ is described by the frequencies present in the signal, this description is also referred to as the spectrum of the time signal. Thus, the frequency spectrum or Fourier transform provides a plot of the relative weight of different frequencies that comprise or represent the given signal. Conversely, if the Fourier transform of a signal is known, the inverse transform of a signal is also known. The inverse transformation, $x(t) = \int_{-\infty}^{\infty} X(f) e^{i2\pi ft} df$, determines the time function $x(t)$.

Discrete Fourier Transform and Fast Fourier Transform. The discrete Fourier transform (DFT) is used to approximate the continuous waveform whenever digital implementation is to be used. A set of integers n and m are defined to represent the equivalent in a sense of the time and frequency variables of the continuous Fourier transform.

If $x(n)$ denotes the sampled signal, and there are N samples of the signal spaced Δt seconds apart, then as n varies from 0 to $N-1$, the N samples of the time signal are generated, and the duration of the time signal is $N\Delta t$. The DFT is defined as

$$X(m) = 1/N \sum_{n=0}^{N-1} x(n) e^{-i2\pi nm/N} \quad (1.4)$$

where, function $X(m)$ represents a discrete spectrum. In general, $X(m)$ is a complex function consisting of a real part and an imaginary part at each frequency. By the definition of DFT, there are approximately N complex multiplications and additions in order to compute the spectrum at one particular value of m .

The Cooley-Tukey algorithm, along with subsequent versions are referred to as the fast Fourier transform (FFT), where its formulation

is the same as the DFT. The FFT is a high speed algorithm for computing the DFT, which reduces the number of computations to $N \log_2 N$, and works best when the number of sample points is an integer power of 2. In other words, if the series to be transformed is of length N and N is a power of 2, the series can be split into $\log_2 N$ subseries, and this doubling algorithm can be applied to compute the finite Fourier transform in $\log_2 N$ doublings (20). Hence, the number of computations in the resulting successive doubling algorithm is proportional to $N \log_2 N$. The symmetries of the sine and cosine functions also reduces the proportionality factor.

Ideal Flowmeter. An ideal flowmeter should possess the following properties (65):

1. A linear response to forward and backward flows.
2. A stable zero reference.
3. A frequency response adequate to follow the phasic phenomena.
4. Independence from blood pressure, internal noise, and other non-related phenomena.
5. Freedom from introducing measurement artifacts; that is, the blood vessel must be unobstructed and non-cannulated and the recording be performed without anticoagulant, anesthesia, or psychic trauma to the experimental subject.

Doppler Ultrasonic Flowmeter. Ultrasonic flowmeters utilize high frequency sound to detect flow velocity by the Doppler principle (36). The transducer, which is situated beside a blood vessel and located outside of the blood stream, emits a sinusoidal beam of

ultrasound. Blood flowing through the vessel contains red cells that act as point scatterers of the incident ultrasound beam. The backscattered ultrasound is a sinusoid shifted in frequency from the transmitted carrier by an amount Δf , where Δf is obtained from the Doppler shift formula (11,27,31,51,77):

$$\Delta f = 2 f_0/c (\cos \theta) v \quad (1.5)$$

where,

- V = particle flow velocity;
- c = speed of sound in the medium;
- f_0 = transmitted carrier frequency;
- θ = transducer orientation angle.

Equation (1.5) is also expressed in the following form (3,48):

$$\Delta \omega = \omega - \omega_0 = \omega_0/c (\cos \alpha + \cos \beta) V \quad (1.6)$$

where,

- ω = angular frequency of the received signal;
- ω_0 = angular frequency of the transmitted signal;
- α = angle between transmitting beam and the direction of the particle velocity;
- β = angle between the receiving beam and the direction of particle velocity.

From Equation 1.6 one can derive the following Equation (3):

$$\Delta \omega_{av.} = \omega_0/c (\cos \alpha + \cos \beta) V_{av.} \quad (1.7)$$

where $\Delta \omega_{av.}$ is the average angular frequency shift.

Equations 1.5, 1.6, and 1.7 do not directly relate Doppler

output to fluid velocity. Equations 1.5 and 1.6 are based on the assumption that all RBC's are moving at the same velocity. Because blood particles travelling through the vessel do not have a uniform velocity, but possess a distribution of velocities or velocity profile across the vessel lumen, the Doppler echoes consist of a combination of frequencies rather than a single frequency (3,4,11,31). Thus, the received signal contains a spectrum of frequencies, where each blood particle gives equal power contribution, but at different frequencies, depending on the magnitude of the quantities in equations 1.5 and 1.6. It is suggested that Doppler frequency is also related to cross-sectional area as well as to the volumetric flow (68).

The average angular frequency shift or mean frequency has been described in terms of spectral power density of the received signal ($\Phi(\omega)$), as for example, expressed by the following equation(3,29):

$$\Delta\omega_{av.} = \left[\int_{-\Delta\omega_m}^{\Delta\omega_m} \Delta\omega \Phi(\omega_0 + \Delta\omega) d\Delta\omega \right] / \int_{-\Delta\omega_m}^{\Delta\omega_m} \Phi(\omega_0 + \Delta\omega) d\Delta\omega \quad (1.8)$$

where $\Delta\omega_m$ is the maximum angular frequency of the received signal corresponding to a maximum velocity of a blood particle expected in a blood vessel, and $\omega = \omega_0 + \Delta\omega$.

Equation (1.8) shows a way to determine $\Delta\omega_{av.}$ from the power density spectrum of the received signal and then from equation (1.7), average velocity of blood can be found.

Statement of the Hypothesis

The following investigations were carried out in order to further

understand the significance of changes in the amplitude of the continuous wave (CW) Doppler signals. The Doppler flowmeter has many worthwhile attributes compared to other techniques; namely, (11,31):

1. It is a non-invasive tool.
2. It has a stable zero-flow reference.
3. It requires simple and inexpensive circuitry.

The scattering of ultrasound from blood has been described by assuming that blood cells act approximately as point scatterers (11,31). This model predicts that the energy backscattered from blood is proportional to hematocrit. The measured root mean square amplitude by means of a pulsed-Doppler flowmeter does not support this hypothesis (8); however, the recorded "intensity of scattered beam" using laser-Doppler technique shows the hypothesis is valid (24). Neither of these studies take into consideration the influence of pressure head, nor do they use the technique of fast Fourier transform (FFT) on the data.

Because a directional ultrasonic flowmeter capable of resolving the net flow into positive and negative components has been used extensively in our laboratory, the initial hypothesis was that blood hematocrit would influence the Doppler amplitude.

In order to answer this question, the mean amplitude of the CW Doppler was calculated for a wide range of blood hematocrits starting from 4.5% to 46.5% at various levels of pressure head under steady blood flow conditions.

As a result of this study, the following objectives were also achieved:

1. The distribution of blood particles in a given hematocrit is dependent upon the change in velocity. A series of experiments were carried out where both instantaneous blood velocity and the corresponding blood hematocrit was measured.
2. Blood viscosity is dependent upon hematocrit. To determine the extent of this dependence, tests were performed for the purpose of obtaining the desired quantitative relationship.

The hypothesis was that the amplitude of the CW Doppler flow-meter is a double variable function of hematocrit and pressure head. This problem will be approached by first processing and Fourier transforming the Doppler signals and then calculating its mean amplitude. Whenever a time-domain approach to a problem is pursued, one should consider taking the FFT of the time record (53); where the frequency spectra reveals peaks which are related to the dynamic events of blood flow (79).

The following properties of blood flow affecting the Doppler signal will be developed:

1. A quantitative description of average velocity in terms of parameters of steady blood flow.
2. The distribution of blood particles inside the vessel.
3. A generalized Doppler amplitude function of 2 variables expressible in terms of hematocrit and pressure head.
4. A mathematical formulation for the description of blood viscosity in terms of hematocrit.

CHAPTER 2
MATERIALS AND METHODS

General

Fluids

Experiments were completed with .9% normal saline, and outdated human blood (Blood Bank, San Bernardino County, CA). In each experiment, the fluid was placed in an elevated container, the height of which maintained the required constant pressure head necessary for steady, laminar flow. Blood of differing hematocrits was obtained by addition and mixing of saline to the packed red cells. In order to prevent blood clots, 169 units/mg heparine was used, where for each milliliter of blood one unit of heparine was mixed with blood.

Measurement Techniques of Blood Flow

The Electromagnetic Flowmeter. Blood flow was measured with a square-wave electromagnetic flowmeter (Carolina Medical Electronics, Inc.). Flow range specification for this instrument was 5 ml/min. to 19.99 L/min. Care was taken to stay completely within this range during the course of each experiment. Electromagnetic flowmeter was used for the purpose of support and comparison to Doppler flowmeter. Principles of operation of electromagnetic flowmeter is described in Appendix A1.

The Ultrasonic Doppler Flowmeter. Blood flow was measured simultaneously by an Ultrasonic Doppler flowmeter (Debitmetre Ultrasonique Directionnel DeLalande Electronique, 30 rue H. Regnault 92402 Courbevoie, France). The Ultrasonic probe was

placed against the glass tube, at a 60 degree angle with an intervening coupling jelly (Sonostat Diagnostic Medical Ultrasonic Couplant, Echo Laboratories, Lewiston, PA 17044). Principles of operation of Continuous-Wave Doppler flowmeter is outlined in Appendix A2.

Blood Flow Monitoring. Electromagnetic flow and Doppler flow were monitored on an oscilloscope (Tektronix, Beaverton, Oregon), and recorded on an eight channel instrumentation tape recorder (Ampex PR 500) or displayed on a polygraph. Pitot tube deflections were displayed on a Grass model 5 ink-writing polygraph.

Pressure Measurements. Pressure was measured with a Statham transducer Model P2310 (Gould Statham, Hato Rey, Puerto Rico).

Steady Flow Procedure

A system consisting of rubber, dialysis, and glass tubing connected to a reservoir was filled with either blood or saline (Fig. 1). An electromagnetic probe was placed around the dialysis tube, and immersed in a saline filled lucite box. The probe will not function in air or in distilled water, which necessitates the use of saline as a conductive liquid (64). Dialysis tube was used because it plays a similar role as an artery for in vitro studies and also because it possesses conductive properties.

The Doppler probe was at a 60 degree angle with respect to the axis of the glass tubing. A pitot tube complex comprised of an axial or straight tube, and a pitot or bent tube held in place with a micromanipulator was placed into a section of rubber tubing. The

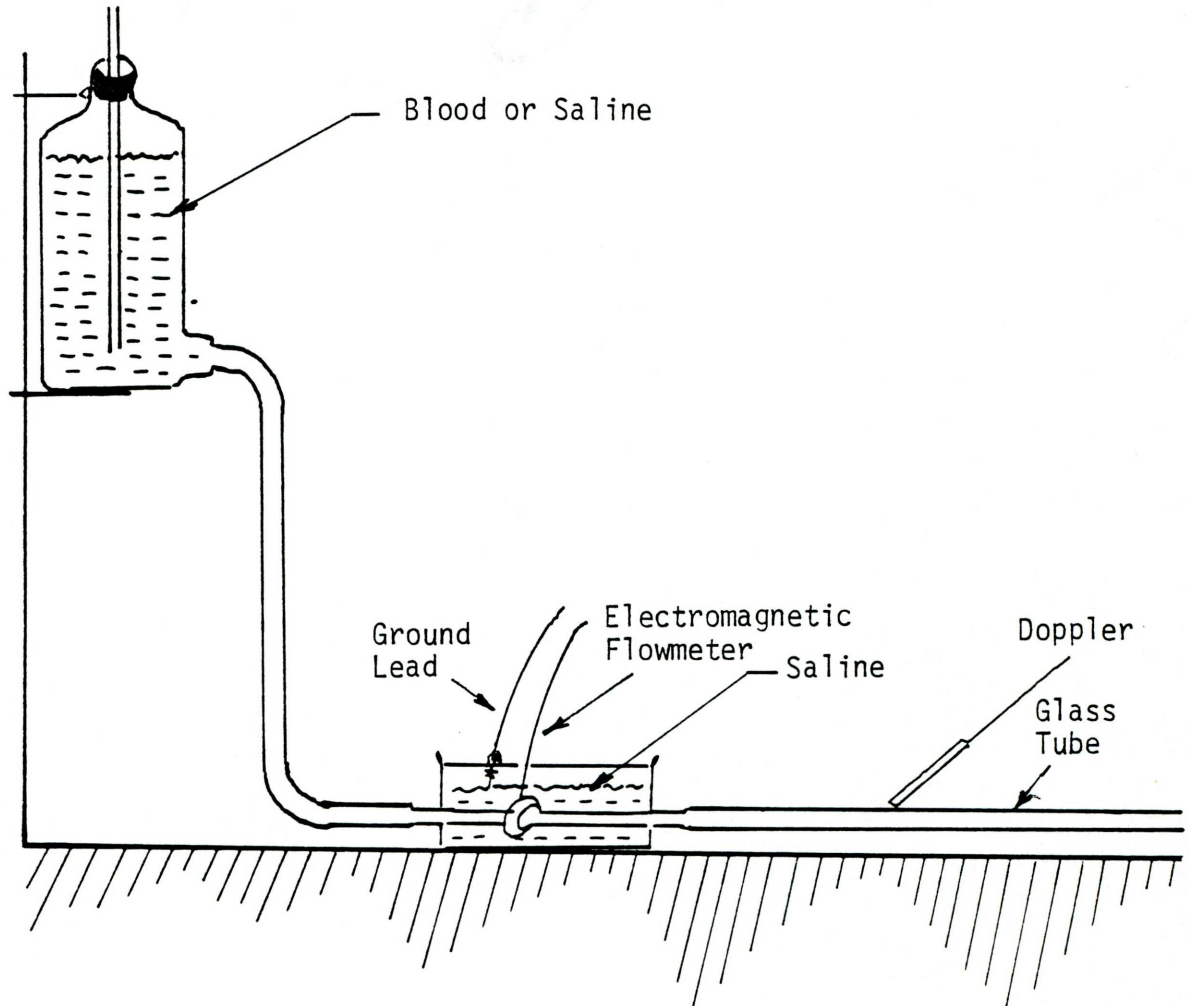


Figure 1. The Experimental Set-Up

axial tube was fixed in position, whereas the pitot tube could be moved vertically in .1 millimeter steps with a micromanipulator. Pressure in each section was monitored by a pressure transducer connected to a polygraph.

In order to study the distribution of particles, blood samples were drawn sequentially at varying radii within the flow stream by means of an array of tubes facing the flow, where each successive one was placed deeper (radically) within the lumen of the rubber tubing, such that the one nearest the flow source was at the top wall. Each of these tubes was connected to a small syringe. Upon maintenance of steady, laminar flow, uniform sampling was carried out (Figure 2). Each sample of blood was centrifuged in a Micro-Capillary Centrifuge, Model MB (International Equipment Company, Needham Heights, MA), and a hematocrit reading was obtained by means of a Micro-Capillary Reader (International Equipment Company, Needham Heights, MA).

Series of Experimental Stages

The Experiments

A sequence of experiments was carried out during each of three stages as described below:

Introductory Stage. A sequence of experiments was conducted to determine the correlation between Doppler and electromagnetic flow measurements. A reservoir containing a mixture of saline and starch was placed at elevations of 40, 50, 60, and 70 cm. respectively for each independent measurement. Starch was used in those early experiments to provide the necessary interfaces for

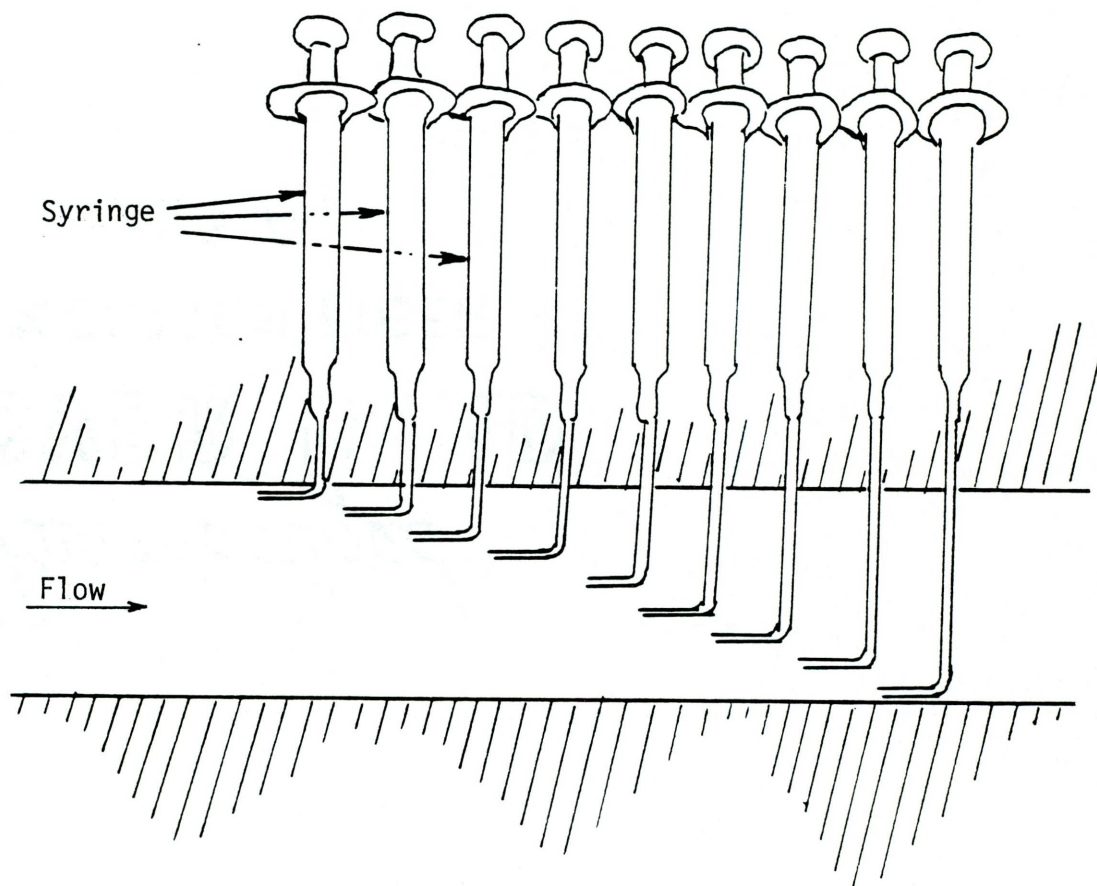


Figure 2. Blood Sampling Method

backscattering.

At each given pressure head, the flow rate was varied by altering the resistance downstream, and flow measurements were recorded for each rate using both the electromagnetic and Doppler flowmeters.

Intermediate Stage. The objective of these experiments was to determine in quantitative terms the simultaneous influence of pressure head and hematocrit on average velocity of blood flow.

Blood reservoir with a total hematocrit of 22.5% was placed at respective heights of 32.5, 42.5, 52.5, and 62.5 cm. As steady, laminar flow was attained, blood was collected in a container, and flow time was measured by a stop watch. Volume of collected blood was measured by a graduated cylinder, and subsequently average velocity was calculated. The experiment was repeated as described above using blood with a total hematocrit of 25.5% and 29.7%.

Final Stage. The investigation of the effect of hematocrit upon the amplitude of the Doppler necessitated that experiments be carried out in three different phases as described below:

The objective of phase 1 was to determine experimentally the distribution of instantaneous velocity of red blood cells by means of a pitot tube complex. Both the straight and bent tubes of the complex was connected to a Statham pressure transducer. An ink-writing polygraph measured these pressures directly with its sensitivity set so 1 mm. deflection was equivalent to 5 mmHg.

Determination of the distribution of the particle population for a given blood hematocrit was the goal of phase 2. Blood

samples were withdrawn at incremental radii with the rubber tubing by means of bent tubes as was discussed on page 22 and illustrated in Figure 2.

The interpretation of the amplitude of the Doppler flowmeter was the purpose of phase 3. Starting from a hematocrit of 46.5%, the blood container was placed at successive heights ranging from 60 to 100 cm. For each given pressure head, stirred blood flowed through the glass tube where the ultrasound was being transmitted by the Doppler transducer. Employing the above procedure, blood was diluted repeatedly and measurements were taken for hematocrits of 40% down to 4.5%. Positive and negative Doppler signals were recorded on magnetic tape along with voice annotation.

Signal Processing

An Apple II personal computer (Apple Computer, Inc.) equipped with 48K bytes of random access memory (RAM) featuring an analogue-to-digital (A/D) converter board was utilized for data reduction and plotting.

Recorded Doppler signals were passed through a 200 Hz to 8 KHz band pass filter (6 pole Butterworth) to eliminate aliasing, and then were digitized at a rate of 8 KHz. A digitization rate of 8 KHz was used because Doppler shifts greater than 4 KHz were not anticipated. Digitized data were Fourier Transformed using Fourier Analyzer, Harmonic Analyzer (Dyna Comp., N.Y. 14580) (82,83), and 6502 Machine Code FFT (Walla Walla College, WA. 98221). The machine code FFT was modified in our laboratory to

accomplish transformation of a file of 8 K points with a resolution of 256 bytes per window (39). The transforming resolution for 8 K bytes of data was 8 windows of 256 samples each.

The FFT'd results were stored on diskettes as textfiles for subsequent processing or plotting. Transformed data were plotted in both time and frequency domain with a digital plotter (Houston Instrument). Appendix B provides a listing of the important programs. To analyze the behavior of experimental data, a "Data Smoother" program (Dynacomp., Inc.) was used (81). A "Curve Fitter" software package (Creative Computing Software, 39 East Hanover Ave., Morris Plains, NJ 07850) was used extensively for the purpose of fitting a wide variety of curves to raw data, smoothed data, and transformed data (74). A 7-point smoothing was performed on transformed data derived from Doppler signals in order to reduce random variations in data values. This technique adjusts the value of a given data point according to the weighted sum of the values of surrounding data points. A least squares polynomial of second degree was sufficient and most appropriate to fit these data, because the coefficients of higher degree terms in polynomials with degrees greater than 2 were quite small. Other fitted curves also resulted in poor correlation coefficients. Mean amplitude was then calculated by evaluating the area under the curve via integration. Lower and upper limits of integration were 0 and 4000 respectively. These limits are used because the Doppler shifts are contained within the

range of 0 to 4000 Hz.

Determination of Blood Viscosity and Density

Blood viscosity and density were determined for a wide range of blood hematocrits. Blood viscosity was determined using a V-1200 viscosimeter, falling ball type, size No. 1 (Roger Gilmonte Instruments, Inc.), where a stainless steel ball type 316 with density 8.02 gm/ml was used. The constant K of the viscosimeter had to be calculated first, where water was used as the fluid and time of descent of the stainless steel ball between a given distance was measured by a stop watch. Subsequently, blood was placed into the viscosimeter and again time of descent was measured.

Viscosity was computed according to the equation:

$$\mu = K(\rho_t - \rho)t$$

where ρ_t was the density of the stainless steel ball, ρ the density of liquid, and t the time of descent in minutes.

To determine blood density of a given blood hematocrit, exactly 5 milliliter of blood was drawn by a TD10 in 1/10 ml No. 37033 pipette (Kimax -51, USA), and then it was weighed on an electronic balance with digital display (Cahn, Model TA 450). A TD pipette has the advantage that it does not require blowing into it. (TD stands for "To Deliver.")

CHAPTER 3

RESULTS

Functional Relationship of Doppler Flow and Electromagnetic Flow.

The Experimental Results

Table 3.1 compares the results of Doppler (\dot{Q}_d) and electromagnetic (\dot{Q}_e) flow measurements. A linear least squares curve was fit to the raw data obtained from each set of independent measurement. The derived equations along with the coefficient of correlation (ξ) and determination coefficient (γ) are given in Table 3.2. The proportion of variance of the dependent variable on the independent variable as explained by a linear regression is referred to as determination coefficient. A value close to 1 indicates a strong linear relation between the two variables (74).

It was not possible to fit other types of curves, such as geometric, exponential, or 2nd degree polynomial least squares to the raw data without first performing a two point smoothing on them. The curve fitting procedure calculates the coefficients of the equation as well as the values of ξ and γ (63,74).

Statistical Analysis

Above results were pooled together using an analysis of covariance (16,21,80). As a final two-step procedure, the null hypotheses H_0 and H'_0 were tested, where they are stated as follows:

H_0 : there is no difference among Q_d 's after adjusting Q_e 's.

H'_0 : one regression line is adequate for all observations.

The computed F value for H_0 was .1947, whereas the tabled F

Table 3.1. Comparison of Electromagnetic and Doppler Flow Measurements

		Height of Saline Reservoir (Cm.)							
		40		50		60		70	
		\dot{Q}_e	\dot{Q}_d	\dot{Q}_e	\dot{Q}_d	\dot{Q}_e	\dot{Q}_d	\dot{Q}_e	\dot{Q}_d
Flow (m/min)	0	0	0	0	0	0	0	0	0
	200	204.28	125	255.35	100	170.24	150	255.35	
	387.5	255.35	200	340.47	125	204.28	325	340.47	
	462.5	340.47	350	425.59	225	238.33	862.5	425.59	
	625	425.59	475	510.71	400	255.35	1162.5	510.7	
			687.5	595.82	537.5	340.47	1200	629.87	
					575	408.56			
					625	510.71			
				875	766.06				

Table 3.2. Linear Equations Describing Doppler Flow as a Function of Electromagnetic Flow Obtained by the Method of Least Squares

Height (cm.)	Linear Equation	ξ	γ
40	$\dot{Q}_d = .6536\dot{Q}_e + 26.18$.98	.96
50	$\dot{Q}_d = .888\dot{Q}_e + 111.06$.94	.89
60	$\dot{Q}_d = .724\dot{Q}_e + 42.97$.95	.91
70	$\dot{Q}_d = .385\dot{Q}_e + 122.7$.92	.85

value with a 95% confidence limit was 3.29. Thus, with a probability of 95%, H_0 was accepted. Similarly, the computed F value for H_0' was 3.395 and its corresponding tabled value with a confidence limit of 99% was 4.82. Hence, H_0' was accepted with a confidence limit of 99%.

A confidence interval was constructed for the coefficients of the regression equation according to the equations:

$$b_0 \pm t_{\alpha/2} S_{b_0} \text{ and } b_1 \pm t_{\alpha/2} S_{b_1} \quad (3.1)$$

where $S_{b_0} = S_{y|x} (1/n + \bar{x}^2 / \sum(x - \bar{x})^2)^{1/2}$

and $S_{b_1} = S_{y|x} / (\sum(x - \bar{x})^2)^{1/2}$

In the expressions 3.11, $t_{\alpha/2}$ is a t value with the appropriate confidence level from the t table having (n-2) degrees of freedom (17,22,37). $S_{y|x}$ is referred to as the standard error of estimate and is computed according to the formula:

$$S_{y|x}^2 = \{[\sum y^2 - (\sum y)^2/n] - b_1 [\sum xy - (\sum x \cdot \sum y)/n]\} / (n-2) \quad (3.2)$$

Ninety-five percent confidence intervals for the coefficients of the regression equation fitted to the unsmoothed data were:

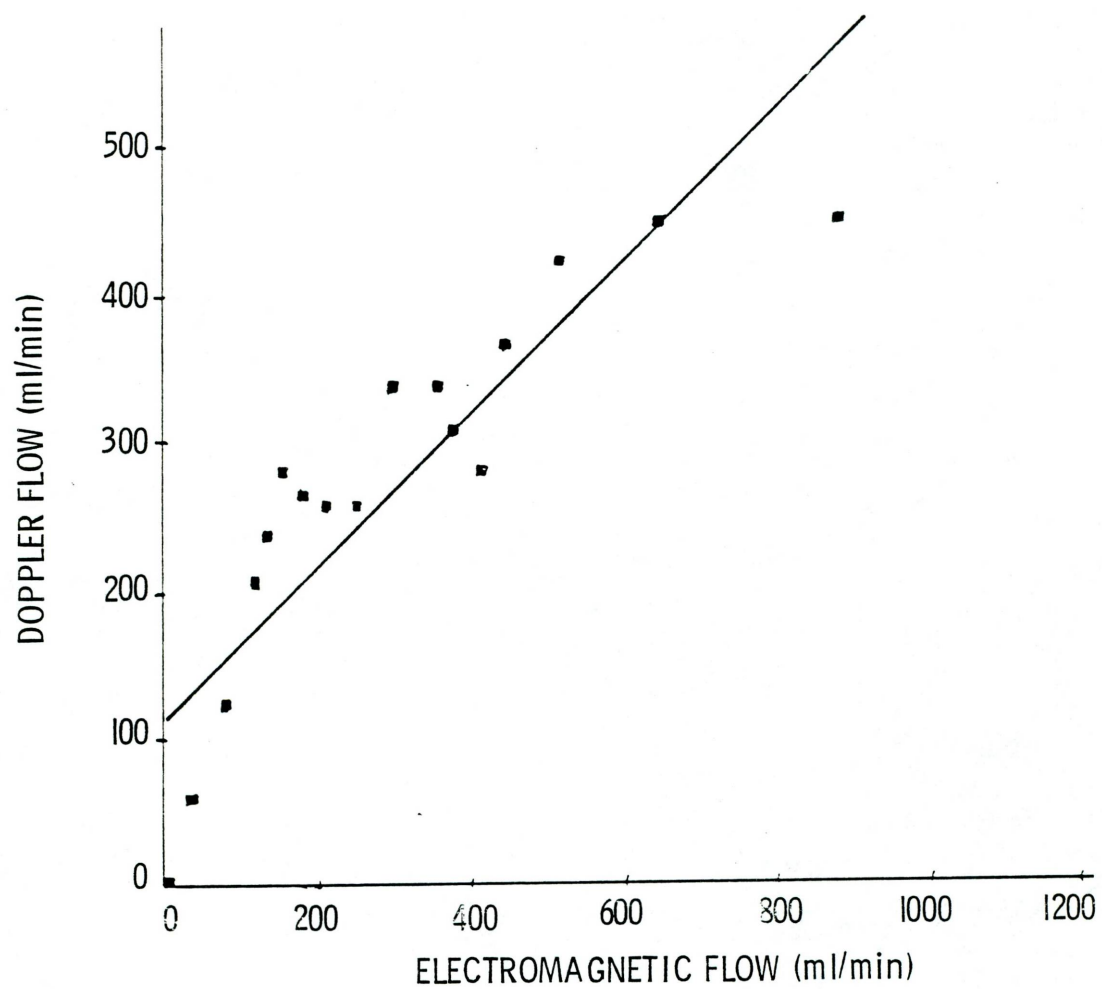
$$122.128 \pm 2.101 (31.751) \text{ and } .43977 \pm 2.101 (.000056096)$$

respectively. Using interval notation, this can also be written as (55.419,188.837) and (0.43965,0.43989).

Figure 3 gives a plot of pooled Doppler as a function of

Figure 3. A scattergram of data representing pooled Doppler flow expressed as a linear function of pooled electromagnetic flow. Results of flow measurements due to constant pressure heads of 40, 50, 60, and 70 Cms were pooled together using analysis of covariance.

Ninety-five percent confidence intervals about the coefficients of linear regression equation are 122.128 ± 66.709 and $.43977 \pm .00011786$.



pooled electromagnetic flow.

A Quantitative Study of Simultaneous Influence of Pressure Head and Hematocrit Upon Velocity of Blood Flow

For a given pressure head (H) and a specified blood hematocrit (\hat{H}), Table 3.3 lists its corresponding average velocity (V). Each value of V is the mean of 5 independent measurements. Using every measured value of V, a multiple linear regression was employed on the raw data. The equation obtained was:

$$V = 59.879 + .74538 H - 1.5053 \hat{H} \quad (3.3)$$

The multiple linear regression model is not valid for $H = \hat{H} = 0$. Although there is no clear cut range of values for this model, upon extrapolation the portion near the origin is more critical than the upper region.

Confidence intervals for the coefficients of the least squares plane were constructed according to the equations 3.7 - 3.10 given in Section 3. The desired 95% confidence intervals obtained were as follows:

$55.3605 \pm (2.365) [(4743.11903)/7]^{1/2}$, $.74538 \pm (2.365) \cdot [(.00064210)(4743.11903)]^{1/2}$, and $-1.5053 \pm (2.365) \cdot [(.0021245)(4743.11903)]^{1/2}$. Using interval notations, these can also be written as $(-6.2017, 116.9227)$, $(-3.38191, 4.87267)$, and $(-9.01273, 6.00213)$ respectively.

Table 3.3. Measurement of Average Velocity (cm/sec) Obtained From a Specified Total Blood Hematocrit and Under a Given Pressure Head

H (cm)	\hat{H} (%)	V (cm.sec)
32.5	22.5	49.152
32.5	25.5	44.337
32.5	29.7	38.865
42.5	22.5	59.275
42.5	25.5	57.019
42.5	29.7	48.519
52.5	22.5	63.007
52.5	25.5	57.973
62.5	22.5	73.722
62.5	29.7	61.736

Determination of Instantaneous and Spatial Velocity of Blood Flow
by Pitot Tube Complex and Doppler Flowmeter, and Hematocrit
Measurement

Distribution of Particle Velocity by Pitot Tube Complex

The supply reservoir, filled with blood of hematocrit 10% was placed at the height of 131 cm. Table 3.4 lists values of particle velocity obtained at intervals of .1 cm across the lumen of the tube, where 0 indicates the top wall. Each value of the instantaneous velocity in Table 3.4 is an average of 4 measurements. Figure 4 illustrates one of these velocity measurements as was recorded by the polygraph.

A least squares polynomial of 2nd degree fit resulted in the equation:

$$V = 11.312 + 5.0236 r - .76072 r^2 \quad (3.4)$$

as shown in Figure 5. In this case, $\xi = .94$, $\gamma = .88$, and standard error of estimate was 1.98.

Confidence intervals for the coefficients of the 2nd degree polynomials can be constructed according to the equations (22):

$$\begin{aligned} b_0 &\pm t_{1-\alpha/2} [S_e^2 (1/n + \bar{x}^2 C_{22})]^{1/2} \\ b_1 &\pm t_{1-\alpha/2} (C_{11} S_e^2)^{1/2} \\ b_2 &\pm t_{1-\alpha/2} (C_{22} S_e^2)^{1/2} \end{aligned} \quad (3.5)$$

where degrees of freedom is equal to $(n-3)$ and were $b_0 = \bar{Y} - b_2 \bar{X}_2$ and $X_2 = \Sigma(X-\bar{X})^2$. S_e^2 , C_{11} , and C_{22} are computed according to the formulas 3.8, 3.9, and 3.10 as defined in

Table 3.4. Measurement of Instantaneous Velocity (cm/sec) Across the Lumen of the Tube. Each Value of Velocity is an Average of Four Measurements.

Radius (cm)	Velocity (cm/sec)	Standard Error of the Mean (\pm SEM)
0	205.57	5.06
.1	205.16	5.42
.2	206.01	4.13
.3	210.13	3.45
.4	207.99	5.07
.5	207.67	6.76
.6	209.23	5.81
.7	197.41	9.53
.8	191.08	7.82

Figure 4. Polygraph recording of axial and pitot deflection from a pitot tube complex. Numbers 1-9 indicate the downward movement of pitot (bent) tube in steps of .1 cm causing a change in pressure.

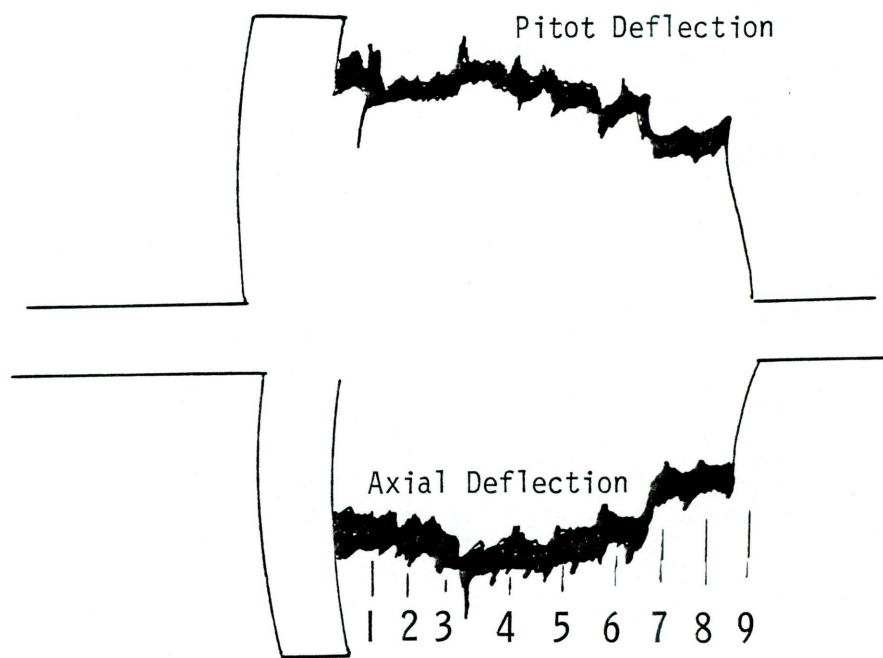
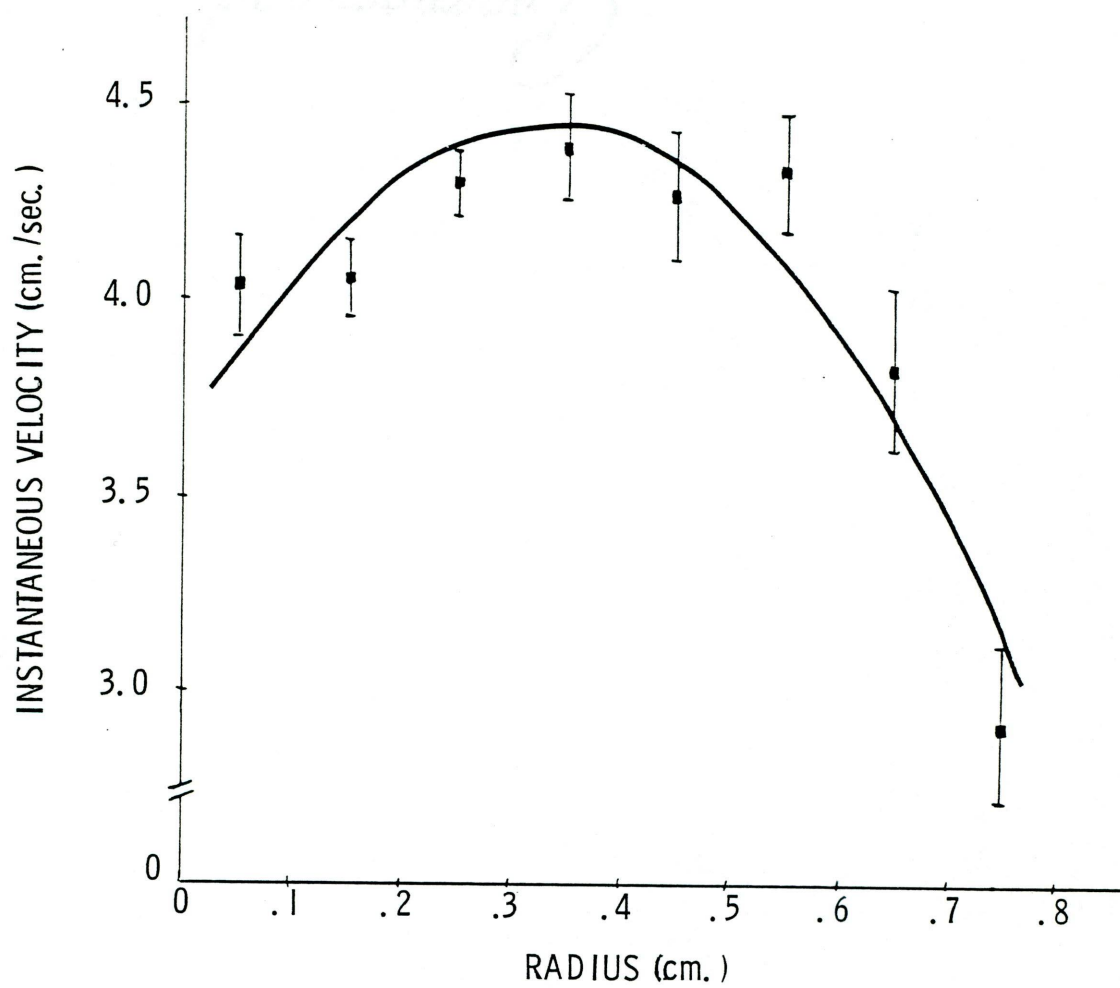


Figure 5. A least squares polynomial of 2nd degree describing the instantaneous velocity of blood as a function of radius. A pitot tube system measured the instantaneous velocity of blood at intervals of .1 cm. across the lumen of the vessel, where 0 indicates the top wall. The values of vessel diameter, pressure head, and total blood hematocrit were .92 cm., 131 cm., and 10% respectively. Radius denotes distance from top wall to bottom wall.

Equation of the fitted curve is $V = 11.312 + 5.0236r - .76072r^2$. Ninety-five percent confidence intervals about the coefficient of the regression equation are 19.52293 ± 72.47879 , 5.0236 ± 62.00851 , and $-.76072 \pm 273.77399$ respectively. Brackets denote ± 1 standard error of the mean.



Section 3, where $x_1 = X - \bar{X}$, $x_2 = X_2 - \bar{X}_2$, and $y = Y - \bar{Y}$.

Ninety-five percent confidence intervals for the coefficients of the equation of the instantaneous velocity are:

$$19.52293 \pm 2.447 [385.28759(1/9 + .066667 \cdot 32.48863)]^{1/2}$$

$$5.0236 \pm 2.447 [(1.66667)(385.28759)]^{1/2}$$

$$- .76072 \pm 2.447 [32.48863)(385.28759)]^{1/2}$$

Using interval notations these can be written as:

(-52.95586, 92.00172), (-56, 98491, 67.03211), and

(-274.53471, 273.01327) respectively.

Measurement of Blood Hematocrit

Using blood with a hematocrit of 10%, the reservoir was set at an elevation of 177 cm. Hematocrit measurement of blood samples drawn at each given radius (r) within the rubber tubing is shown in Table 3.5, where 0 indicates top wall.

Geometric, exponential, and linear least squares fit to the data resulted in a low correlation coefficient. Least squares polynomial of 2nd, 3rd, and 4th degrees yielded the information shown in Table 3.6.

Figure 6-8 show the graphs of these polynomials. Ninety-five percent confidence intervals for the coefficients of the 2nd degree regression equation are:

$$3.6920 \pm 2.365 [.71316(1/10 + .0825^2 \cdot 18.96726)]^{1/2}$$

$$.56481 \pm 2.365 [(1.21390)(.71316)]^{1/2}$$

$$-.072719 \pm 2.365 [(18.96726)(.71316)]^{1/2}$$

Table 3.5. Measurement of Blood Hematocrit (\hat{H}) Across the Lumen of the Tube. Each Value of \hat{H} is an Average of Three Measurements.

r (cm)	\hat{H} (%)	\pm SEM
0	8.21	.18
.1	8.67	.17
.2	9.03	.29
.3	9.42	.30
.4	9.59	.26
.5	9.40	.20
.6	8.91	.33
.7	8.31	.21
.8	7.64	.36

Table 3.6. Least Squares Polynomial Fitting Describing Hematocrit (\hat{H}) as a Function of Radius (r)

<u>Degree of Polynomial</u>	<u>Resulting Equation</u>	<u>ξ</u>	<u>γ</u>
2	$\hat{H} = 3.2402 + .56481r - .072719r^2$.91	.83
3	$\hat{H} = 2.8159 + 1.1109r - .22331r^2 + .011155r^3$.95	.90
4	$\hat{H} = 3.4961 - .25104r + .43744r^2 - .10207r^3 + .0062918r^4$.99	.99

Figure 6. A least squares polynomial of 2nd degree fit describing the hematocrit of blood as a function of radius. Hematocrit value was measured across the lumen of the rubber tubing, where 0 marks the top wall. Equation of the fitted curve is $\hat{H} = 3.2402 + .56481r - .072719r^2$.

Pressure head and total blood hematocrit were 177 cm. and 10% respectively.

Ninety-five percent confidence intervals about the coefficients of the regression equation are $3.6920 \pm .95595$, $.56481 \pm 2.20047$, and $-.072719 \pm 8.69815$ respectively.

Brackets denote ± 1 standard error of the mean.

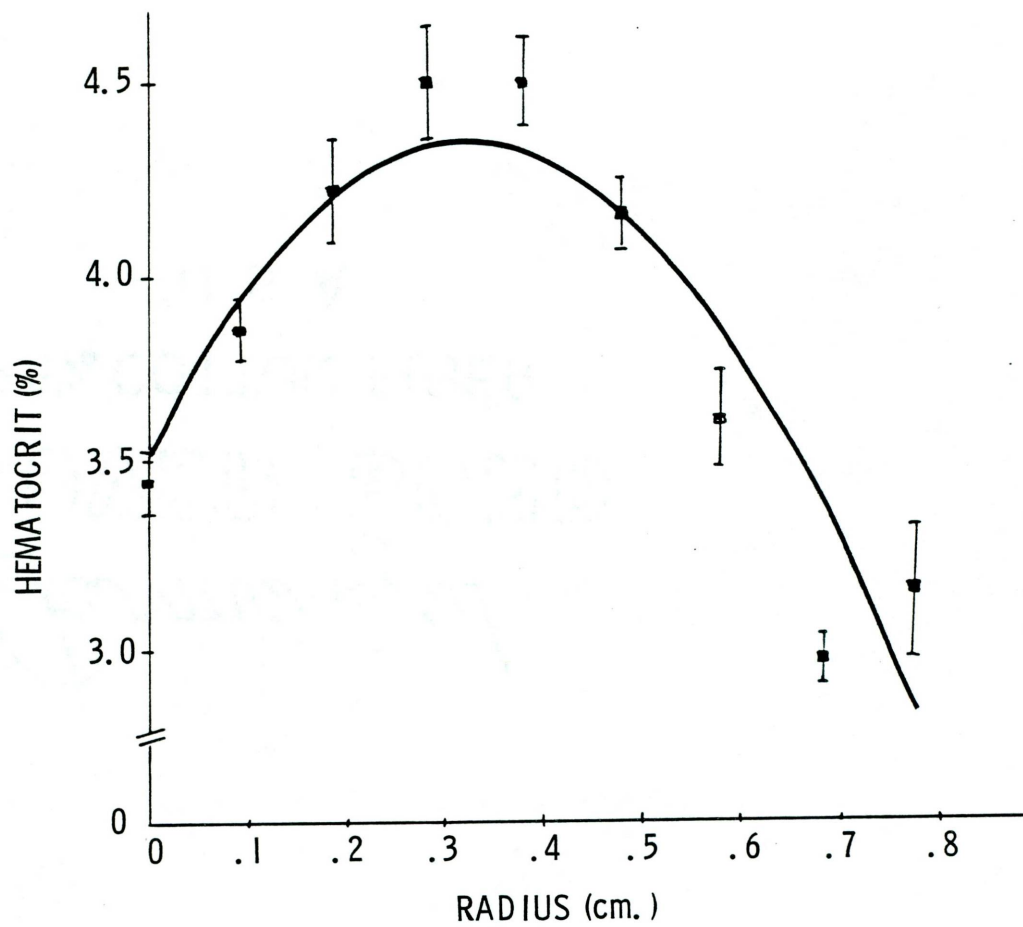


Figure 7. A least squares polynomial of 3rd degree fit describing the hematocrit of blood as a function of radius. Hematocrit was measured across the lumen of the vessel in steps of .1 cm., where 0 marks the top wall. Equation of the fitted curve is $\hat{H} = 2.8159 + 1.1109r - .22331r^2 + .011155r^3$.

Pressure head and total blood hematocrit were 177 cm. and 10% respectively.

Brackets denote ± 1 standard error of the mean.

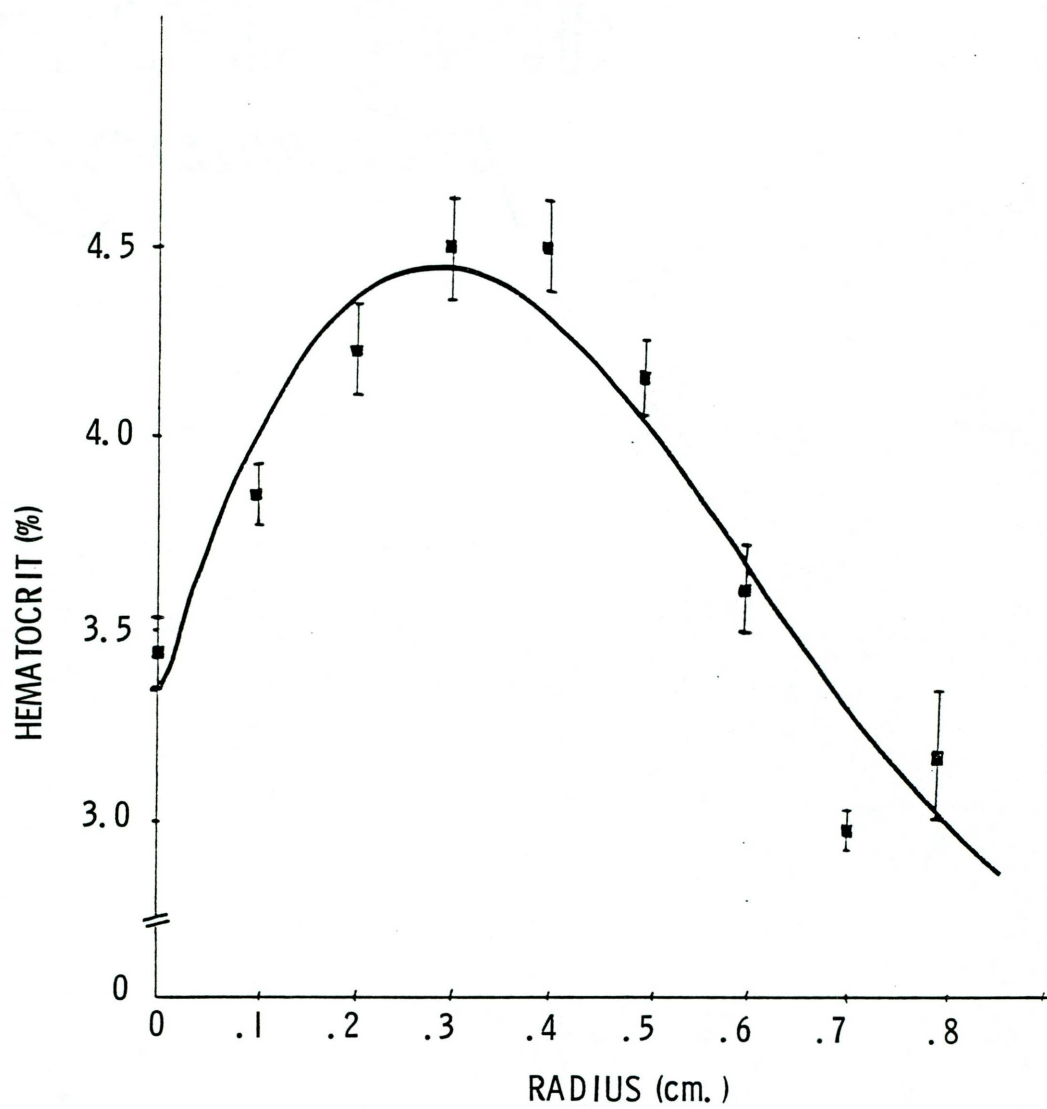
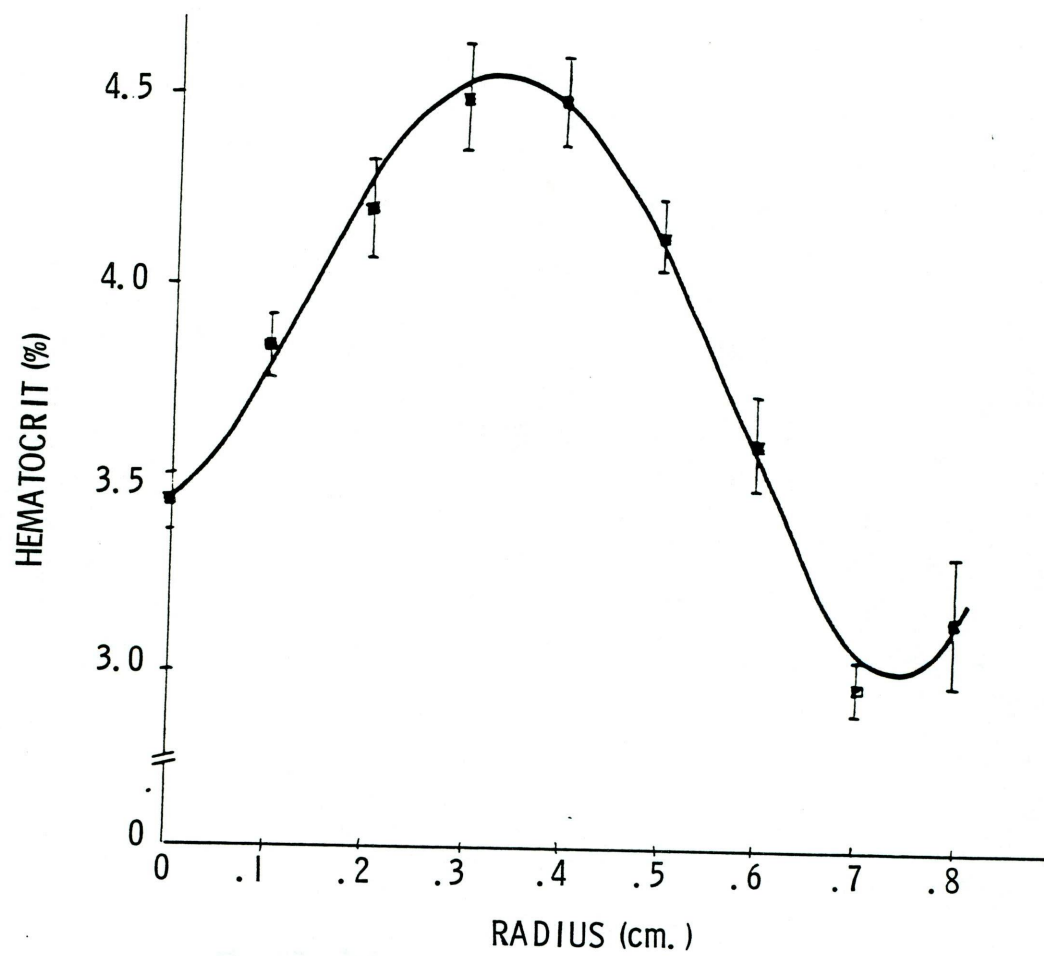


Figure 8. A least squares polynomial of 4th degree fit describing the hematocrit of blood as a function of radius. Hematocrit was measured across the lumen of the vessel at intervals of .1 cm., where the top wall is marked by 0. Equation of the fitted curve is $\hat{H} = 3.4961 - .25104r + .43744r^2 - .10207r^3 + .0062918r^4$.

Brackets denote ± 1 standard error of the mean.



Using interval notations these can be written as:

(2.73605,4.64795), (-1.63566,2.76528), and (-8.77087,8.62543) respectively.

The following results shown in Table 3.7 were obtained when the supply reservoir was set at the height of 131 cm. and total blood hematocrit was 10% and 7% respectively. Standard error of estimate is denoted by ϵ . Figure 9-10 illustrate the graphs of least squares polynomials of 2nd, 3rd, 4th, and 5th degrees for blood hematocrit of 7%.

Calculation of Mean Doppler Amplitude

The area under the curve which was fit to the Fourier transformed data was calculated. Each mean amplitude of the Doppler signal for a given blood hematocrit was an average of 3 separate measurements. Table 3.8 shows the calculated values of mean amplitude (A) of Doppler signals, where blood hematocrit was in the range 4.5% to 46.5% and pressure head (H) varied from 60 cm. to 100 cm. of blood. A linear and a 2nd degree polynomial least squares were fit to the data. Table 3.9 lists the resulting equation together with coefficients of correlation and determination.

Figure 11-15 show the graphs of least squares linear and quadratic fittings which describe Doppler amplitude as a function of blood hematocrit. A 95% confidence interval about the coefficients for each of the linear equations is also included in each legend.

For the purpose of generalization, the effect of pressure

Table 3.7. Least Squares Polynomial Fitting Describing Hematocrit (\hat{H}) as a Function of Radius (r).

\hat{H} (%)	Resulting Equation	ξ	ϑ	ϵ
10	$\hat{H} = 2.1802 + .1248r - .020599r^2$.85	.72	.16
7	$\hat{H} = .91050 + .12542r - .018690r^2$.52	.27	.21
7	$\hat{H} = .54743 + .64649r - .18005r^2$ $+ .013447r^3$.79	.63	.17
7	$\hat{H} = .81022 + .069348r + .13228r^2$ $- .046627r^3 + .0037546r^4$.85	.71	.17
7	$\hat{H} = .028271 + 2.31138 - 1.6478r^2$ $+ .52372r^3 - .075371r^4$ $+ .0039564r^5$.97	.95	.09

Figure 9. Least squares polynomials of 2nd and 3rd degree fit describing the hematocrit of blood as a function of radius. Hematocrit was measured across the lumen of the vessel in steps of .1 cm., where 0 marks the top wall. Equations of the fitted curve are $\hat{H} = .91050 + .12542r - .018690r^2$ and $\hat{H} = .54743 + .64649r - .18005r^2 + .013447r^3$.

Pressure head and total blood hematocrit were 131 cm., and 7% respectively.

Brackets denote ± 1 standard error of the mean.

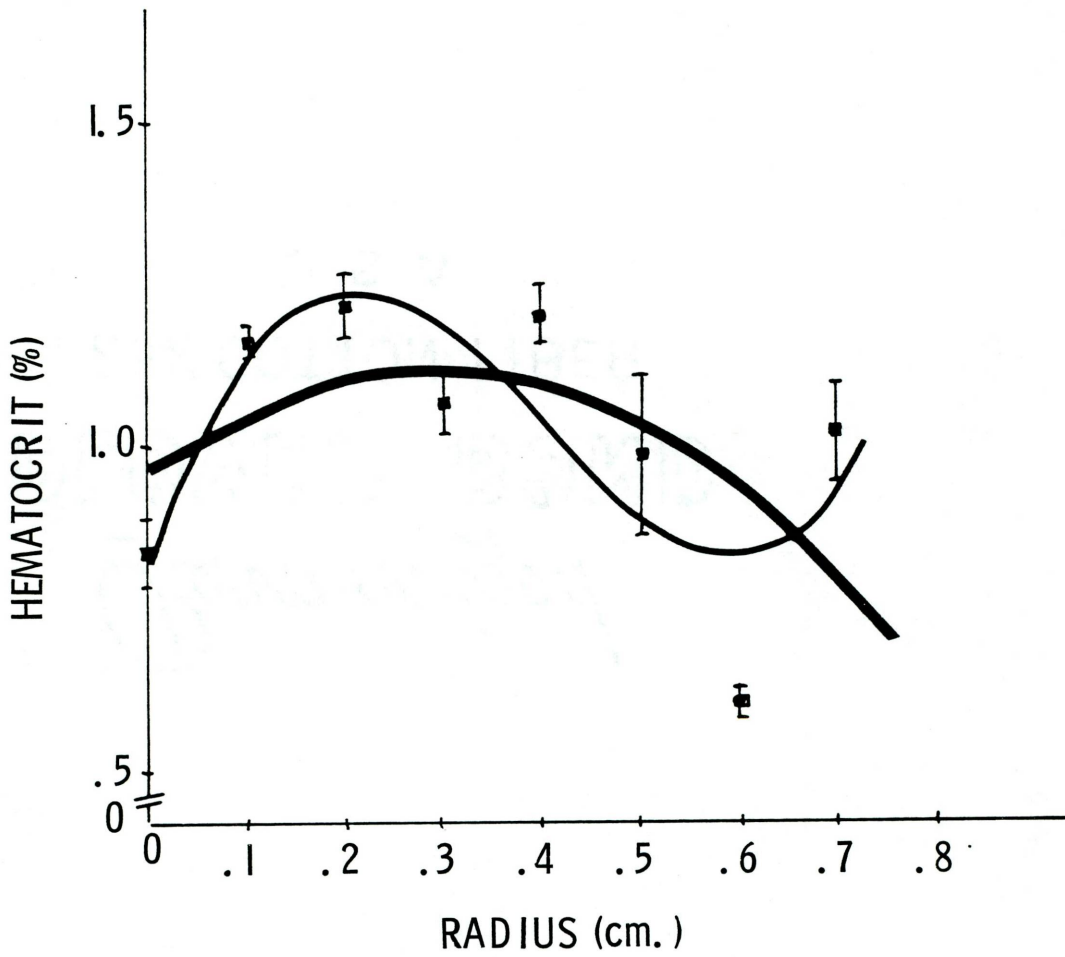


Figure 10. Least squares polynomials of 4th and 5th degree fit describing the hematocrit of blood as a function of radius. Hematocrit was measured across the lumen of rubber tubing at intervals of .1 cm., where 0 marks the top wall. Total blood hematocrit is 7%. Equations of the fitted curves are $\hat{H} = .81022 + .069348r + .13238r^2 - .046627r^3 + .0037546r^4$ and $\hat{H} = .028271 + 2.3113r - 1.6478r^2 + .52372r^3 - .075371r^4 + .0039564r^5$ respectively.

Brackets denote ± 1 standard error of the mean.

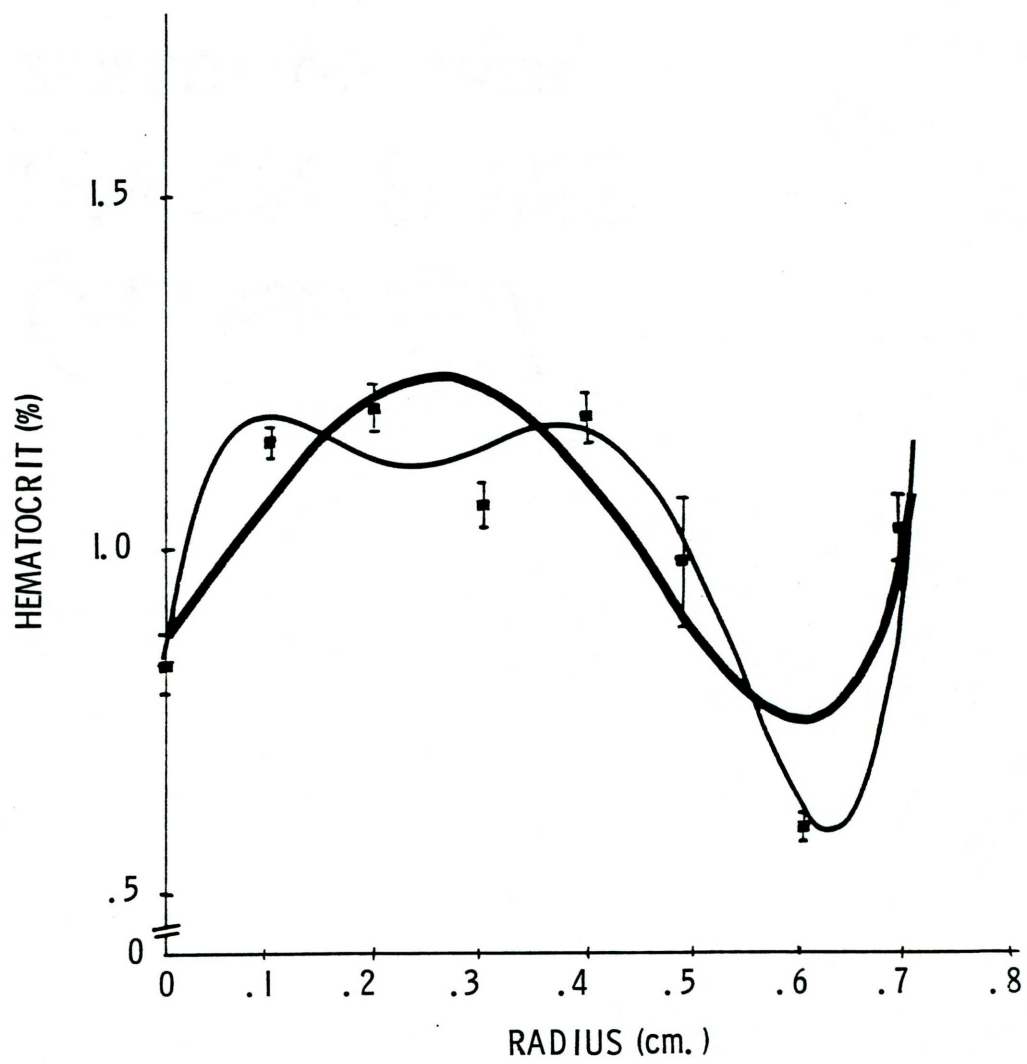


Table 3.8. Calculated Values of Mean Doppler Amplitude (A) for a Range of Blood Hematocrits (\hat{H}) Under a Given Pressure Head (H).

H (cm)	A		A		A		A		A	
	A	\pm SEM	A	\pm SEM	A	\pm SEM	A	\pm SEM	A	\pm SEM
4.5	23.3	.43	22.5	.12	22.7	.63	24.6	.20	23.5	.088
7.0	23.6	.61	21.5	.93	20.1	.79	23.1	.22	22.7	.73
10.0	23.6	1.21	24.0	.79	23.5	1.06	21.8	.033	23.1	.95
14.5	22.6	.52	20.7	.59	23.3	.58	20.0	1.26	20.3	.23
19.5	22.7	.53	25.3	1.21	21.6	.24	24.2	.50	23.3	.62
24.0	24.5	.71	23.3	.27	23.4	.28	24.0	2.19	23.8	.92
29.0	23.8	.94	24.4	.61	25.8	.74	23.4	.66	21.2	.25
34.0	23.8	.45	24.8	1.25	24.5	.85	26.2	.81	24.1	2.42
40.0	28.2	1.54	27.2	.32	28.1	1.16	23.2	2.73	26.1	1.52
46.5	26.3	1.78	27.6	.94	27.1	.68	30.0	1.11	28.0	.59

Table 3.9. Linear and Quadratic Least Squares Equations Describing Doppler Amplitude (A) as a Function of Blood Hematocrit (H).

<u>H (cm)</u>	<u>Resulting Equation</u>	<u>ξ</u>	<u>γ</u>
60	$A = 22.213 + .088492 \hat{H}$.73	.53
70	$A = 21.150 + .13014 \hat{H}$.83	.69
80	$A = 20.724 + .14348 \hat{H}$.84	.71
90	$A = 21.411 + .11521 \hat{H}$.62	.38
100	$A = 21.271 + .10214 \hat{H}$.66	.44
.....			
60	$A = 23.729 - .088839 \hat{H} + .0035878 \hat{H}^2$.81	.65
70	$A = 22.107 + .018173 \hat{H} + .0022653 \hat{H}^2$.85	.72
80	$A = 21.523 + .050031 \hat{H} + .0018906 \hat{H}^2$.85	.72
90	$A = 24.407 - .23528 \hat{H} + .0070912 \hat{H}^2$.77	.59
100	$A = 24.346 - .25776 \hat{H} + .0072817 \hat{H}^2$.87	.74

Figure 11. Doppler amplitude (A) as a function of blood hematocrit (\hat{H}) as described by a least squares linear fit and a polynomial of 2nd degree fit. Points in the plot represent an average of 3 measurements. Pressure head for the steady flow equals 60 cm. Equations of the fitted curves are $A = 22.213 + .088492 \hat{H}$ and $A = 23.729 - .088839\hat{H} + .0035878\hat{H}^2$ respectively.

Ninety-five percent confidence intervals about the coefficients of linear regression are (20.41776, 24.00824) and (.02110, .15590).

Brackets denote ± 1 standard error of the mean.

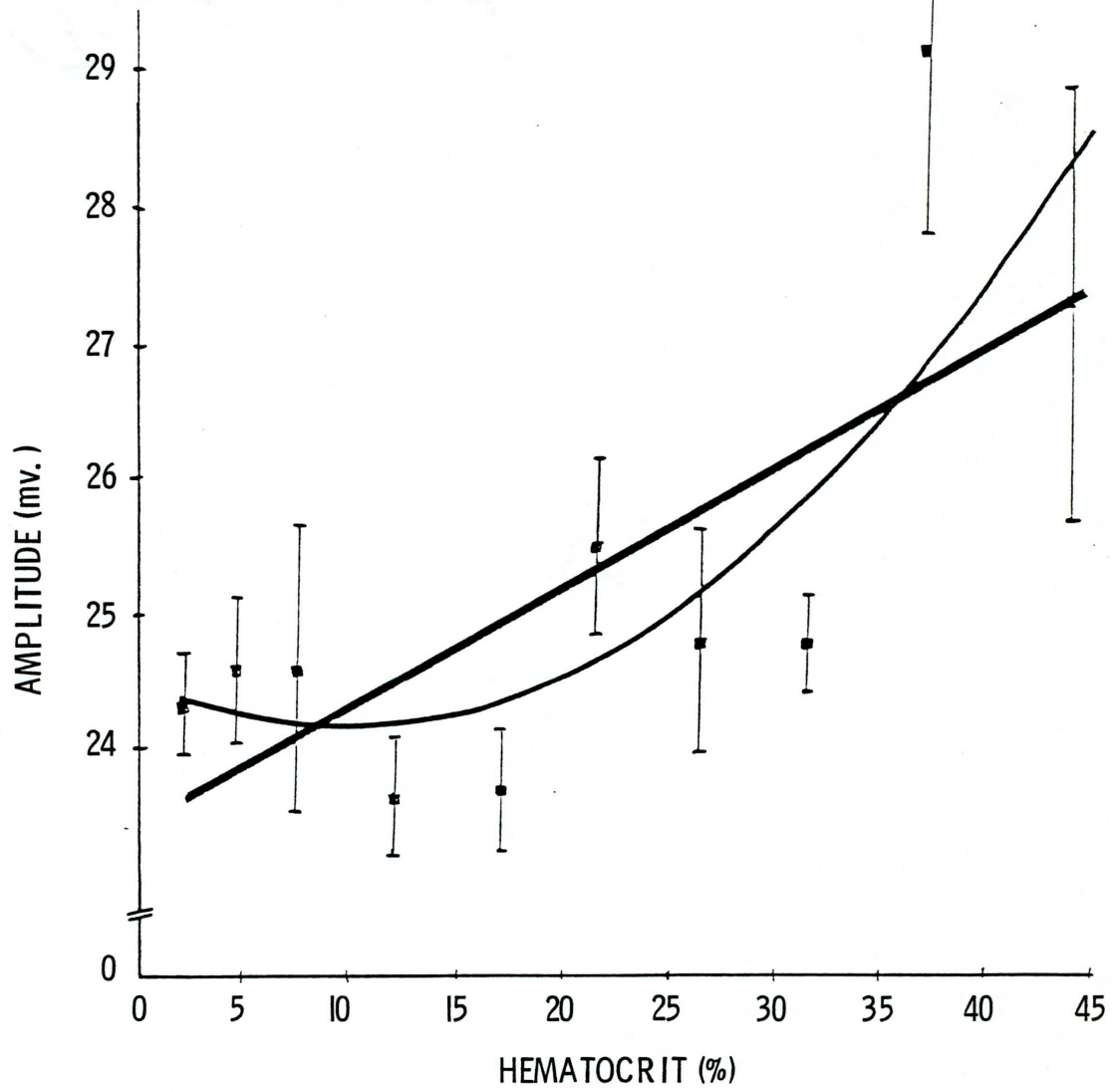


Figure 12. Linear and 2nd degree polynomial least squares fit describing Doppler amplitude (A) as a function of blood hematocrit (\hat{H}). Points in the plot are average of 3 measurements. Pressure head for the steady flow is equal to 70 cm. Equation of the fitted curves are $A = 21.150 + .13014\hat{H}$ and $A = 22.107 + .018173\hat{H} + .0022653 \hat{H}^2$ respectively.

Ninety-five percent confidence intervals about the coefficients of linear regression equation are (19.25744,23.04196) and (.05909,.20118).

Brackets denote ± 1 standard error of the mean.

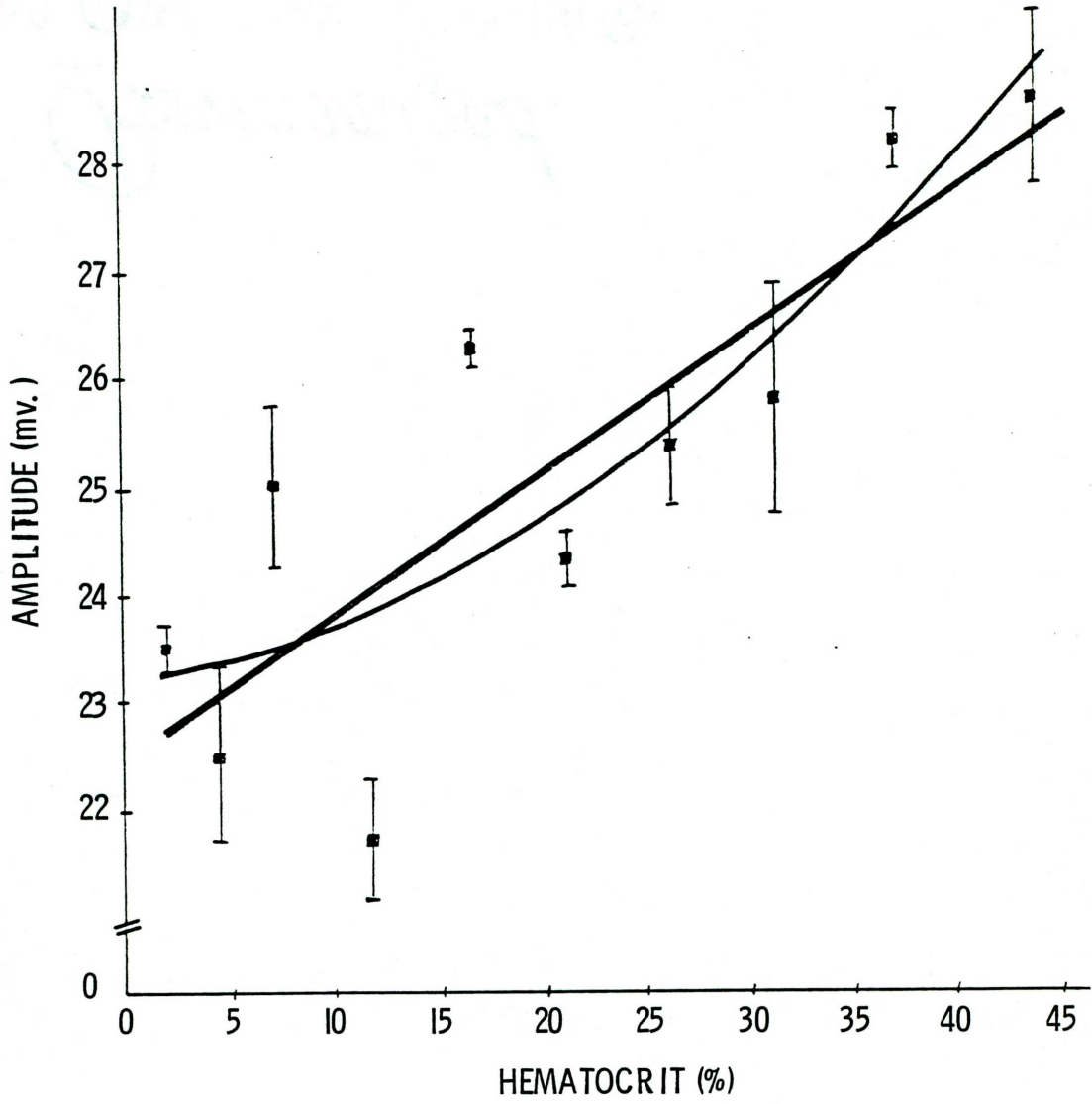


Figure 13. Linear and 2nd degree polynomial least squares fit describing Doppler amplitude (A) as a function of blood hematocrit (\hat{H}). Points in the plot are average of 3 measurements. Pressure head for the steady flow equals 80 cm. Equations of the fitted curves are $A = 20.724 + .14348\hat{H}$ and $A = 21.523 + .050031\hat{H} + .0018906\hat{H}^2$ respectively.

Ninety-five percent confidence intervals about the coefficients of linear regression equation are (18.73245,22.71555) and (.06872,.21824).

Brackets denote ± 1 standard error of the mean.

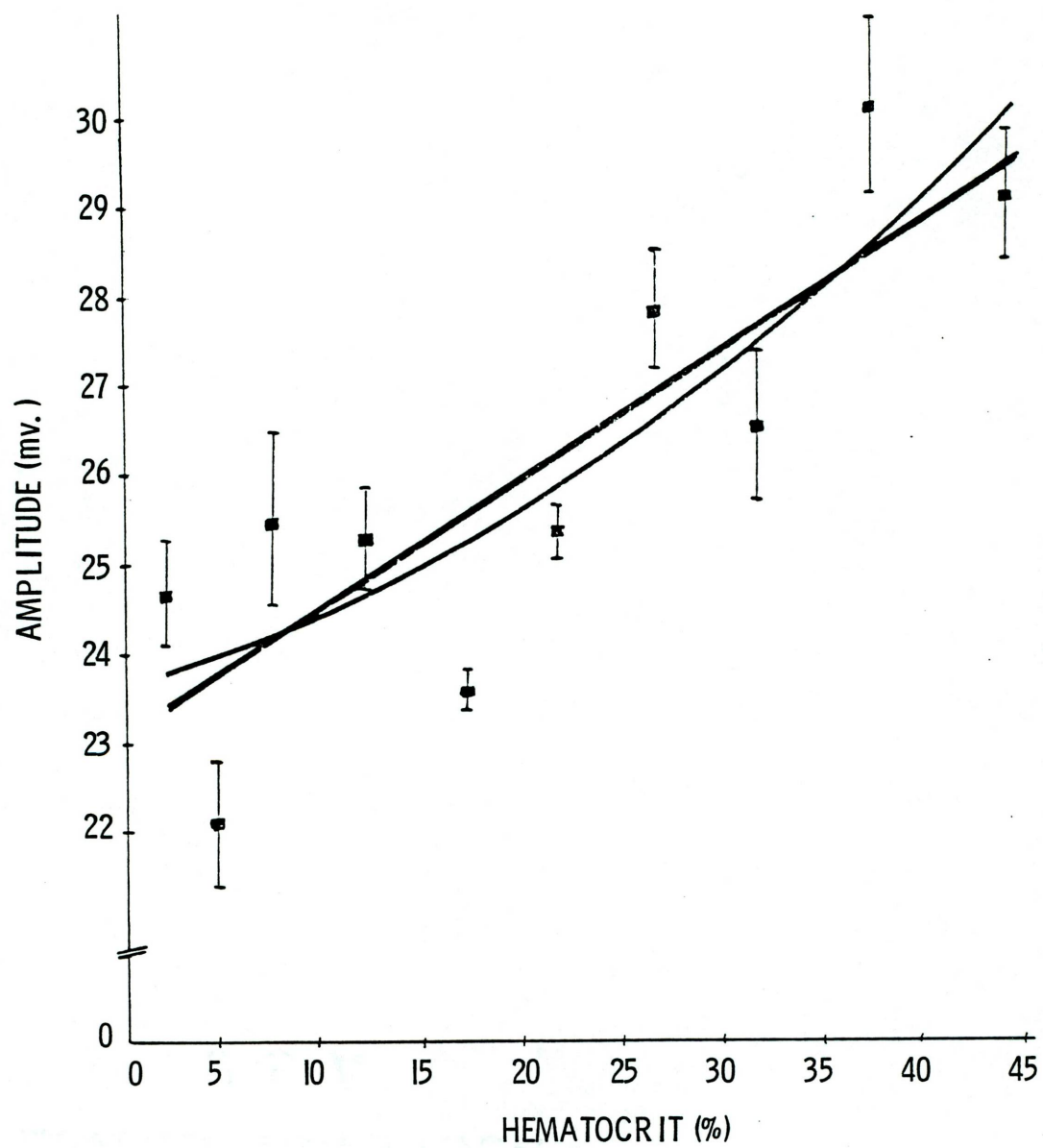


Figure 14. Linear and 2nd degree polynomial least squares fit describing Doppler amplitude (A) as a function of blood hematocrit (\hat{H}). Points in the plot are average of 3 measurements. Pressure head for the steady flow is equal to 90 cm. Equations of the fitted curves are $A = 21.411 + .11521\hat{H}$ and $A = 24.407 - .23528 \hat{H} + .0070912\hat{H}^2$ respectively.

Ninety-five confidence intervals about the coefficients of linear regression equation are (18.24673, 24.57527) and (-.00360, .23402).

Brackets denote ± 1 standard error of the mean.

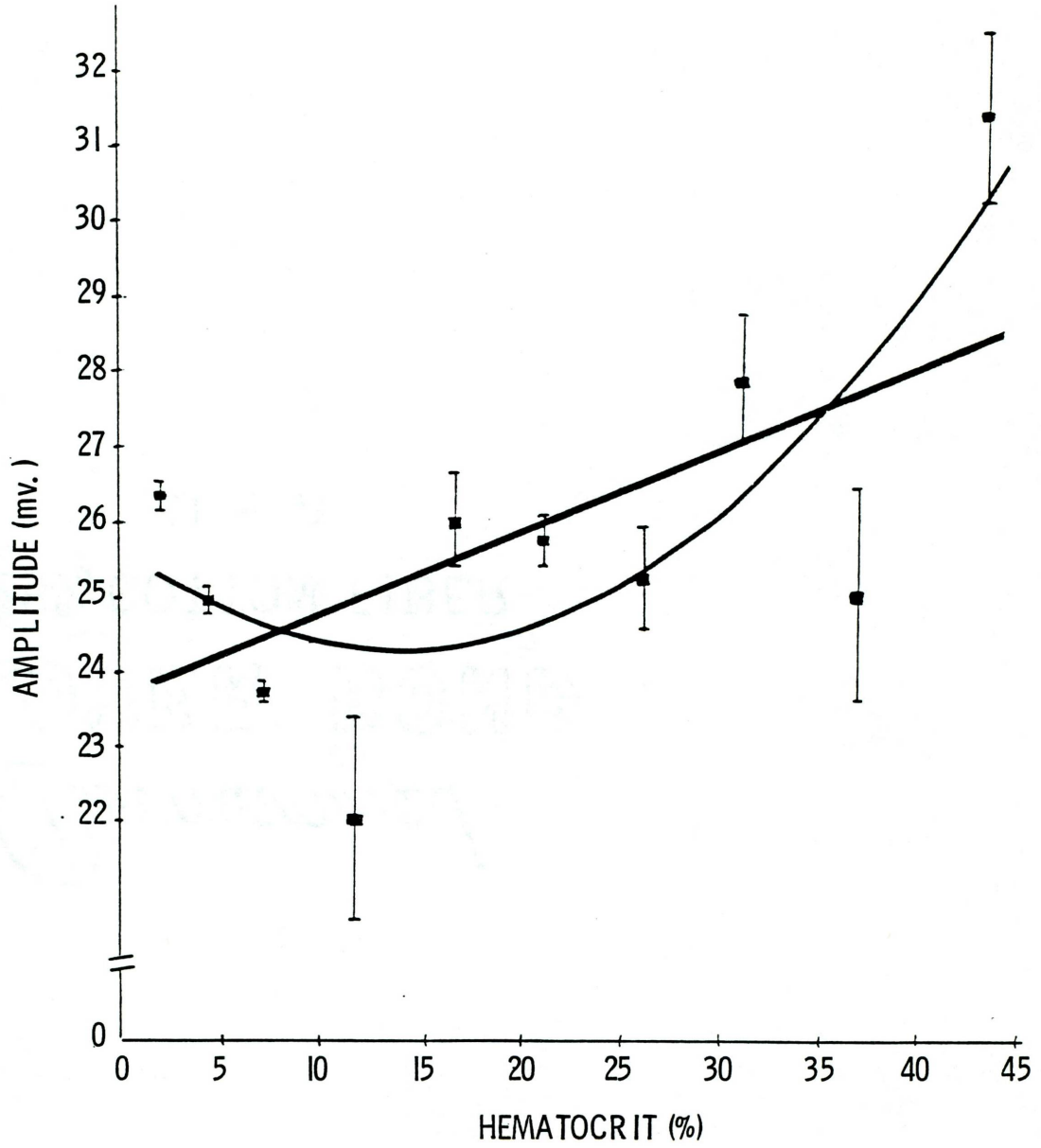
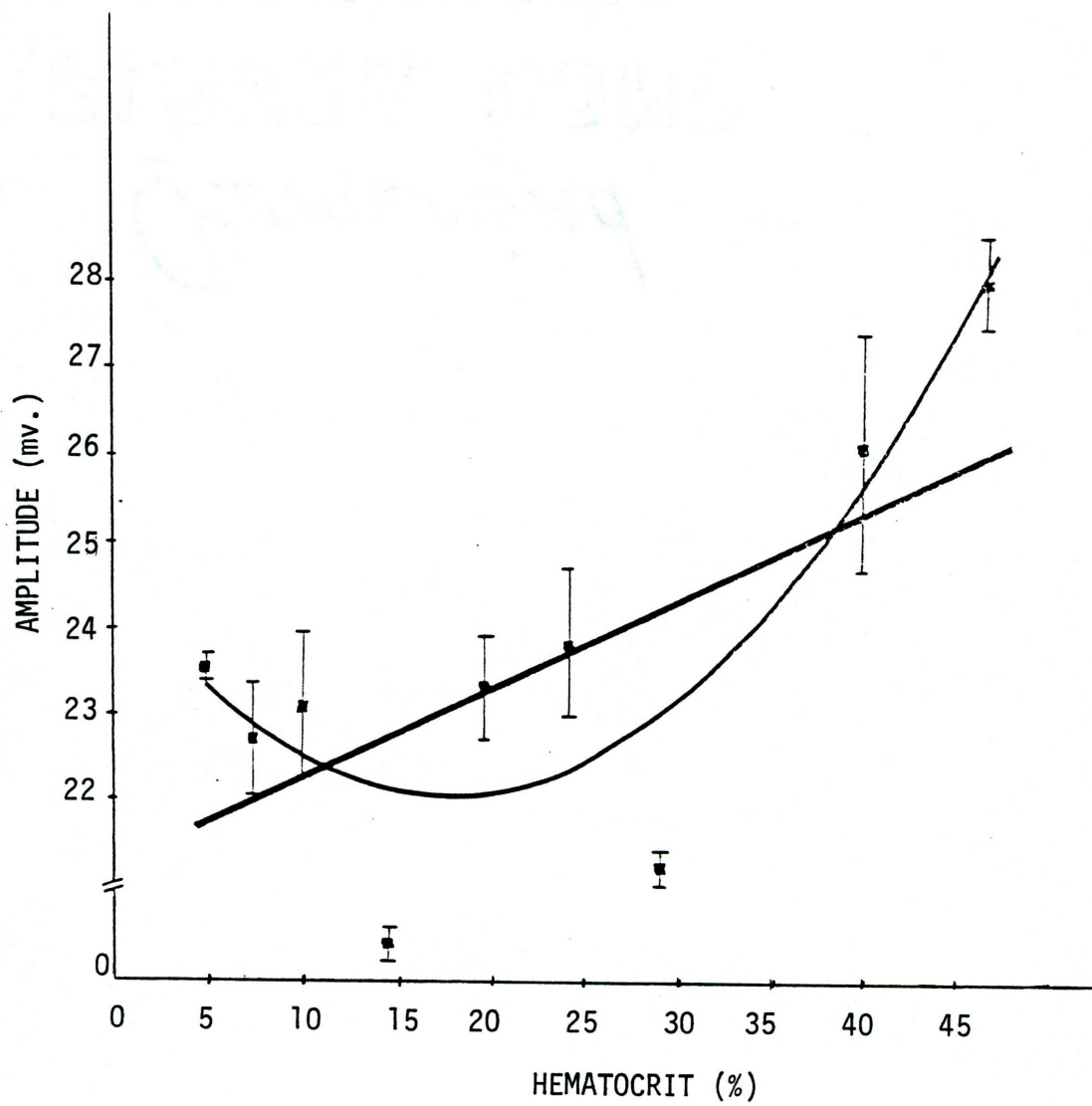


Figure 15. Linear and 2nd degree polynomial least squares fit describing Doppler amplitude (A) as a function of blood hematocrit (\hat{H}). Points in the plot represent an average of 3 measurements. Pressure head for the steady flow equals 100 cm. Equations of the fitted curves are $A = 21.271 + .10214\hat{H}$ and $A = 24.346 - .25776\hat{H} + .0072817\hat{H}^2$ respectively.

Ninety-five percent confidence intervals about the coefficients of linear regression equation are (18.77768,23.76432) and (.0085348,.19575).

Brackets denote ± 1 standard error of the mean.



head on the amplitude of the Doppler must also be taken into account. Because blood hematocrit and pressure head are the independent variables, and the Doppler amplitude the dependent variable, a multiple linear regression was used on the data.

The following equation was obtained:

$$A(H, \hat{H}) = 23.154 - .021200 H + .10794 \hat{H} \quad (3.6)$$

where the coefficient of multiple correlation was .69 and standard error of estimate 1.6.

A confidence interval for the coefficients of the least squares plane was constructed according to the equations (22):

$$\bar{Y} \pm t_{1-\alpha/2} (S_e^2/n)^{1/2} \quad (3.7)$$

$$b_1 \pm t_{1-\alpha/2} (C_{11} S_e^2)^{1/2}$$

$$b_2 \pm t_{1-\alpha/2} (C_{22} S_e^2)^{1/2}$$

where

$$S_e^2 = (\Sigma y^2 - b_1 \Sigma x_1 y - b_2 \Sigma x_2 y) / (n-3) \quad (3.8)$$

C_{11} and C_{22} were calculated from the system of equations:

$$(\Sigma x_1^2) C_{11} + (\Sigma x_1 x_2) C_{12} = 1 \quad (3.9)$$

$$(\Sigma x_1 x_2) C_{11} + (\Sigma x_2^2) C_{12} = 0$$

$$(\Sigma x_1^2) C_{21} + (\Sigma x_1 x_2) C_{22} = 0 \quad (3.10)$$

$$(\Sigma x_1 x_2) C_{21} + (\Sigma x_2^2) C_{22} = 1$$

The desired 95% confidence intervals obtained were as follows:

$23.93 \pm 2.012 (592.0875/50)^{1/2}$, $-.021200 \pm 2.012 [(.000010698)(592.0875)]^{1/2}$, and $.10794 \pm 2.012 [(.000099507)(592.0875)]^{1/2}$ respectively. Using interval notations, these can also be written as (17.00634,30.85366),(-.18133),.13893), and (-.38043,.59631).

Figures 16-19 show plots of Fourier transformed data in the time domain and in frequency domain.

Functional Relationship of Blood Viscosity and Blood Hematocrit

Using a falling ball type viscosimeter, time of descent was measured for a blood of specified hematocrit, where room temperature was 26°C. Table 3.10 displays the measured values of descent time (t) expressed in minutes, as well as calculated values of blood viscosity (μ) in centipoise (c.p.) and blood density (ρ) in gm/cm³ for a given hematocrit (\hat{H}).

At 26°C, the viscosity of water is listed as .8705 c.p. (75).

Exponential, geometric, and polynomial of 2nd degree least squares fitting were applied to the data. The results are shown in Table 3.11. The graph of exponential least squares fitting, described by the equation:

$$\mu = .78256e^{.026521\hat{H}}, \quad (3.11)$$

is shown in Figure 20.

A 95% confidence interval for coefficients of the exponential function was constructed by taking the logarithms of the equation 3.11 and then treating it as a linear regression equation. The confidence intervals are: (.74354,.813760) and (.02433,.02871).

Figure 16. Time-domain representation of 8 windows of Fourier transformed data, obtained from digitized Doppler signals. Steady-laminar flow attained by a pressure head equal to 60 cm., where total blood hematocrit was 24%, 29%, 34%, 40%, and 46.5%.

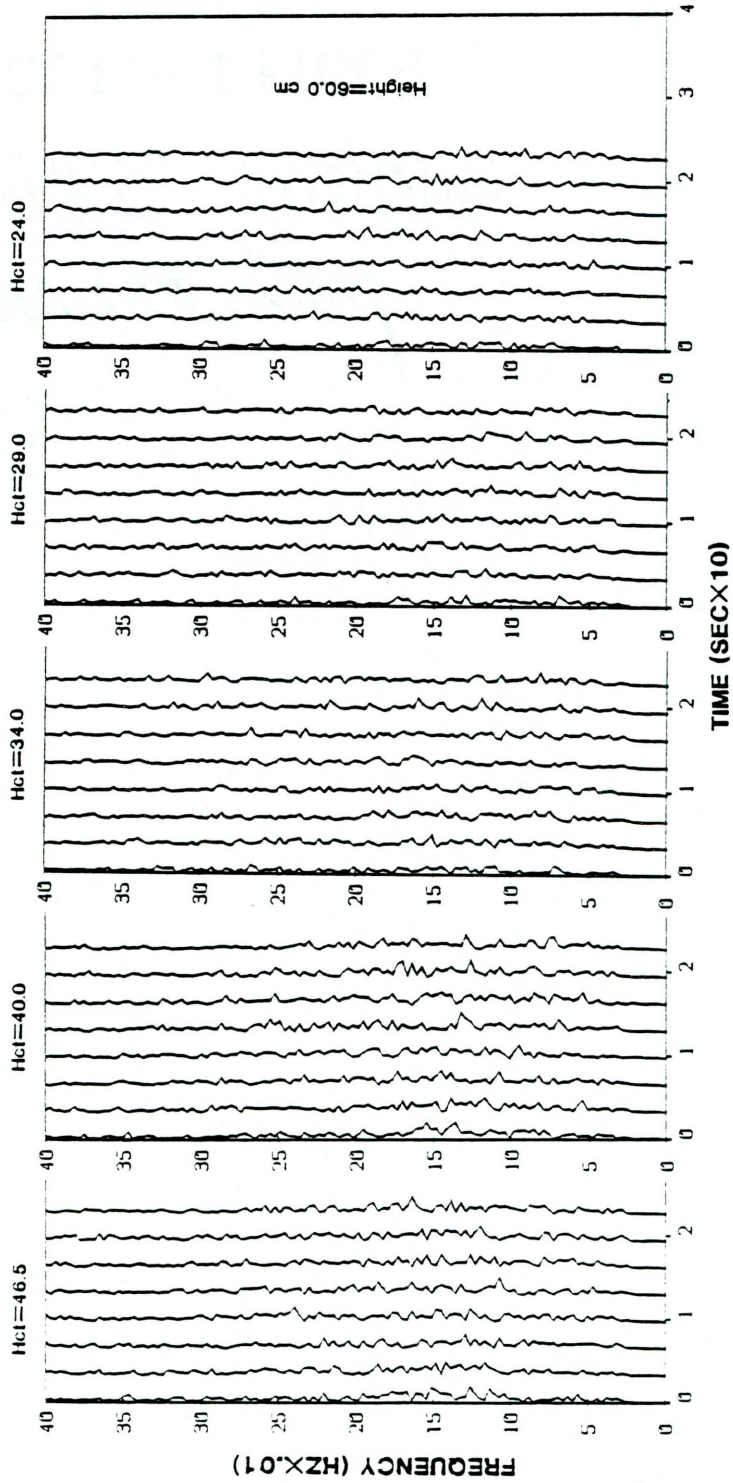


Figure 17. Time-domain representation of 8 windows of Fourier transformed data, which is obtained from digitized Doppler signals. Steady-laminar flow maintained by means of pressure head equalling 60 cm., where total blood hematocrit was 4.5%, 7%, 10%, 14.5%, and 19.5%.

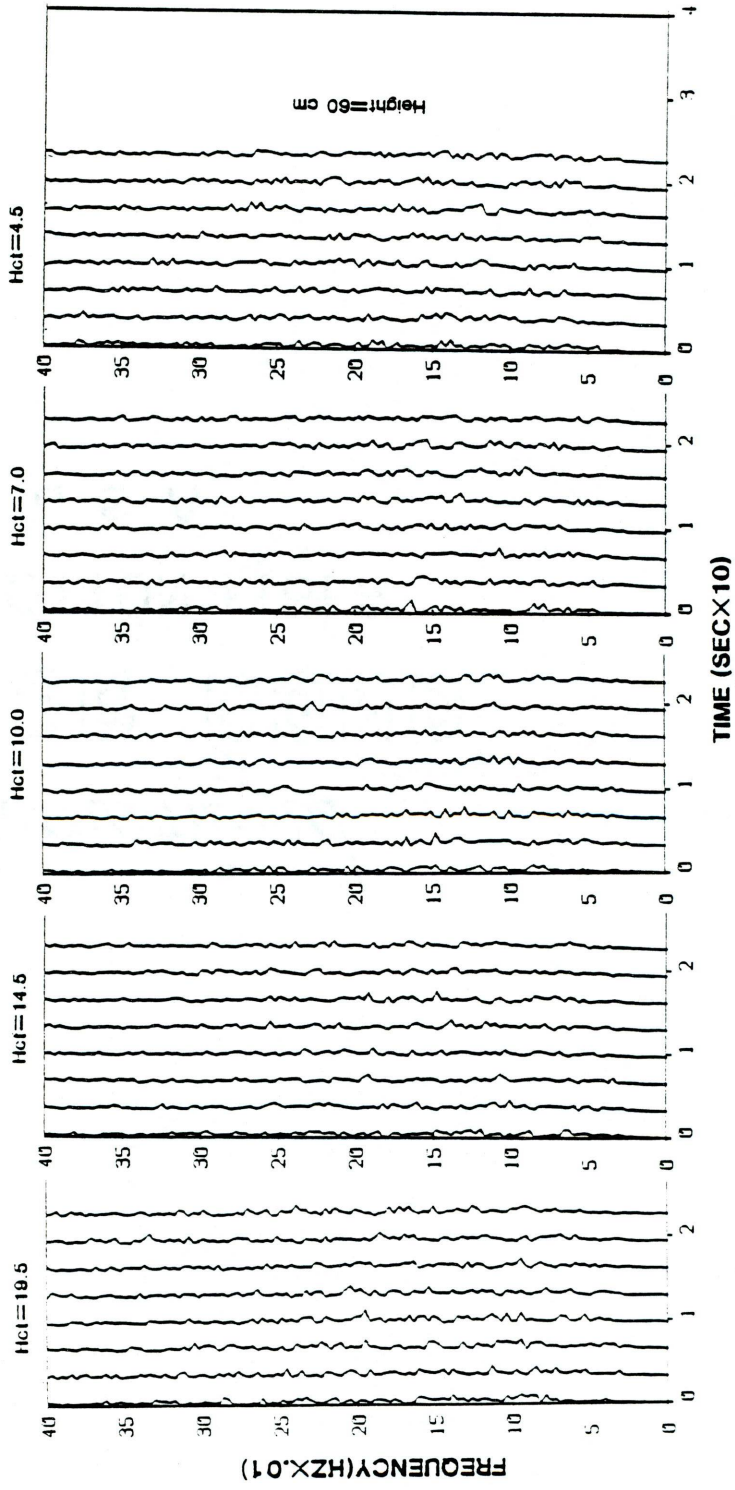


Figure 18. Frequency domain representation of Fourier transformed data (Window 1) obtained from digitized Doppler signals. Blood hematocrit was 40% and pressure head was 60 cm.

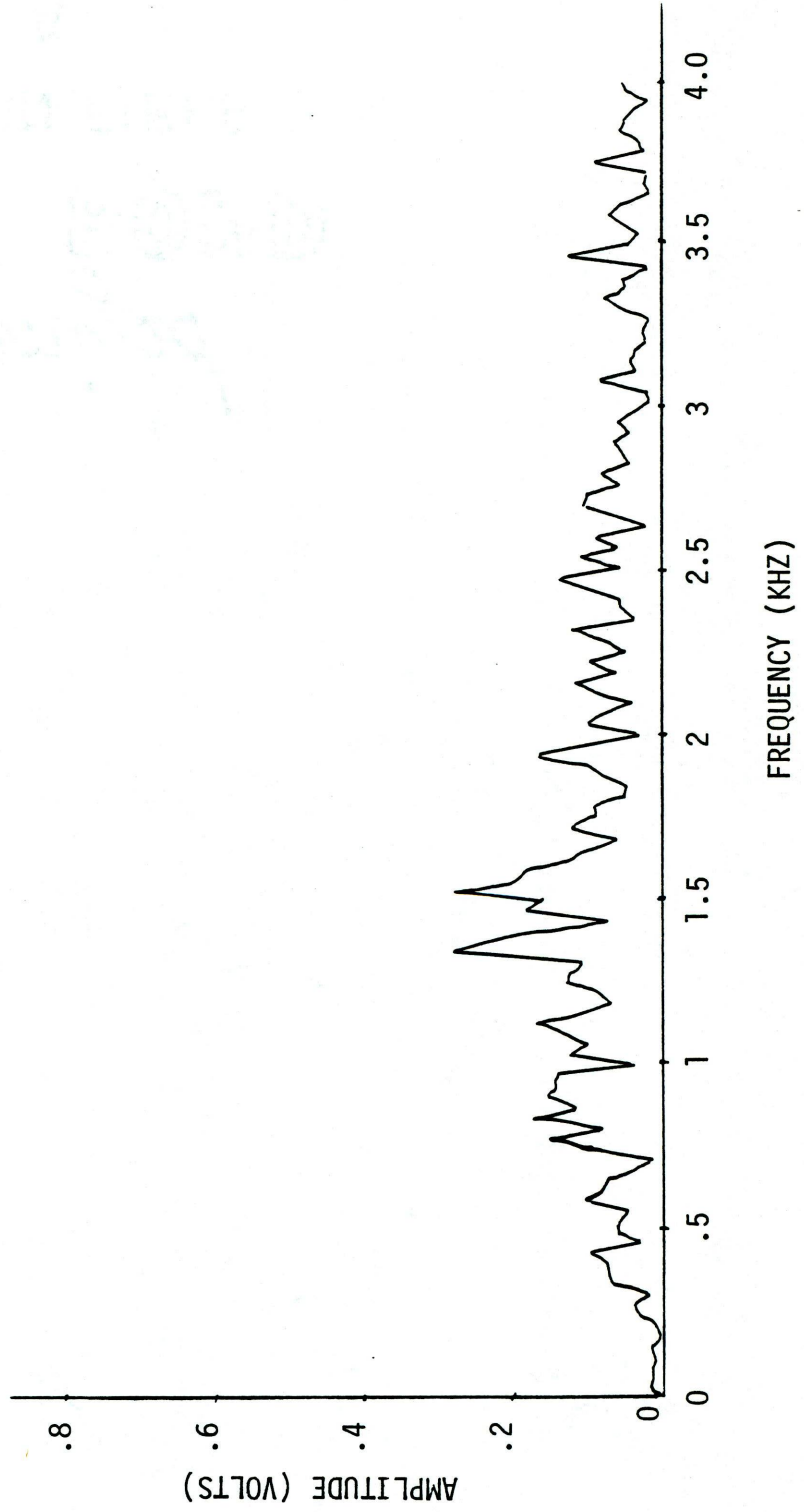


Figure 19. Frequency domain representation of Fourier transformed data (Window 1) obtained from digitized Doppler signals. Blood hematocrit was 4.5% and pressure head was 60 cm.

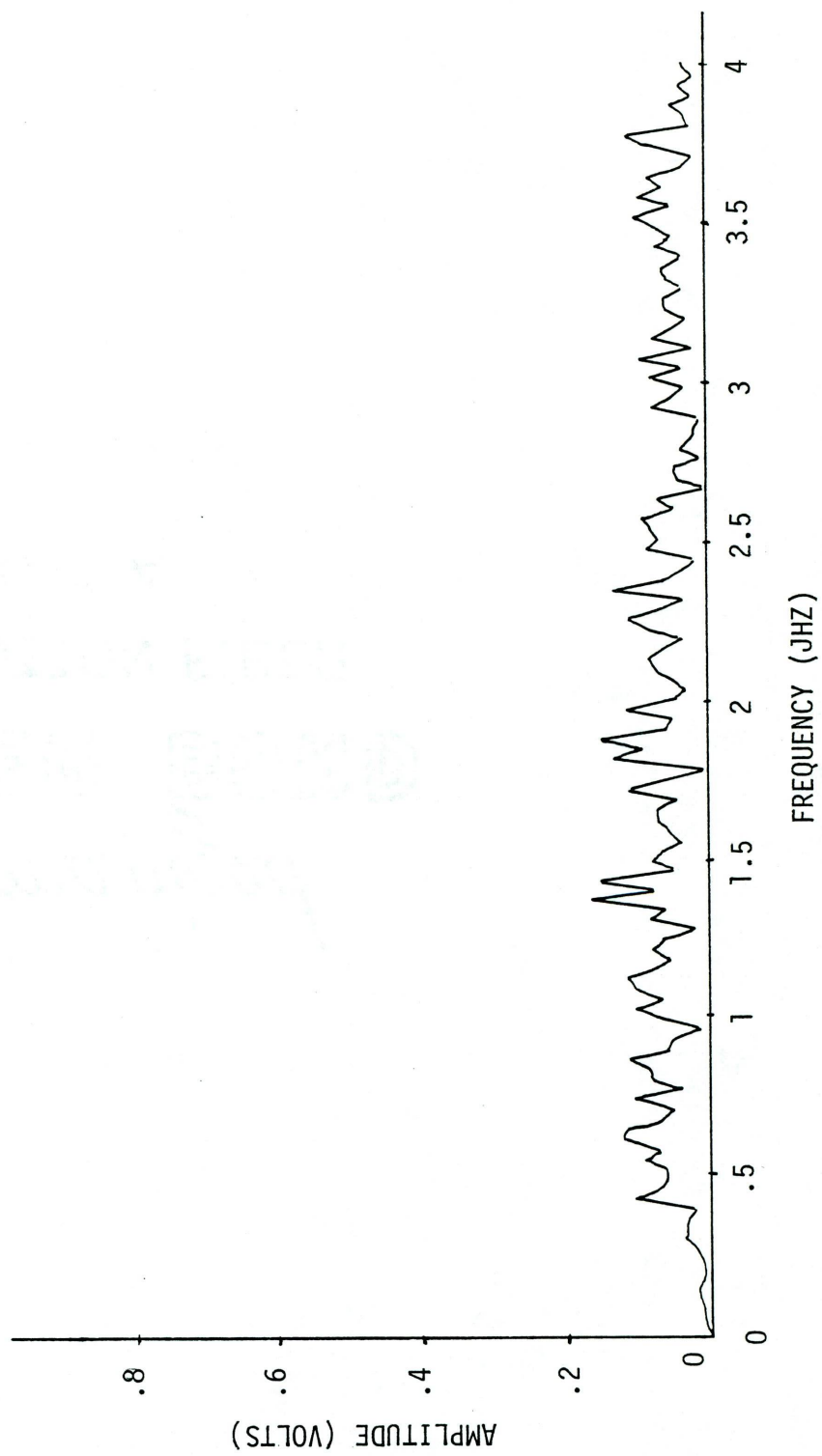


Table 3.10. Measured Values of Descent Time (t), Blood Density (ρ) and Blood Viscosity (μ) for a Given Hematocrit (\hat{H}). Each Value of μ is an Average of 3 Trials.

\hat{H} (%)	t (min)	ρ (gm/cm ³)	μ (c.p.)	\pm SEM
29.7	.8350	1.0217	1.7163	.00052
26.7	.7917	1.01815	1.6281	.00048
22.5	.6850	1.0149	1.4094	.00025
17.9	.5983	1.0129	1.2313	.00029
13.3	.5350	1.0086	1.1017	.00025
10.0	.4950	1.0003	1.0206	.00025
7.0	.4650	.9956	.9593	.00038

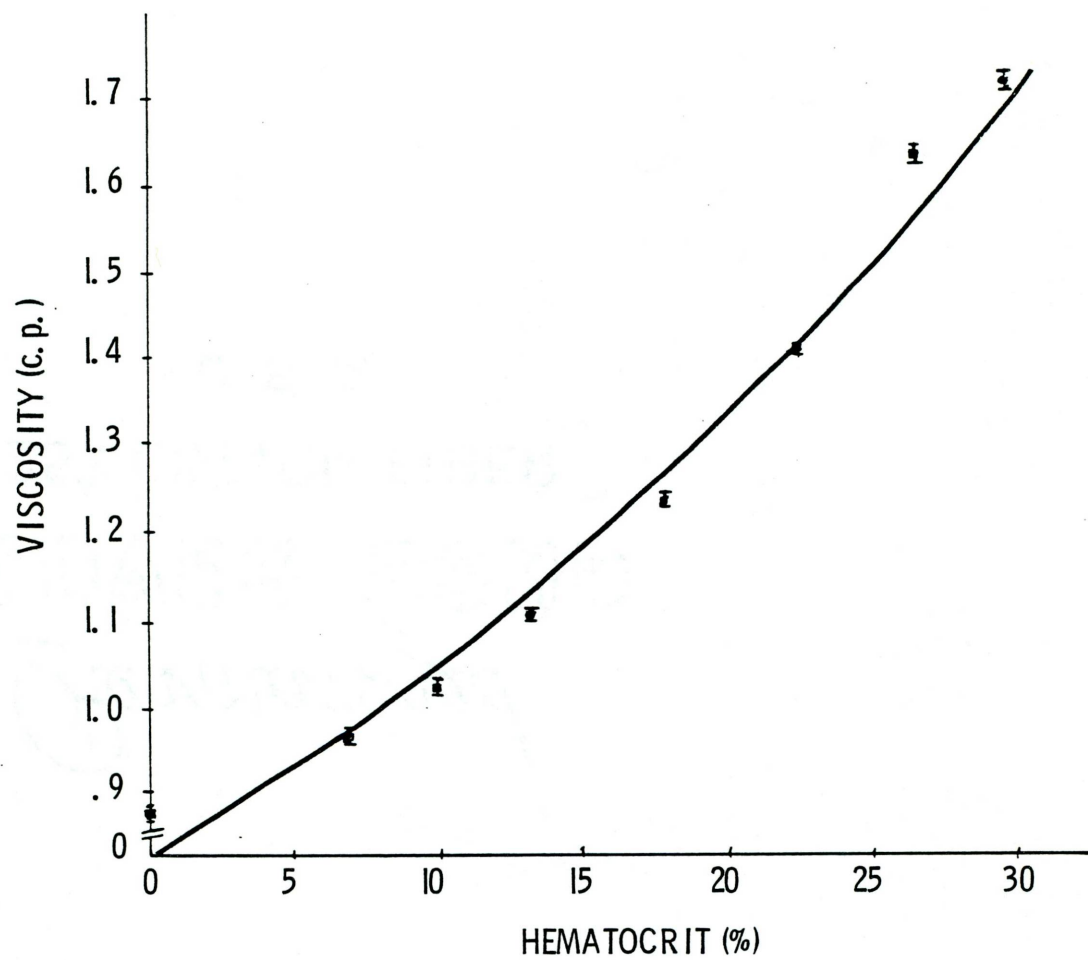
Table 3.11. Least Squares Equations Describing Viscosity (μ) as a Function of Hematocrit (\hat{H}).

<u>Least Squares Method Used</u>	<u>Resulting Equation</u>	<u>ξ</u>	<u>γ</u>	<u>ϵ</u>
Exponential	$\mu = .78256e^{.026521\hat{H}}$.99	.99	.018
Geometric	$\mu = .40044 (\hat{H})^{.41316}$.97	.94	.061
2nd Degree Polynomial	$\mu = .85830 + .0092583\hat{H} + .00068494\hat{H}^2$.99	.99	.021

Figure 20. Exponential least squares fit describing blood viscosity (μ) as a function of blood hematocrit (H). Points in the plot are average of 3 measurements. Equation of the fitted curve is $\mu = .78256 \exp (.026521H)$.

Ninety-five percent confidence intervals about the coefficients of the exponential function are (.74534, .813760) and (.02433, .02871).

Brackets denote ± 1 standard error of the mean.



CHAPTER 4

DISCUSSION

Functional Relationship of Doppler Flow and Electromagnetic Flow.

Because electromagnetic flowmeter has been used for a long time, it is considered as the standard for evaluation of all varieties of ultrasonic flowmeters (59,73). The accuracy of the Doppler flowmeter technique is satisfactory if a good linear relation can be found between the known flow, as derived by the electromagnetic flowmeter (\dot{Q}_e) and the flow, ultrasonically derived (\dot{Q}_d).

The following discussion pertains to evaluation of the Doppler flowmeter by other investigators. S.F. Vatner, et al., compared the output of both flowmeters and concluded that the contours of the simultaneous analog waveforms were similar over a wide range of volume flows (73). They graphed the output of each flowmeter as a function of volume flow. However, they did not derive \dot{Q}_d as a function of \dot{Q}_e . J.R. Haywood, et al., tested the validity of the pulsed Doppler flowmeter by making a simultaneous comparison of electromagnetic and Doppler responses (43). They noted that a linear relationship exists between electromagnetic and Doppler flow measurements and concluded that their individual regression lines for several experiments were consistent. They did not use analysis of covariance in order to test for adjustment (removal) of the extraneous effect of pressure head. Guldvog, et al., compared blood flow measured transcutaneously in dog arteries by the use of a pulsed ultrasound Doppler equipment with blood flow as measured simultaneously by an electromagnetic flowmeter applied on the exposed vessels (40). They obtained a good fit between ultrasound velocity

measurements and the electromagnetic flow measurements, and concluded that the output from the ultrasound equipment is proportional to flow as measured by the electromagnetic flowmeter.

My results indicate that for various rates of flow, a very good linear relation exists between the \dot{Q}_e and the \dot{Q}_d . Thus, I can conclude that the Doppler flowmeter used in all my experiments is reliable and accurate. The analysis of covariance was used in order to further strengthen this idea. It showed that a good linear relationship exists between measurements of \dot{Q}_e and \dot{Q}_d over all rates of flow. The regression line should have passed through the origin based on deductions from physical principles. The linear regression line which adequately described all rates of flow was given by:

$$\dot{Q}_d = 113.69 + .51428\dot{Q}_e$$

A nonzero intersect may be possible due to:

1. Orientation of Doppler probe to the vessel in each experiment.
2. The coupling medium between Doppler probe and vessel and the requirement of a close fit for electromagnetic probe around the dialysis tubing without actually compressing it.
3. Both transducers must be identical in size, otherwise a perfect linear relation may be difficult to find.
4. Intrinsic characteristics of each probe.

A Quantitative Study of Simultaneous Influence of Pressure Head and Hematocrit Upon Velocity of Blood Flow.

Two important parameters in my steady, laminar flow experiments are the hematocrit and the pressure head of blood.

Poiseuille's equation:

$$\dot{Q} = (\pi r^4 \Delta P) / (8L\mu) \quad (4.2)$$

asserts that flow is proportional to pressure gradient, which for a tube with uniform radius may be determined from the difference between inlet and outlet pressures divided by the tube length (14,26,41). The average velocity of flow times the cross sectional area of the tube equals the flow (26):

$$\therefore \dot{Q} = \bar{v} \cdot A \quad (4.3)$$

Equations 4.2 and 4.3 together imply that an increase in pressure head results in an increase in average velocity of flow.

Another way of looking at this is by considering the maximum velocity at the central axis of the tube, which is expressed by the following equation:

$$v_{\max} = (\Delta P / 4L\mu) r^2$$

Then, the average velocity is $1/2 v_{\max}$ (26). From this it can simply be stated that head pressure is positively correlated with average velocity.

The resistance to flow of blood is due to friction between adjacent laminae of blood, that is, the inner friction, or viscosity (14). Equation 4.2 asserts that flow is inversely proportional to viscosity and,

since hematocrit is the principle factor in blood viscosity, it can be said that hematocrit is negatively correlated with average velocity.

Due to the fact that hematocrit (\hat{H}) and pressure head (H) constitute two independent variables influencing the average velocity (v), multiple linear regression was used on the data.

The equation:

$$v = 59.879 + .74538H - 1.5053\hat{H} \quad (4.4)$$

obtained by using multiple regression, shows the simultaneous influence of H and \hat{H} in quantitative terms.

Equation 4.4 reveals that my experimental findings are in agreement with theoretical results explained above. More importantly, it gives a measure of the weight of each of these variables \hat{H} and H upon v. Equation 4.4 indicates that the negative influence of the \hat{H} upon average velocity is almost twice as great as the positive influence of H.

This finding implies that blood hematocrit may indeed influence the amplitude of the Doppler signals backscattered from blood.

Velocity-Hematocrit Correlation

Distribution of Particle Velocity

First of all, it is necessary to discuss in some detail how a pitot tube system can be used to measure the instantaneous velocity of blood flow.

Consider Bernoulli's equation for a steady, incompressible flow along a streamline (33):

$$P/\rho + 1/2 v^2 + g Z = \text{Const.} \quad (4.5)$$

where P is the pressure, v the velocity, ρ the density, g the acceleration due to gravity, and Z the elevation component.

Equation 4.5 relates pressure changes to velocity and gives elevation changes along a streamline. The pressure P is called the static pressure. Experimentally, static pressure is measured in a flowing fluid with a wall pressure tap. In order to achieve this, I placed a narrow straight tube through the rubber tubing with its axis perpendicular to the wall.

Because the flow is incompressible, elevation differences can be neglected and Equation 4.5 is reduced to:

$$P/\rho + \frac{1}{2} v^2 = \text{Const.} \quad (4.6)$$

Equation 4.6 can be applied between any two arbitrary points (in radial direction) in the system. This gives rise to:

$$P_0/\rho + \frac{1}{2} v_0^2 = P_1/\rho + \frac{1}{2} v_1^2 \quad (4.7)$$

In particular, if P_0 is that value obtained when a flowing fluid is decelerated to zero velocity (in my experiments, it would be at the wall), then Equation 4.7 is reduced to:

$$P_0 = P_1 + \frac{1}{2} \rho v_1^2 \quad (4.8)$$

Equation 4.8 can be rewritten in terms of velocity:

$$v = \sqrt{2(P_0 - P)/\rho} \quad (4.9)$$

The pressure P_0 is called the stagnation pressure, which can be measured by a probe with a hole that faces directly upstream. Such a probe is referred to as a stagnation pressure probe, or a

pitot tube. With the measurement of static and stagnation pressure at a point, the instantaneous flow velocity can be calculated. The importance of the velocity profile measurement is twofold, first, because a parabolic velocity profile is assumed, and second, because the velocity profile varies from vessel to vessel.

Velocity measurement is a technique to measure flow characteristics within vessels. The characteristics of the movement of red blood corpuscles (RBC's) are important in understanding the nature of the Doppler signals. In laminar flow, the velocity components of RBC's are axial, as will be explained later in Section 3. In steady flow, where time is invariant, the velocity profile or the distribution of particle velocities ($V(r)$) across the vessel lumen can be described by a parabola.

Model predictions for the CW Doppler flowmeter are based on the assumption of parabolic velocity profile, and under this assumption specific predictions can be made regarding the shape of the spectrum (6,11). W.R. Brody points out that an independent velocity profile measurement is necessary because changes appearing in the spectral shape are believed to be caused by a change in velocity profile (10). Since observed spectra vary with average flow rate, it can be concluded that the velocity profile changes with flow rate, and the assumption of a parabolic velocity profile may not be realistic. Brody suggests that the pulsed Doppler flowmeter provides a technique for the measurement of velocity profile. F. Mahler, et al., also lend support in this respect, and

remark that integration of the velocity profile over the cross-sectional area of the vessel will give volume flow (49). In a similar fashion, P.J. Fish points out that the flow is calculated assuming a uniform velocity within a semi-annulus of the vessel. The flow through the semi-annulus is equal to the velocity times the cross-sectional area of the annulus, and the total flow through the vessel is calculated by summing the flows through the individual annuli (20).

Other investigators have employed expensive and sophisticated instruments to determine the instantaneous velocity of blood flow. For example, S. Einav, et al., measured velocity at about 10 distinct sample locations across the vessel diameter by means of laser Doppler anemometry (LDA) (23). They reported that velocities were greatest at the center of the vessel, and, in general, were parabolic in shape. An increase in vessel diameter led to the blunting of the parabolic velocity. G. Tomonaga, et al., used laser Doppler velocimeter (LDV) with an optical fiber to measure point velocity in the coronary artery. The fiber tip was inserted into the artery and was traversed stepwise from the near to the far wall of the lumen (72). However, the practical application of the LDV has been restricted to the measurement of the flow velocity within small, thin walled vessels (47).

If the shape of the velocity profile is distorted from the true profile, then it may be concluded that the velocity measurements extend beyond the physical dimensions of the tube and in such cases the extraction of true velocity is a non-trivial

problem (19).

Often the term "instantaneous" velocity has been used incorrectly or ambiguously. For example, Franklin, et al., concluded that the mean Doppler shift in frequency can be employed as a measure of the instantaneous flow velocity of blood (36). He should have said "mean flow velocity." M.G.J. Arts, et al., use the term "instantaneous average velocity" to mean the measurement of average velocity by ultrasonic means at a given instant of time (3). C. Risqe, et al., use the term "instantaneous velocity" in connection with electromagnetic and Doppler flowmeter in an ambiguous manner (58).

In my experiments, the highest value of measured velocity was in the center, and the lowest was in the bottom wall of the tube. Examination of Figure 5 indicates that there is a slight distortion of the velocity profile near the top wall. A 94% correlation between the measured particle velocities and the fitted parabola indicates that there is good agreement between the experimentally measured profile and the fitted theoretical parabolic curve.

The equation of the velocity profile:

$$v(r) = 11.312 + 5.0236 r - .76072 r^2 \quad (4.10)$$

reveals that each coefficient is significant relative to one another, and therefore, not a mere perturbation.

It has been remarked that an unusual velocity profile may cause an additional source of inaccuracy for the Doppler (73). Errors of this type were minimal in my experiments. I evaluated

the Reynolds number for each experiment, where its value was found to be well below the given threshold value, and hence, I can conclude that laminar flow was maintained in all my experiments.

Measurement of Blood Hematocrit

S.W. Flax, et al., citing H.L. Goldsmith, states that blood cells exhibit a strange behavior in a flowing plasma stream. Depending on the differential velocities and shear forces in the plasma, the blood cells form aggregates known as rouleaux. In some regions of the stream, one finds rouleaux, while in other regions only single cells can be found. Also, there is a red cell free layer near the vessel walls. Both of these effects make the red cell distribution non-homogenous. A quantitative description that would describe this non-homogeneity is lacking. For lack of a better description and for the sake of simplicity, most investigators assume a homogenous description when using Doppler flowmeter (31). (In Section 3, this assumption is listed and will be elaborated further.) A discussion of the distribution of particles or particle profile as found in my experiments may help to clarify the picture. Because geometric, exponential, and linear least squares fitting showed a low correlation coefficient, only the case of polynomial least squares will be discussed.

According to Table 3.6, higher degree polynomials show a greater coefficient of correlation. However, a higher correlation coefficient does not necessarily guarantee that a better fit is obtained, as will be discussed below. I will invoke Descarte's

rule of signs in analysis of each of these polynomials.

Appendix A3 provides the mathematical formulation of Descarte's rule of signs.

For the sake of brevity, only 2 significant figures will be carried out in all subsequent analyses.

$$\text{Case 1) Let } g(r) = 3.2 + .56 r - .073 r^2$$

$$\text{Then, } g(-r) = 3.2 - .56 r - .073 r^2$$

The number of variations of signs for $g(r)$ is 1 and for $g(-r)$ is also 1. By Descarte's rule of signs, it can be said that \hat{H} has one positive and one negative root. That is, the hematocrit will approach zero for a positive radius as well as for a negative one, as is suggested by Figure 6. Examination of this figure indicates that hematocrit is greatly reduced as one approaches the walls of the tube, and, is greatest in the central region.

$$\text{Case 2) Let } g(r) = 2.8 + 1.1 r - .22 r^2 + .011 r^3$$

$$\text{Then, } g(-r) = 2.8 - 1.1 r - .22 r^2 - .011 r^3$$

The number of variations of sign for $g(r)$ is 2, whereas for $g(-r)$ is 1. Thus, $g(r)$ has either 2 or no positive roots and 1 negative root. Hence, \hat{H} has either 2 positive and 1 negative roots, or 1 negative and 2 imaginary roots.

Examination of Figure 7 indicates that it is not feasible to have imaginary roots. It strongly suggests that there must be a double positive root and a negative one. Thus, it can be

concluded that hematocrit tends to approach zero as it approaches the wall, and is greatest near the central region.

$$\text{Case 3) Let } g(r) = 3.5 - .25 r + .44 r^2 - .10 r^3 + .0063 r^4$$

$$\text{Then, } g(-r) = 3.5 + .25 r + .44 r^2 + .10 r^3 + .0063 r^4$$

Number of variations of signs for $g(r)$ is 4 and for $g(-r)$ is 0. Thus, \hat{H} may have 4 positive roots, or 2 positive and 2 imaginary roots, or all 4 roots may be imaginary. Examination of Figure 8 indicates that \hat{H} has either 2 or 4 imaginary roots. In other words, the hematocrit approaches zero somewhere in the middle of the tube. This contradicts the physical reality of laminar flow, hence a polynomial of 4th degree fit is not appropriate.

Notice that the coefficient of the 4th degree term is quite small, indicating that in the fitting of higher degree polynomials, higher order terms will be correspondingly smaller making such an evaluation inappropriate.

In summary, the similarity between Figures 6 and 7, and the parabolic shape of the cubic polynomial strongly suggests that a polynomial of 2nd degree fit is the most appropriate choice to represent hematocrit as a function of radius.

In a similar fashion, I will do an analogous analysis for a blood hematocrit of 7%, where pressure head was lowered to 131 cm.

$$\text{Case 1) Let } g(r) = .91 + .13 r - .019 r^2$$

$g(r)$ has 1 positive and 1 negative root. Figure 9 indicates

that hematocrit is reduced at the walls, which agrees with our expectation.

$$\text{Case 2) Let } g(r) = .55 + .65 r - .18 r^2 + .013 r^3$$

Figure 9 suggests the existence of imaginary roots for this 3rd degree polynomial. This means that hematocrit will be zero somewhere in the middle of the tube, which contradicts physical reality. Thus, a 3rd degree polynomial least squares fit is inappropriate.

$$\text{Case 3) Let } g(r) = .81 + .069 r + .13 r^2 - .047 r^3 + .0037 r^4$$

$g(r)$ may have 2 positive and 2 imaginary roots, or it may have 2 positive and 2 negative roots, or it has 2 negative and 2 imaginary roots, or possibly it has 4 imaginary roots. Examination of Figure 10 reveals existence of imaginary roots. Hence, I can conclude that a 4th degree least squares polynomial fit is inappropriate.

$$\text{Case 4) Let } g(r) = .028 + 2.3 r - 1.6 r^2 + .52 r^3 + .075 r^4 + .0039 r^5$$

It can be concluded that $g(r)$ has 2 positive, 1 negative, and 2 imaginary roots, or it has 1 negative and 4 imaginary roots. Alternatively it may have 3 negative and 2 imaginary roots, or 2 positive and 3 negative roots. Graph of 5th degree polynomial in Figure 10 suggests that there are no positive roots. Thus, $g(r)$ has either 2 or 4 imaginary roots from which one can conclude that a 5th degree polynomial is not an appropriate fit.

It can be summarized that hematocrit can be properly

expressed as a function of radius in terms of a second degree polynomial.

Table 3.7 does not list higher degree polynomials for a blood hematocrit of 10%, because a similar analysis showed that hematocrit was best expressible as a second degree polynomial.

The discussion of particle profile will be complemented by a mapping of particle velocity onto set of hematocrit values.

Although it will be assumed in Section 3 that particle velocity is equal to the velocity of the surrounding fluid, it is necessary to elaborate on this matter. If the particles of a suspension move with the surrounding fluid without any slip velocity, then the velocity obtained from these particles will represent that of the surrounding fluid. In other words, particle velocity and fluid velocity are the same, provided there is no relative motion between the particles and the fluid (24).

Distribution of velocities and particle profile are both parabolic, and instantaneous velocity of flow and particle velocity are the same, which suggests that there is a one to one correspondence between changes in velocity and changes in hematocrit values. This can be described by means of mapping the set of velocities onto the set of hematocrit values.

For a constant pressure head of 131 cm. and a total blood hematocrit of 10%, this mapping is described by the following equation:

$$\hat{H}_v = 2.39 + .326 v - .0123 v^2 \quad (4.11)$$

In similar fashion, when the constant pressure head was raised to 177 cm. and where total blood hematocrit was unchanged, the equation of mapping obtained was:

$$\hat{H}_V = 2.59 + .154 v - .00314 v^2 \quad (4.12)$$

T. Cochrane, et al., used the empirical relation of Charm and Kurland which relates the velocity of RBC's to the fractional concentration (C_f), where C_f is defined as the ratio of volume of red cells to volume of suspending medium (19). The empirical formula is given as:

$$v(C_f) = v(0) (1 - C_f)^\alpha \quad (4.13)$$

where $v(0)$ denotes the center line velocity. The parameter α in Equation 4.13 varies greatly with the suspending medium, the age, and the quality of blood cells used. When the suspending medium is plasma and fresh RBC's are used, α is 2.5. Their graph indicates that velocity rapidly decreases as the value of fractional concentration increases. It will be shown later that an increase in hematocrit value will cause velocity to decrease exponentially based on a derived rather than empirical relationship.

Note that $v(C_f)$ can be regarded as the inverse relation to the mapping which was just described above.

Calculation of the Mean Doppler Amplitude

Before discussing the results obtained, it would be beneficial to provide the necessary background and present the relevant information. The Doppler shift formulas 1.5 and 1.6 are valid

provided the following assumptions are made (77):

1. The red cells are uniformly distributed in the blood.
2. The red cells behave like point scatterers.
3. The sound beam illuminates the entire cross section of the vessel with uniform intensity.
4. The sensitivity of the receive is uniform over the whole vessel cross section.
5. The frequency shift is only caused by red cells inside the vessel.

I have shown that the first assumption is not fulfilled for large vessels as depicted by Figure 6, and it is not justified for small vessels. The second assumption is justified because the dimensions of the cells are much smaller than the wavelength of the sound waves. The third and fourth assumptions depend upon the geometry of the ultrasonic beam, as the width of the ultrasonic beam needs to be almost equal to the diameter of the vessel. I used a large transducer in my experiments to comply with these assumptions. The fifth assumption may be justified in some situations and not in others. Appropriate filtering satisfies this assumption, as was carried out in all my experiments.

The following assumptions are valid for showing the dependence of Doppler amplitude on blood hematocrit:

1. In the sample blood volume under consideration the transmitter and receiver beam are homogenous with respect to the intensity of radiation and receiver gain

respectively. These beams are also assumed to be well defined. This assumption is not justified in my project because it was not possible to measure the size of the transducer.

2. Only particles in the sample volume contribute to the power of the received signal. Every particle is assumed to give the same contribution with respect to magnitude of this power.
3. The average velocity of blood in the measuring volume is equal to that across the cross section of the blood vessel.
4. The velocity of a particle is equal to the velocity of the surrounding liquid.
5. The center of gravity of the cross section of the blood vessel remains always in the same place.
6. At any moment the blood vessel is a cylinder.

Assumption (5) implies that the average liquid velocity has an axial component only. Assumption (6) permits a consideration of an axial direction of the blood flow in the volume under consideration. All these assumptions together mean that in the sample volume under consideration the average liquid velocity is equal to the average particle velocity at any instant of time, and that this velocity is axially directed (3).

Now I will briefly present views expressed by other investigators who support the hypothesis of functional dependence

of Doppler amplitude upon the number of particles. S.W. Flax, et al., hypothesize that amplitude is related to the number of particles reflecting sound, moving at a given velocity (32).

S. Wille asserts that the intensity of a certain Doppler frequency is proportional to the number of red cells causing the frequency shift. That is, $I(f_i) \propto N(f_i)$, where $I(f_i)$ is the intensity and $N(f_i)$ is the number of red cells (77). S. Einav and S.L. Lee asserted that the amplitude of the Doppler signal was related to the number density of the scattering particles in the measuring volume (24). Later in 1975, Einav, et al., suggested that the amplitude of the Doppler signal was greatest in the center of the vessel (23). J.M. Reid, et al., in employing single scattering theory suggest that scattering is approximately proportional to the hematocrit in the range from 7% to 40% (57). K.K. Shung, et al., found that scattering of ultrasound from blood increases with hematocrit, reaching a maximum for a hematocrit of about 30%, and decreasing as hematocrit increases further (61). They showed that the scattering coefficient is a parabolic function of hematocrit, and attribute its decline after reaching a hematocrit of 30% to multiple scattering and gradual disappearance of the random nature of the motion of RBC's.

Researchers such as S.W. Flax, et al., point out that parameters influencing the power spectral content are so complex that an exact determination would be impossible, mainly because what occurs is the phenomena of sound scattering and not simple

reflection (31). For example, B.A.J. Angelsen (2) has modeled the received radio frequency (RF) signal in the CW ultrasonic blood velocity instrument by the equation:

$$e(t) = \text{Re} \{ \hat{X}(t) e^{i\omega_0 t} \} \quad (4.14)$$

He asserts that $\hat{X}(t)$ is a complex signal which contains both amplitude and phase information in the RF signal, where the invariant velocity field $\hat{X}(t)$ with respect to time can be written as:

$$\hat{X}(t) = x(t) + i y(t) \quad (4.15)$$

Finally, he expresses the complex process in Equations 4.14 and 4.15 in terms of its time-variable amplitude $A(t)$ and phase $\phi(t)$:

$$\begin{aligned} \hat{X}(t) &= A(t)e^{i\phi(t)} \\ A(t) &= \sqrt{x^2(t) + y^2(t)} \\ \phi(t) &= \tan^{-1} \{y(t)/x(t)\} \end{aligned} \quad (4.16)$$

Notice that the amplitude and phase in Fourier transformation is analogous to $A(t)$ and $\phi(t)$ of Equation 4.16.

I claim to differ with these researchers in at least one of the following ways:

1. Some researchers, like Angelsen, stress only theoretical aspects without verification against experimental results.
2. Usually, the method of the Fourier transformation was not employed in processing the information, although some authors suggested that spectrum analyzer would facilitate visualization of the frequency range and

content of the Doppler shift (62).

3. The tendency was towards complex stochastic modeling. In this respect, deterministic model was either ignored or if pursued, no exact functional relationship was derived (11,23,61,77).

In order to determine the relationship between the amplitude of the Doppler signal and the number of red cells, I applied Fourier analysis on the digitized Doppler signals because of the following reasons:

1. It reduces the complexity of the problem by identifying different frequency sinusoids and their respective amplitudes, which combine to form the arbitrary waveform.
2. Spectrogram analysis provides a unified framework for ultrasonic diagnosis. It has been remarked that simple computation of the spectrogram is becoming feasible because real-time FFT's are becoming available as integrated circuits (1).
3. It results in estimates of the power spectrum of a time signal. That is, the square of the magnitude of the set of complex Fourier coefficients is used to estimate the power spectrum of the original signal (7,9). Physically, the Fourier transform represents the distribution of signal strength with frequency which is a density function (78).
4. Fourier transformation is ideal for model experiments which use a steady-state flow, because properties of

Fourier integral, such as periodicity are being utilized (41).

The mean amplitude of the Doppler signal, for a given blood hematocrit, was calculated by evaluating the area under the curve which was fitted to the transformed data. The lower and upper limits of integration were 0 and 4000 respectively, since the data were between 0 and 4000 Hz. This is a suitable procedure because it is based on "Consequence of Mean Value Theorem" as outlined in Appendix A4.

Table 3.9 lists Doppler amplitude (A) as a function of blood hematocrit (\hat{H}) for various rates of constant flow. In each case the amplitude is expressed as a linear and as a quadratic function of hematocrit. Notice that the quadratic functions display a greater correlation coefficient in 80% of my cases. However, Doppler amplitude may be described more suitably as a linear function of the hematocrit for the following reasons:

1. In general, the curve fitting procedure improves the correlation coefficient as polynomials of higher degrees are selected (74).
2. The constant and the coefficient of the first degree term in each of the linear functions, under different pressure heads, are comparable in magnitude and in sign. On the other hand, the coefficient of the first degree term in quadratic functions is positive for pressure heads of 70 and 80 cms., and is negative for 60, 90, and

100 cms.

3. The coefficient of the 2nd degree term in all quadratic functions are rather small.
4. There is a close proximity between the linear and quadratic curves corresponding to pressure heads of 70 and 80 cms. as shown in Figures 12 and 13.

Note that quadratic functions in Figures 11 and 15 seem to indicate that amplitude increases proportionally to hematocrit for hematocrits exceeding 15%. This somewhat parallels the findings of J.M. Reid, et al., who assert that this proportionality is true when hematocrit is greater than 7% (57,62).

Thus, I can conclude that the amplitude of the Doppler signal is a linear function of blood hematocrit. For the Doppler instrument used in my experiments, the constant term averages about 21 with a standard deviation of .54 and the coefficient of the first degree term averages about .11 with a standard deviation of .021. Hence, the Doppler amplitude function of the single variable A can be written as:

$$A(\hat{H}) = 21 + .11 \hat{H} \quad (4.17)$$

where \hat{H} is the blood hematocrit. When the variable H, the pressure head, is also allowed to vary, the Doppler amplitude becomes a function of double variables H and \hat{H} , that is, $A = A(H, \hat{H})$. Multiple linear regression is the appropriate model and can be suitably used on data. In this manner, the function $A(H, \hat{H})$ was expressed as:

$$A(H, \hat{H}) = 23.154 - .021200H + .10794 \hat{H} \quad (4.18)$$

which asserts that \hat{H} is the primary and H the secondary factor influencing the Doppler amplitude.

The influence of \hat{H} is 5 times greater than H and as can be observed from the sign of the coefficients, $A(H, \hat{H})$ monotonically increases as \hat{H} does, but is a monotone decreasing function of H .

Functional Relationship of Blood Viscosity and Blood Hematocrit.

It has been stated that changes in the properties of the blood, such as its viscosity, may be accompanied by alterations in the pattern of blood flow (19). Since viscosity of blood is primarily dependent on the hematocrit, it would be useful to understand the nature of their relationship.

The viscosity of blood greatly increases as the percentage of the volume of whole blood occupied by red cells increases (13). This suggests that blood viscosity (μ) may be an exponential function of blood hematocrit (\hat{H}).

Examination of Table 3.11 reveals that geometric least squares fitting is inferior to both exponential and 2nd degree polynomial least squares because its correlation coefficient (ξ) is smaller and its standard error of the estimate (ϵ) is higher.

Examination of the 2nd degree polynomial shows that coefficients of higher degree terms are smaller. Hence, it was not necessary to fit higher degree polynomials to the data, as coefficients of higher degree terms are negligible.

Both the exponential and 2nd degree polynomial fit showed excellent

correlation, although ϵ was slightly higher for the 2nd degree polynomial least squares fit. Each case will be discussed separately.

Case 1) Viscosity is an Exponential Function of the Hematocrit.

That is, $\mu = Ae^{B \hat{H}}$, where A and B are both constants.

Constants A and B cannot both be negative at the time time, otherwise, regardless of the value of the hematocrit, viscosity will be negative. If $B > 0$ and $A < 0$, then as hematocrit value increases, viscosity will decrease and its value will be negative. If $B < 0$ and $A > 0$, then an increase in value of \hat{H} will cause μ to decrease exponentially, which is a contradiction to the assumption that μ increases exponentially with increasing \hat{H} . Thus, A and B are positive constants.

Because water was used to determine the constant K of the viscosimeter, and for water $\hat{H} = 0$, it can be concluded that A is equal to viscosity of water. It should be mentioned that blood proteins contribute significantly to blood viscosity. However, plasma was not used in determination of K, hence the role of these plasma proteins was not considered. Constant A has the dimensions of viscosity and depends on the temperature, but for a given temperature A is independent of \hat{H} . For example, at 26°C, $A = .8705$ c.p.

To study the nature of constant B, we examine Table 3.10 more closely. For example, for a blood hematocrit of 29.7%, $\mu = 1.7163$ c.p. which implies that $e^{29.7B} = 1.7163 \text{ c.p.} / .8705 \text{ c.p.}$ or $B = .02296$, a dimensionless number. In a similar fashion,

the constant B can be evaluated for any other value of hematocrit. Thus, constant B is dimensionless and its value is dependent upon the hematocrit. The extent of this dependence was determined by a least squares linear fitting, which resulted in the equation:

$$B = .011723 + .00042180 \hat{H} \quad (4.19)$$

The coefficient of correlation was .99 and the standard error of the estimate was .00039, with 95% confidence intervals of (.01078, .01268) and (.00036, .00046). Thus, B is dimensionless and is a linear function of blood hematocrit.

Notice that the slope is positive which means that as hematocrit increases, so does the value of constant B. Also notice that my experimental findings are in close agreement with the theoretical results.

The significance of the above constants becomes apparent when one considers the role of viscosity on velocity distribution. Classically, this relationship is as follows:

$$V = (\Delta P / 4L\mu)(r_0^2 - r^2) \quad (4.20)$$

(See Appendix A5 for derivation of Equation 4.20). Normally, Equation 4.20 is treated in such a way that μ is held fixed. That is to say, within the normal range of blood flow under in vivo conditions, viscosity is relatively constant. On the other hand, when contrasted with anemia (hematocrit < 45%) or polycythemia (hematocrit > 48%), viscosity can no longer be treated as a

constant factor.

In order to discuss this situation, Equation 4.20 can be rewritten in the following form:

$$\begin{aligned} v &= \mu^{-1} (\Delta P/4L)(r_0^2 - r^2) \\ &= (1/A)e^{-B \cdot \hat{H}}(\Delta P/4L)(r_0^2 - r^2) \end{aligned} \quad (4.21)$$

Because $A > 0$, $1/A$ is also positive, and for fixed values of L , r_0 , and Δp , Equation 4.21 is reduced to:

$$v = K (r_0^2 - r^2) e^{-B \hat{H}} \quad (4.22)$$

A change in \hat{H} causes a corresponding change in B , consequently one can set $B \cdot \hat{H} = \hat{H}$. Thus, Equation 4.22 simplifies to:

$$v = K (r_0^2 - r^2) e^{-\hat{H}} \quad (4.23)$$

Note that $K > 0$, and at a given radius r where $r \leq r_0$ an increase in hematocrit value will, in turn, cause \hat{H} to increase. As a result, velocity will decrease exponentially. In other words, with values of r being held constant, velocity is an exponentially decreasing function of hematocrit.

Equation 4.23, as it stands, is a product of a quadratic function and an exponential function. If the quadratic function is the dominant factor, then parabolic characteristics of the velocity profile prevail.

My experiments showed that hematocrit is a parabolic function of the velocity. Then, in terms of its inverse relation, velocity will also be a parabolic function of hematocrit provided either μ is held constant or the quadratic factor dominates over

exponential term.

Case 2) Viscosity is a quadratic function of hematocrit.

From Table 3.11 and retaining only 3 significant figures, one can write the equation of velocity profile as:

$$V = K (r_0^2 - r^2) / (.858 + .00926 \hat{H} + .000685 \hat{H}^2) \quad (4.24)$$

Again, Equation 4.24 can be compared with the empirical equation 4.13, that is, $v(C_f) = v(0) (1-C_f)^\alpha$. Both of these equations show a sharp decrease in velocity as \hat{H} or C_f increases; however, the empirical equation is limited to variations of center-line velocity. Equation 4.24 is more general and can be applied to any other radius (r) within the vessel.

The principle objective of this research was to determine if blood hematocrit influenced the amplitude of the Doppler signal; and if so, to establish a generalized Doppler amplitude function $A = A(H, \hat{H})$.

As a first step, in order to gain an insight about the importance of each of the parameters H and \hat{H} , I determined that:

$$V = 59.879 + .74538 H - 1.5053 \hat{H}$$

The relative importance of these parameters with respect to one another is reflected in the function $A = A(H, \hat{H})$.

Measurement of velocity profile is a prerequisite to $A(H, \hat{H})$ not only because a parabolic velocity profile is assumed, but also because the profile varies from vessel to vessel. The equation:

$$V(r) = 11.312 + 5.0236 r - .76072 r^2$$

obtained by using the pitot tube system guarantees that errors

associated with unusual velocity profiles are minimal.

Although it has been assumed that the red cells are uniformly distributed, I showed that this assumption is not valid. The particle profile is parabolic and in general can be represented by the equation of the form:

$$\hat{H}(r) = a_1 + 2_2 r - a_3 r^2$$

where a_1 's are positive.

Calculation of the mean Doppler amplitude showed that the amplitude was a linear function of hematocrit. For the Doppler instrument used in my experiments, this equation was expressed as:

$$A(\hat{H}) = 21 + .11 \hat{H}$$

The generalized Doppler amplitude is a function of double variables H and \hat{H} as given by

$$A(H, \hat{H}) = 23.154 - .021200 H + .10794 \hat{H} ; H \in [60, 100], \hat{H} \in [4.5, 46.5]$$

This equation shows that amplitude increases as hematocrit increases, but it decreases slowly as pressure head is increased.

Finally, because changes in viscosity bring about alteration in pattern of blood flow and since viscosity depends on hematocrit, it was shown that viscosity can be expressed as:

$$= A \exp (B \hat{H})$$

where A and B are positive constants.

Many parameters influence the amplitude of the Doppler signal, as for example, H and \hat{H} . This research could be extended to determine if

blood viscosity affects the amplitude of the Doppler. Because viscosity also depends on temperature, an experiment could be conducted, where for a specified blood hematocrit, the temperature of blood reservoir is allowed to vary. Doppler signal could then be recorded for different viscosities produced by a range of temperatures.

CHAPTER 5

SUMMARY AND CONCLUSIONS

Due to the fact that red cells act as point scatters or reflectors of ultrasound, and because the classical Doppler equation does not provide amplitude information, the question centered around whether or not the amplitude of the Doppler corresponded to the number of particles, and if so, could Doppler amplitude be expressed as a precise algebraic or transcendental function of hematocrit? To answer this question the problem was attacked in 3 stages.

In the preliminary stage, my aim was twofold. The first was to test the reliability and accuracy of the Doppler instrument itself, and the second was to find out in quantitative terms the simultaneous influence (or the relative weight) of the two important parameters in steady, laminar flow; namely, pressure head and hematocrit upon the velocity of flow.

In the second stage, the strategy was to arrive at the particular form of the function which represented Doppler amplitude in terms of blood hematocrit. In this respect, it was necessary to determine the distribution of velocities, particle profile, one-to-one map of particle velocities onto set of hematocrit values, and finally calculation of Doppler amplitude for a range of blood hematocrits.

In the final stage, my objective was to develop and expand on the relationship between blood viscosity and hematocrit based on mathematical analysis and supported by experimental results. This last stage of my research served two important purposes. In the first place, because changes in viscosity can bring about alterations

in the pattern of blood flow and also because viscosity of blood is mainly due to number of red cells present, one must ultimately take into consideration the viscosity factor when Doppler flowmeter is used for in vivo measurements of blood flow. This can be significant especially if polycythemia is encountered in patients. In the second place, because many parameters influence the amplitude of the Doppler signal, it may be hypothesized the amplitude is also dependent upon the viscosity, hence future studies and/or experiments can be designed to answer this question.

Now, I will briefly summarize each component of the project and correspondingly state the derived conclusions.

1. Accuracy and reliability of the Doppler flowmeter used in my experiments was tested against known volume flows measured simultaneously by an electromagnetic flowmeter. Under steady, laminar flow conditions, a range of flow rates was measured simultaneously by both flowmeters. The experiment was repeated for various pressure heads, and in each case the relation between electromagnetic flow (\dot{Q}_e) and Doppler flow (\dot{Q}_d) was found to be linear.

Applying analysis of covariance, I found a single linear function which represented all applied pressure heads. The equation of this linear function was described by:

$$\dot{Q}_d = .51428 \dot{Q}_e + 113.69 \quad (5.1)$$

Equation 5.1 guarantees the reliability and accuracy of the

Doppler ultrasonic flowmeter which was used in all my experiments.

2. Blood hematocrit (\hat{H}) and pressure head (H) are two important parameters which influence the velocity of blood flow (V). Volumetric flow was measured under steady, laminar flow conditions by means of a graduated cylinder and a stop watch.

Multiple linear regression was applied on data, as a result of which the equation of velocity in terms of H and \hat{H} was found to be:

$$V = 59.879 + .74538 H - 1.5053 \hat{H} \quad (5.2)$$

As expected, the influence of pressure head upon velocity is positive, whereas that of hematocrit is a negative one. But, more importantly, Equation 5.2 reveals the relative weight of these parameters upon velocity. In other words, the negative influence of hematocrit upon average velocity is almost twice as great as that of pressure head, giving us a clue as to hierarchy of parameters.

3. Under steady flow conditions, the velocity profile is parabolic, but it also varies from vessel to vessel. Thus, the instantaneous particle velocity across the lumen of the vessel was measured by means of a pitot tube system. A least square polynomial of 2nd degree fit resulted in the following equation:

$$V(r) = 11.312 + 5.0236 r - .76072 r^2 \quad (5.3)$$

Equation 5.3 does not represent an unusual velocity profile, hence one can conclude that there does not exist any additional source of inaccuracy for the Doppler.

Because the distribution of particles within the vessel is actually inhomogenous, particle profile was also determined simultaneously with the aid of a series of bent tubes facing the flow. It was shown that the distribution of particles within the tube is appropriately described by means of a 2nd degree polynomial.

For $\hat{H} = 10\%$ and $H = 177$ cm the equation of particle profile was:

$$\hat{H}(r) = 3.2402 + .56481 r - .072719 r^2 \quad (5.4)$$

Similarly, the equation of particle profile for $H = 7\%$ and $H = 131$ cm. was:

$$\hat{H}(r) = .91050 + .12542 r - .018690 r^2 \quad (5.5)$$

As H and \hat{H} reduced, the profile was blunted.

A 1-1 mapping of particle velocities onto set of hematocrit values was described by a parabola. The equation of the mapping for $\hat{H} = 10\%$ and $H = 131$ cm. was:

$$\hat{H}_V = 2.39 + .326 V - .0123 V^2 \quad (5.6)$$

and when $H = 177$ cm., it resulted in:

$$\hat{H}_V = 2.59 + .154 V - .00314 V^2 \quad (5.7)$$

The amplitude of the CW Doppler flowmeter can be expressed as a linear function of hematocrit. For the Doppler instrument used in my experiemnts, the overall linear function obtained was:

$$A(\hat{H}) = 21 + .11\hat{H} \quad (5.8)$$

The generalized Doppler function of hematocrit and pressure head was found to be:

$$A(H, \hat{H}) = 23.154 - .021200 H + .10794 \hat{H} \quad (5.9)$$

4. Viscosity (μ) is an exponential function of hematocrit. In its most general form it can be written as:

$$\mu = A e^{B \hat{H}} \quad (5.10)$$

where A and B are constants. In order to understand the nature of constants A and B and develop the theory further, viscosity of blood was measured for a wide range of blood hematocrits using a Falling ball type viscosimeter. Constant A has the dimension of viscosity, is dependent on temperature, but independent of hematocrit. Constant B is dimensionless but is a function of hematocrit.

As an application of Equation 5.10, it was shown that velocity decreases exponentially as hematocrit increases. A 2nd degree polynomial least squares also showed good correlation with experimental data. The curve is concave upward, and looks very much like the curve shown on Figure 18. Its application also indicates a sharp decrease in velocity as hematocrit increases.

LITERATURE CITED

1. Altes, R.A., and W.J. Faust. A unified method of broad-band echo characterization for diagnostic ultrasound. *IEEE Trans. Biomed. Eng.*, 27 (9):500-508, 1980.
2. Angelsen, B.A.J. Instantaneous frequency, mean frequency, and variance of mean frequency estimators for ultrasonic blood velocity Doppler signals. *IEEE Trans. Biomed. Eng.*, 28 (H): 733-741, 1981.
3. Arts, M.G.J., and J.M.J.G. Roevros. On the instantaneous measurement of blood flow by ultrasonic means. *Med. Biol. Eng.*, 10:23-34, 1972.
4. Baskett, J.J., M.G. Beasley, G.J. Murphy, D.E. Hyams, and R.G. Gosling. Screening for carotid junction disease by spectral analysis of Doppler signals. *Cardiovasc. Res.*, XI (2):147-155, 1977.
5. Bauer, R.D., T. Pasch, and W. Sperling. Studies on the accuracy of directional Doppler flowmetry with regard to steady and pulsatile flow. *Ultrasonics Med.*:290-294, 1974.
6. Bentley, P.B. Advanced recording and preprocessing of physiological signals. *Stanford Res. Inst.*: 1-50, 1975.
7. Bergland, G.D. A guided tour of the fast Fourier transform. *IEEE Spect.*, 6 (7):41-52, 1969.
8. Borders, S.E., A. Fronek, W.S. Kemper, and D. Franklin. Ultrasonic energy backscattered from blood: An experimental determination of the variation of sound energy with hematocrit. *Ann. Biomed. Eng.*, 6:83-92, 1978.
9. Brigham, E.O., and R.E. Morrow. The fast Fourier transform. *IEEE Spect.*, 4 (12):63-70, 1967.
10. Brody, W.R. Theoretical analysis of the ultrasonic blood flowmeter. (Ph.D. Diss.), Stanford Univ., 1971.
11. Brody, W.R., and J.D. Meindl. Theoretical analysis of the C.W. Doppler ultrasonic flowmeter. *IEEE Trans. Biomed. Eng.*, 21 (3): 183-192, 1974.
12. Burton, A.C. Composition of blood. In: Physiology and Biophysics of the Circulation. Chicago: Year Book Med. Publ., Inc., 1968, p. 16.
13. Burton, A.C. Hemodynamics and the physics of the circulation. In: Physiology and Biophysics. Edited by T.C. Ruch and H.D. Patton. Philadelphia: W.B. Saunders Co., 1966, pp. 523-542.

14. Burton, A.C. Viscosity and the manner in which blood flows. In: Physiology and Biophysics of the Circulation. Chicago: Year Book Med. Publ., Inc., 1968, pp. 50-57.
15. Caro, C.G., T.J. Pedley, R.C. Schroter, and W.A. Seed. In: The Mechanics of the Circulation. New York: Oxford Univ. Press, 1978, pp. 151-161.
16. Choi, S.C. Analysis of Covariance. In: Introductory Applied Statistics in Science. New Jersey: Prentice-Hall, Inc., 1978 pp. 216-221.
17. Christensen, H.B. Regression and Correlation. In: Statistics Step by Step. Boston: Houghton Mifflin Co., 1977, pp. 544-611.
18. Cochran, W.T., J.W. Cooley, D.L. Favin, H.D. Helms, R.A. Kaenel, W.W. Lang, G.C. Maling, Jr., D.E. Nelson, C.M. Rader, and P.D. Welch. What is the fast Fourier transform? *IEEE Trans. Audio Electroacoust.*, AU-15 (2):45-55, 1967.
19. Cochran, T., J.C. Earnshaw, and A.H.G. Love. Laser Doppler measurement of blood velocity in microvessels. *Med. Biol. Eng. Comp.*, 19:589-596, 1981.
20. Cooley, L.W., P.A.W. Lewis, and P.D. Welch. Historical notes on the fast Fourier transform. *IEEE Trans. Audio. Electroacoust.*, AU-15 (2):76-79, 1967.
21. Dixon, W.J., and F.J. Massey, Jr. Analysis of Covariance. In: Introduction to Statistical Analysis. New York: McGraw-Hill Book Co., Inc., 1969, pp. 226-234.
22. Dunn, O.J., and V.A. Clark. Multiple Regression and Correlation. In: Applied Statistics: Analysis of Variance and Regression. New York: John Wiley & Sons, 1974, pp. 252-294.
23. Einav, S., H.J. Berman, R.L. Fuhro, P.R. DiGiovanni, S.Fine, and J.D. Fridman. Measurement of velocity profiles of red blood cells in the microcirculation by Laser Doppler Anemometry (LDA). *Biorheol.*, 12:207-210, 1975.
24. Einav, S., and S.L. Lee. Measurement of velocity distribution in two-phase suspension flows by the laser-Doppler technique. *Rev. Sci. Instrum.*, 44 (10):1478-1480, 1973.
25. Emerson, P.L. Fast Fourier transform: Fundamentals and applications. *Creat. Comp.*, 6 (7):58-63, 1980.

26. Feigl, E.O. Physics of the Cardiovascular System. In: Physiology and Biophysics II. Edited by T.C. Ruch, and H.D. Patton. Philadelphia: W.B. Saunders Co., 1974, pp. 10-22.
27. Felix, W.R., B. Sigel, and C.L. Popky. Doppler ultrasound in the diagnosis of peripheral vascular disease. Seminars Roentgenol., X (4):315-321, 1975.
28. Finkelstein, L., and E.R. Carson. Transfer functions. In: Mathematical Modeling of Dynamic Biological Systems. Forest Grove, Oregon: Res. Stud. Press, 1979, pp. 65-76.
29. Fish, P.J. Transcutaneous blood flow measurement--The problems and a solution. Brit. Med. Ultrasound Soc. Meet., 1-21, 1980.
30. Fishman, A.P., and D.W. Richards. The Output of the Heart. In: Circulation of the Blood Men and Ideas. New York: Oxford Univ. Press, Inc., 1964, pp. 81-93.
31. Flax, S.W., J.G. Webster, and S.J. Updike. Statistical evaluation of the Doppler ultrasonic blood flowmeter. Biomed. Sci. Instrument., 201-222, 1970.
32. Flax, S.W., J.G. Webster, and S.J. Updike. Theoretical and experimental evaluation of Doppler blood flow information. Proc. 8th Int. Conf. Med. Biol. Eng. 22nd Ann. Conf. Eng. Med. and Biol., paper 10-8, 1969.
33. Fox, R.W., and A.T. McDonald. Dynamics of incompressible inviscid flow. In: Introduction to Fluid Mechanics. New York: John Wiley and Sons, 1978, pp. 265-304.
34. Fox, R.W., and A.T. McDonald. Newtonian Fluid. In: Introduction to Fluid Mechanics. New York: John Wiley and Sons, 1978, p. 33.
35. Franklin, D.L. Techniques for measurement of blood flow through intact vessels. Med. Electron. Biol. Eng., 3:27-37, 1965.
36. Franklin, D.L., W. Schlegel, and R.F. Rushmer. Blood flow measured by Doppler frequency shift of back-scattered ultrasound. Sci., 134:564-565, 1961.
37. Freund, J.E. Regression. In: Modern Elementary Statistics. New Jersey: Prentice-Hall, Inc., 1973, pp. 386-419.
38. Giles, R.V. Fluid flow in pipes. In: Fluid Mechanics and Hydraulics. New York: McGraw-Hill Book Co., 1965, pp. 96-114.

39. Gonzalez, R.R., Jr., and W.J. Koh. The personal computer as a tool for spectral analysis of Doppler ultrasonic signals. *Suppl. J. Ultrasound Med.*, 1 (7):207, 1982.
40. Guldvog, I.M. Kjaernes, M. Thoreson, and L. Walloe. Blood flow in arteries determined transcutaneously by an ultrasonic Doppler velocimeter as compared to electromagnetic measurements on the exposed vessel. *Acta Physiol. Scand.*, 109:211-216, 1980.
41. Gupta, R., J.W. Miller, A.P. Yoganathan, F.E. Udwadia, W.H. Corcoran, and B.M. Kim. Spectral analysis of arterial sounds: a non-invasive method of studying arterial disease. *Med. Biol. Eng.*: 700-705, 1975.
42. Guyton, A.C. Physics of blood flow and pressure: hemodynamics. In: Textbook of Medical Physiology, 6th ed. Philadelphia: W.B. Saunders Co., 1981, p. 209.
43. Haywood, J.R., R.A. Shaffer, C. Fastenow, G.D. Fink, and M.J. Brody. Regional blood flow measurement with pulsed Doppler flowmeter in conscious rat. *Amer. J. Physiol.*, 241:H-273 - H-278, 1981.
44. Hughes, W.F., and J.A. Brighton. Boundary layer flow and flow in pipes and ducts. In: Fluid Dynamics. New York: Mc-Graw Hill Book Co., 1967, pp. 87-92.
45. Jensen, D. Hydrostatic and hydrodynamic principles as applied to hemodynamics: Laplace's law. In: The Principles of Physiology. New York: Appleton-Century-Crofts Publ., 1980, pp. 588-589.
46. Johnston, K.W., B.C. Maruzzo, and R.S.C. Cobbold. Errors and artifacts of Doppler flowmeters and their solution. *Arch. Surg.*, 112:1335-1342, 1977.
47. Kajiya, F., N. Hoki, G. Tomonaga, and H. Nishihara. A laser-Doppler-veocimeter using an optical fibre and its application to local velocity measurement in the coronary artery. *Experientia* 37, (Birkhäuser Verlag, Basel, Schweiz):1171-1173, 1981.
48. Louis, P. Directional ultrasonic flowmeter. Paris: Delalande Electron. manual.
49. Mahler, F., H.H. Brummer, A. Bollinger, M. Casty, and M. Anliker. Changes in phasic femoral artery flow induced by various stimuli: a study with percutaneous pulsed Doppler ultrasound. *Cardiovasc. Res.*, 11:454-460, 1977.
50. McDonald, D.A. The nature of flow in a liquid. In: Blood Flow in Arteries. London: Edward Arnold (Publ.) LTD., 1960, pp. 11-37.

51. Michie, D.D., and C.P. Cain. Effect of hematocrit upon the shift in Doppler frequency. *Proc. Soc. Exp. Biol. Med.*, 138:768-772, 1971.
52. Noordergraef, A. Hemodynamics. In: Biological Engineering. New York: McGraw-Hill Book Co., 1969, pp. 391-527.
53. Parzan, E., and B.P. Bogert. Informal comments on the uses of power spectrum analysis. *IEEE Trans. Aud. Electroacoust.*, AU-15 (2):74-76, 1967.
54. Peterson, R.D., and G.G. Myers. Fourier Series. In: Waveform Analysis in Medicine. Springfield, Illinois: Charles C. Thomas Publ., 1976, pp. 119-135.
55. Ramirez, R.W. The fast fourier transforms errors are predictable, therefore manageable. *Electron.*, 47 (12):96-102, 1974.
56. Ramirez, R.W. The FFT: Fundamentals and Concepts. Tektronix, Inc Publ., 1975.
57. Reid, J.M., R.A. Sigelmann, M.G. Nasser, and D.W. Baker. The scattering of ultrasound by human blood. *Proc. 8th Int. Conf. Med. Biol. Eng. 22nd Ann. Conf. Eng. Med. Biol.*, paper 10-7, 1969.
58. Risqe, C., and S.O. Wille. Blood velocity in human arteries measured by a bidirectional ultrasonic Doppler flowmeter. *Acta Physiol. Scand.*:370-378, 1978.
59. Rushmer, R.F., D.W. Baker, and H.F. Stegall. Transcutaneous Doppler flow detection as a non-destructive technique. *J. Appl. Physiol.*, 21 (2):554-566, 1966.
60. Shepherd, J.T., and P.M. Vanhoutte. From historical hallmarks to modern concepts of cardiovascular control. In: The Human Cardiovascular System. New York: Raven Press, 1979, pp. 1-12.
61. Shung, K.K., R.A. Sigelmann, and J.A. Reid. Scattering of ultrasound by blood. *IEEE Trans. Biomed. Eng.*, 23 (6):460-467, 1976.
62. Sigel, B., R.J. Gibson, K.V. Amatneek, W.R. Felix, Jr., A.L. Edelstein, and G.L. Popky. A Doppler ultrasound method for distinguishing laminar from turbulent flow. *J. Surg. Res.*, 10 (5):221-224, 1970.
63. Skidmore, R., and J.P. Woodcock. Physiological interpretation of Doppler-shift waveforms-I Theoretical Considerations. *Ultrasound Med. & Biol.*, 6:7-10, 1980.

64. Spencer, M.P., and A.B. Denison. Measurement of blood flow through intact vessels with the square-wave electromagnetic flowmeter. Fribourg (Switzerland): Comptes rendus du II Congres international d'Angeiologie, 1955.
65. Spencer, M.P., and A.B. Denison, Jr. Pulsatile blood flow in the vascular system. In: Handbook of Physiology-Circulation II. Washington, D.C.: Amer. Physiol. Soc., 1963, pp. 839-864.
66. Spencer, M.P., and A.B. Denison, Jr. The squarewave electromagnetic flowmeter: Theory of operation and design of magnetic probes for clinical and experimental application. IRE Trans. Med. Electron.:220-228, 1959.
67. Spencer, M.P., H. Okino, F.R. Johnston, and A.R. Cordell. Blood flow research with electronic techniques. 4th Int. Conf. Med. Electron., 1961.
68. Spencer, M.P., and J.M. Reid. Quantitation of carotid stenosis with continuous-wave (C-W) Doppler ultrasound. Stroke, 10 (3): 326-330, 1979.
69. Stanley, W.D., and S.J. Peterson. Fast Fourier transforms on your home computer. Byte Publ., Inc., 1978.
70. Streeter, V.L. Fluid properties and definitions. In: Fluid Mechanics. New York: McGraw-Hill Book Co., Inc., 1958, pp. 3-10.
71. Swokowski, E.W. Applications of the definite integral. In: Calculus with Analytic Geometry. Boston: Prindle, Weber & Schmidt, Inc., 1975, pp. 256-257.
72. Tomonaga, G., H. Mitake, N. Hoki, and F. Kajiya. Measurement of point velocity in the canine coronary artery by laser Doppler velocimeter with optical fiber. Jap. J. Surg., 11 (4):226-231, 1981.
73. Vatner, S.F., D. Franklin, and R.L. Van Citters. Simultaneous comparison and calibration of the Doppler and electromagnetic flowmeter. J. Appl. Physiol., 29 (6):907-910, 1970.
74. Warne, R.K. Curve fitter. Creat. Comp., 1981.
75. Weast, R.C. (Editor-in-Chief). C.R.C. Handbook of Chemistry and Physics (53rd ed.). Cleveland: The Chem. Rubber Co., 1972, p. F-36.
76. Welch, P.D. The use of fast Fourier transform for the estimation of power spectra: A method based on time averaging over short, modified periodograms. IEEE Trans. Aud. Electroacoust., AU-15 (2):70-73, 1967.

77. Wille, S. A computer system for on-line decoding of ultrasonic Doppler signals from blood flow measurement. *Ultrasonics*: 226-230, 1977.
78. Yoganathan, A.P., R. Gupta, and W.H. Corcoran. Fast Fourier transform in the analysis of biomedical data. *Med. Biol. Eng.*: 239-244, 1976.
79. Yoganathan, A.P., R. Gupta, F.E. Udwadia, J.W. Miller, W.H. Corcoran, R. Sarma, J.L. Johnson, and R.J. Bing. Use of the fast Fourier transform for frequency analysis of the first heart sound in normal man. *Med. Biol. Eng.*:69-73, 1976.
80. Zar, J.H. Comparing Simple Linear Regression Equations. In: Biostatistical Analysis. New Jersey: Prentice-Hall, Inc., 1974, pp. 228-235.
81. _____. Data Smoother. New York: Dynacomp, Inc., 1979.
82. _____. Fourier Analyzer. New York: Dynacomp, Inc. 1980.
83. _____. Harmonic Analyzer. New York: Dynacomp, Inc., 1980.

APPENDIX A

DERIVATION OF FORMULAS AND THEORIES

A1. PRINCIPLES OF OPERATION OF ELECTROMAGNETIC FLOWMETER

Electromagnetic flowmeter operates on the principle of electromagnetic induction, described by Faraday's law, which states that an electrical potential will be developed across a conductor (in this case blood) that is moving through a magnetic field. The transducer associated with the flowmeter contains an electromagnet which produces a magnetic field across the vessel. Motion of blood through the magnetic field generates an induced voltage proportional to velocity. For a given vessel diameter, the induced voltage is also proportional to volumetric flow rate. This electrical voltage (signal) is amplified and processed by the flowmeter and made available for presentation on an oscilloscope or a recorder (35,42). The average output voltage is an indication of mean flow rate. The square-wave electromagnetic flowmeter is energized from a high resistance square-wave source, and hence the field is essentially a "dc" field reversing periodically in polarity (66).

A2. PRINCIPLES OF OPERATION OF CONTINUOUS-WAVE (CW) DOPPLER FLOWMETER

The ultrasonic Doppler flowmeter consists of an electronic apparatus which energizes a minute piezoelectrical transmitting crystal. The crystal, upon being energized, transmits sound at a frequency of several million cycles per second. The flowing particles reflect a portion of the sound waves towards a receiving crystal with a lower or higher frequency depending upon sensor to artery orientation and velocity. The electronic apparatus greatly amplifies the reflected waves (11,42).

The mean differences (ΔF) between the frequency of the transmitted wave and that of the reflected wave is such that:

$$\Delta F/F = v/c \ 2 \cos \theta$$

where F is the transmission frequency, v the mean flow speed or particle flow velocity, c is the rate of propagation of ultrasonic waves through the blood ($\sim 1.5 \times 10^5$ cm/sec) and θ the transducer orientation angle (11,27,48). The ΔF can be recorded as to the spectrum, or it can be converted to an analog signal suitable for a galvanometric recorder (48).

A3. DESCARTES' RULE OF SIGNS

If $f(x)$ is a polynomial with real coefficients, then the number of positive roots of the equation $f(x) = 0$ cannot exceed the number of variations of sign in $f(x)$, and the difference between the number of variations of sign and the number of positive roots must be an even integer.

A4. CONSEQUENCE OF MEAN VALUE THEOREM

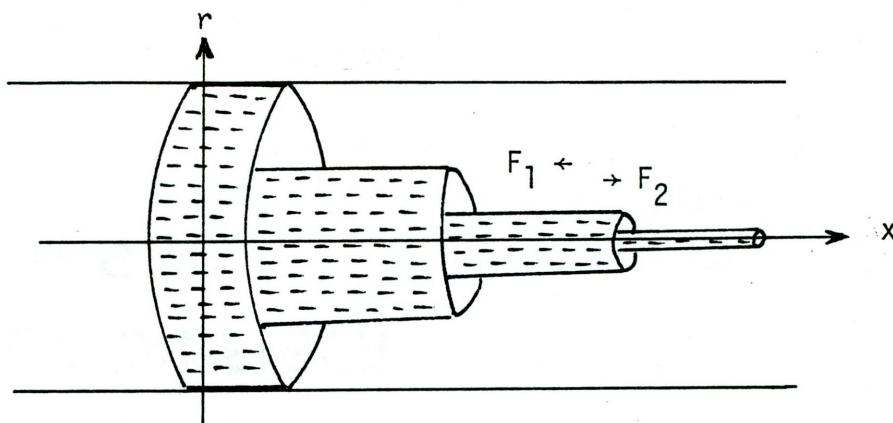
If the function f is integrable on a closed, bounded interval $[a,b]$, then

$$m \leq \frac{1}{b-a} \int_a^b f(x)dx \leq M \quad (1)$$

where m and M are lower and upper bounds for the function f .

The quantity $(1/b-a) \int_a^b f(x)dx$ is called the mean or average of f over $[a,b]$. Thus, equation 1 asserts that the average or mean of the function f lies between its smallest and largest values.

A5. EQUATION OF THE VELOCITY PROFILE FOR STEADY, LAMINAR FLOW



Assuming the flow is steady, each blood particle moves to the right without acceleration, where the flow is in layers as shown above. Suppose that the viscous force which opposes the flow over the unit area is proportional to product of blood viscosity (μ) and the velocity gradient (dv/dr) in the blood. Because velocity is constant, the sum of the forces along x-axis must be zero.

Let us consider a cylindrical unit of blood whose length is L and whose radius is r . The viscous force F_1 is given by

$F_1 = (2\pi rL)\mu(dv/dr)$, where $2\pi rL$ is the surface area of the cylindrical unit of blood. On the other hand, the force F_2 exerted by the pressure on the end of cylinder is equal and opposite in direction to the force F_1 , and is given by $F_2 = \pi r^2 \Delta P$, where ΔP is the pressure difference across the tube. Thus, $F_2 + F_1 = 0$ which implies (\Rightarrow)

$$\pi r^2 \Delta P = -2\pi rL\mu(dv/dr) \Rightarrow dv = (-r\Delta P)/(2L\mu)dr. \quad (1)$$

If we denote the center of tube by $r=0$ and velocity at the center by v_c , then integration of Equation 1 yields:

$$\int_{v_c}^v dv' = \int_0^r (\Delta P/2L\mu)r' dr' \Rightarrow v = v_c - (\Delta P/4L\mu)r^2$$

In the layer closest to the wall of the tube, the blood tends to stick to the wall, and its velocity may be considered zero.

Thus, denoting the distance between center of the tube and the wall by r_0 , we can write $v(r_0) = 0$

$$\therefore 0 = v_c - (\Delta P/4L\mu) r_0^2 \quad \rightarrow \quad v_c = (\Delta P/4L\mu) r_0^2$$

Hence, we have

$$v = (\Delta P/4L\mu) (r_0^2 - r^2) \quad (2)$$

Equation 2 represents the distribution of velocity or velocity profile for steady, laminar flow (23,38,50).

APPENDIX B

LISTING OF PROGRAMS

PROGRAM LISTING FOR DIGITIZER

```

5 TEXT : HOME
10 DIM D(2000)
15 D$ = CHR$(4): VTAB 4
20 PRINT "CHOOSE FROM THE FOLLOWING"
30 VTAB 10
40 PRINT TAB(5)"1) ONE CHANNEL"
50 PRINT TAB(5)"2) FOUR CHANNELS"
60 PRINT TAB(5)"3) DOPPLER"
70 PRINT : INPUT C
80 IF C = 1 THEN V = 1023: GOTO 120
90 IF C = 2 THEN V = 4095: GOTO 110
100 PRINT D$;"BLOAD WJSAMPLE": GOTO 125
110 PRINT D$;"BLOAD SAMPLE34A": GOTO 125
120 PRINT D$;"BLOAD SAMPLE2"
125 PRINT : INPUT "NEED TO ENTER CALIBRATION DATA? ";Q$
130 GOSUB 500
135 INPUT "READY TO GO? ";Q$
140 R$ = LEFT$(Q$,1): IF R$ < > "Y" THEN 135
165 CALL 768
170 FOR I = 0 TO V
180 IF I / 1024 = INT(I / 1024) THEN PRINT : PRINT "NEXT CHANNEL"
190 PRINT PEEK(16384 + I);" "
200 NEXT I
205 PRINT :D$ = CHR$(4)
220 PRINT D$;"BSAVE DATA." + F$ + ",A$4000,L$2000"
250 GOTO 1000
499 REM **** PARAMETER INFO ****
500 HOME :D$ = CHR$(4)
510 DIM N$(10)
520 PRINT "ROUTINE TO DEFINE PARAMETERS - DEFAULT VALUES IN PARENTHESIS"
530 PRINT : INPUT "FILE NAME? ";F$
535 IF LEFT$(Q$,1) < > "Y" THEN RETURN
540 PRINT : PRINT "INPUT CALIBRATION INFO FOR EACH OF 4 CATEGORIES"
550 PRINT "(EG. DATA 0 AT -4V WITH 100 MMHG*3.1V)"
560 PRINT : INPUT "EKG (NONE)? ";N$(1)
565 IF N$(1) = "" THEN N$(1) = "NONE"
570 PRINT : INPUT "AORTIC PRESSURE (3.2V=100MMHG)? ";N$(2)
575 IF N$(2) = "" THEN N$(2) = "3.2V=100MMHG"
580 PRINT : INPUT "PRESSURE DOWNSTREAM (4.25V=100MMHG)? ";N$(3)
585 IF N$(3) = "" THEN N$(3) = "4.25V=100MMHG"
590 PRINT : INPUT "EM FLOW (8.5V=1L/MIN)? ";N$(4)
595 IF N$(4) = "" THEN N$(4) = "8.5V=1L/MIN"
600 PRINT : INPUT "HEART RATE? ";N$(5)
610 PRINT : INPUT "STROKE VOLUME? ";N$(6)
620 PRINT : INPUT "FLASK VOLUME? ";N$(7)
630 FOR I = 8 TO 10
640 PRINT : INPUT "ADDITIONAL COMMENTS? ";N$(I)
650 IF N$(I) = "" THEN N = I - 1: GOTO 700
660 NEXT I
670 N = 10
700 HOME : PRINT "STORING INFORMATION"
710 A1$ = F$ + ".INFO"
720 PRINT D$;"OPEN ";A1$ + ",L100"
722 PRINT D$;"DELETE ";A1$
725 PRINT D$;"OPEN ";A1$ + ",L100"
727 PRINT D$;"WRITE ";A1$ + ",RO"
728 PRINT N
730 FOR I = 1 TO N
740 PRINT D$;"WRITE ";A1$ + ",R ";I
750 PRINT N$(I)
760 NEXT I
770 PRINT D$;"CLOSE ";A1$
800 RETURN
1000 END

```

```

0300- 4C 07 03  JMP  $0307
0303- 71 00      ADC  ($00),Y
0305- 40          RTI
0306- 00          BRK
0307- 78          SEI
0308- 48          PHA
0309- 8A          TXA
030A- 48          PHA
030B- 98          TYA
030C- 48          PHA
030D- A0 00      LDY  ##00
030F- AE 03 03  LDX  $0303
0312- AD 04 03  LDA  $0304
0315- 8D 3B 03  STA  $033B
0318- AD 05 03  LDA  $0305
031B- 8D 3C 03  STA  $033C
031E- 4C 25 03  JMP  $0325 ; BYPASS TRIGGER
0321- C9 D0      CMP  ##D0
0323- 30 F9      BMI  $031E
0325- BD 80 C0  LDA  $C080,X ; BOGUS READ
0328- 8A          TXA
0329- 48          PHA
032A- A2 15      LDX  ##15 ; DELAY
032C- CA          DEX
032D- E0 00      CPX  ##00
032F- D0 FB      BNE  $032C
0331- 68          PLA
0332- AA          TAX
0333- EA          NOP
0334- 4C 37 03  JMP  $0337
0337- BD 80 C0  LDA  $C080,X ; REAL READ
033A- 99 00 60  STA  $6000,Y ; STORE IN BUFFER
033D- C8          INY
033E- C0 00      CPY  ##00
0340- D0 1E      BNE  $0360
0342- EE 3C 03  INC  $033C ; INCREMENT BUFFER COUNTER AND
0345- AD 3C 03  LDA  $033C ; CHECK TO SEE IF BUFFER IS FULL
0348- C9 60      CMP  ##60
034A- D0 25      BNE  $0371
034C- 68          PLA ; RESTORE REGISTER AND INTERRUPTS
034D- A8          TAY
034E- 68          PLA
034F- AA          TAX
0350- 68          PLA
0351- 58          CLI
0352- 60          RTS ; BACK TO BASIC
0353- 00          BRK
0354- 00          BRK
0355- 00          BRK
0356- 00          BRK
0357- 00          BRK
0358- 00          BRK
0359- 00          BRK
035A- 00          BRK
035B- 00          BRK
035C- 00          BRK
035D- 00          BRK
035E- 00          BRK

```

035F-	00	BRK	
0360-	9A	TXA	
0361-	48	PHA	; LOW ADDRESS DELAY
0362-	A2 13	LIX	##13
0364-	CA	DEX	
0365-	E0 00	CPX	##00
0367-	D0 FB	BNE	\$0364
0369-	68	PLA	
036A-	AA	TAX	
036B-	4C 6E 03	JMP	\$036E
036E-	4C 37 03	JMP	\$0337
0371-	9A	TXA	; HIGH ADDRESS DELAY
0372-	48	PHA	
0373-	A2 10	LIX	##10
0375-	CA	DEX	
0376-	E0 00	CPX	##00
0378-	D0 FB	BNE	\$0375
037A-	68	PLA	
037B-	AA	TAX	
037C-	EA	NOP	
037D-	EA	NOP	
037E-	4C 37 03	JMP	\$0337

PROGRAM LISTING FOR SERIAL FFT

```

10 TEXT : HOME : GOTO 50
20 POKE 37657,A: POKE 37681,A: POKE 37705,A: POKE 37813,A: POKE 37832,A: POKE
   37837,A: POKE 37851,A: POKE 37854,A: POKE 37963,A: POKE 38029,A: POKE
   38071,A: POKE 38076,A: POKE 38105,A: POKE 38110,A
22 B1 = 128: IF I / 2 = INT ( I / 2 ) THEN B1 = 0
25 POKE 37659,B1: POKE 37711,B1: POKE 37790,B1: POKE 37817,B1: POKE 37823
   ,B1: POKE 37828,B1: POKE 37842,B1: POKE 37845,B1: POKE 37967,B1: POKE
   38033,B1: POKE 38062,B1: POKE 38067,B1: POKE 38096,B1: POKE 38101,B1
27 IF B1 = 128 THEN 40
28 B = B + 1
30 POKE 37660,B: POKE 37712,B: POKE 37791,B: POKE 37818,B: POKE 37824,B: POKE
   37829,B: POKE 37843,B: POKE 37846,B: POKE 37968,B: POKE 38034,B: POKE
   38043,B: POKE 38068,B: POKE 38097,B: POKE 38102,B
40 RETURN
50 D$ = CHR$ ( 4 )
52 INPUT "HOW MANY FILES? ";N
55 DIM F$(N)
57 PRINT "ENTER FILE(S): "
60 FOR J = 1 TO N
62 PRINT J;: INPUT F$(J)
65 NEXT J
70 INPUT "FROM WHICH DISK? ";N$
75 INPUT "SAVE ON WHICH DISK? ";N1$
77 PRINT "LOADING DATA AND FFT ROUTINE..."
82 PRINT D$;"BLOAD FFTMOD,D";N$
85 FOR J = 1 TO N
87 A = 65:B = 32
90 PRINT D$;"BLOAD DATA. ";F$(J);",D";N$
100 FOR I = 1 TO 8
105 HOME : PRINT J;". ";I
110 CALL 37632
120 GOSUB 20
130 A = A + 1
140 NEXT I
145 PRINT : PRINT "LOADING FFT'D DATA..."
150 PRINT D$;"BSAVE FFT. ";F$(J);",A$2000,L$400,D";N1$
155 I = I + 1:A = 64:B = 31
160 GOSUB 20
165 NEXT J
170 HOME : PRINT "DONE": PRINT D$;"CATALOG"
175 END

```

9300-	A2 00	LDX	##00	; ENTRY POINT FOR MAGNITUDE RESULT
9302-	F0 01	BEQ	\$9305	; ENTRY POINT FOR REAL & IMAG RESULTS
9304-	CA	DEX		
9305-	BE 44 93	STX	\$9344	
9308-	A2 00	LDX	##00	; BIT REVERSAL
930A-	86 EI	STX	\$ED	
930C-	A0 08	LDY	##08	
930E-	A9 00	LDA	##00	
9310-	46 ED	LSR	\$ED	
9312-	2A	ROL		
9313-	88	DEY		
9314-	D0 FA	BNE	\$9310	
9316-	A8	TAY		
9317-	BD 00 40	LDA	\$4000,X	
931A-	99 00 20	STA	\$2000,Y	
931D-	EB	INX		
931E-	D0 EA	BNE	\$930A	
9320-	A9 02	LDA	##02	; ILOC = 2
9322-	85 ED	STA	\$ED	
9324-	A9 40	LDA	##40	; JEND = 64
9326-	85 EE	STA	\$EE	
9328-	A9 80	LDA	##80	; NL = 128
932A-	85 EF	STA	\$EF	
932C-	A9 00	LDA	##00	
932E-	AA	TAX		
932F-	9D 00 40	STA	\$4000,X	
9332-	9D 00 8F	STA	\$8F00,X	
9335-	9D 00 90	STA	\$9000,X	
9338-	EB	INX		
9339-	D0 F4	BNE	\$932F	
933B-	20 AF 93	JSR	\$93AF	; CALL FFT
933E-	2C 44 93	BIT	\$9344	; CALC. MAGN ?
9341-	10 02	BPL	\$9345	
9343-	60	RTS		; N ? , RETURN
9344-	00	BRK		; MAGN FLAG
9345-	A2 00	LDX	##00	; SQRT (R^2 + I^2)
9347-	BD 00 40	LDA	\$4000,X	
934A-	85 FD	STA	\$FD	
934C-	85 FA	STA	\$FA	
934E-	BD 00 20	LDA	\$2000,X	
9351-	85 FE	STA	\$FE	
9353-	85 FB	STA	\$FB	
9355-	20 3C 95	JSR	\$953C	
9358-	20 10 95	JSR	\$9510	
935B-	A5 1D	LDA	\$1D	
935D-	85 1B	STA	\$1B	
935F-	A5 1E	LDA	\$1E	
9361-	85 1C	STA	\$1C	
9363-	BD 00 8F	LDA	\$8F00,X	
9366-	85 FD	STA	\$FD	
9368-	85 FA	STA	\$FA	
936A-	BD 00 90	LDA	\$9000,X	
936D-	85 FE	STA	\$FE	
936F-	85 FB	STA	\$FB	
9371-	20 3C 95	JSR	\$953C	

9374-	20 10 95	JSR	\$9510	
9377-	18	CLC		
9378-	A5 1C	LDA	\$1C	
937A-	65 1E	ADC	\$1E	
937C-	85 1C	STA	\$1C	
937E-	A5 1B	LDA	\$1B	
9380-	65 1D	ADC	\$1D	
9382-	85 1B	STA	\$1B	
9384-	A0 00	LDY	#\$00	; SQRT
9386-	A9 01	LDA	#\$01	
9388-	85 E3	STA	\$E3	
938A-	A5 1C	LDA	\$1C	
938C-	38	SEC		
938D-	E5 E3	SBC	\$E3	
938F-	B0 12	BCS	\$93A3	
9391-	48	PHA		
9392-	A5 1B	LDA	\$1B	
9394-	38	SEC		
9395-	E9 01	SBC	#\$01	
9397-	85 1B	STA	\$1B	
9399-	68	PLA		
939A-	B0 07	BCS	\$93A3	
939C-	98	TYA		
939D-	9D 00 20	STA	\$2000,X	
93A0-	4C AB 93	JMP	\$93AB	
93A3-	C8	INY		
93A4-	E6 E3	INC	\$E3	
93A6-	E6 E3	INC	\$E3	
93A8-	4C 8C 93	JMP	\$938C	
93AB-	EB	INX		
93AC-	D0 99	BNE	\$9347	
93AE-	60	RTS		; DONE
93AF-	A2 00	LDX	#\$00	
93B1-	A0 01	LDY	#\$01	
93B3-	BD 00 40	LDA	\$4000,X	
93B6-	85 06	STA	\$06	
93B8-	BD 00 20	LDA	\$2000,X	
93BB-	85 07	STA	\$07	
93BD-	18	CLC		
93BE-	B9 00 20	LDA	\$2000,Y	; RE (X) = RE (X) +-RE (Y)
93C1-	65 07	ADC	\$07	
93C3-	9D 00 20	STA	\$2000,X	
93C6-	B9 00 40	LDA	\$4000,Y	
93C9-	65 06	ADC	\$06	
93CB-	9D 00 40	STA	\$4000,X	
93CE-	38	SEC		
93CF-	A5 07	LDA	\$07	; RE (Y) = RE (X) - RE (Y)
93D1-	F9 00 20	SBC	\$2000,Y	
93D4-	99 00 20	STA	\$2000,Y	
93D7-	A5 06	LDA	\$06	
93D9-	F9 00 40	SBC	\$4000,Y	
93DC-	99 00 40	STA	\$4000,Y	
93DF-	C8	INY		; ADDRESSES OF NEXT PAIR
93E0-	C8	INY		
93E1-	EB	INX		
93E2-	EB	INX		
93E3-	D0 CE	BNE	\$93B3	; DO NEXT TRANSFORM PAIR
93E5-	A9 01	LDA	#\$01	; INITIALIZE J-INDEX
93E7-	85 08	STA	\$08	
93E9-	46 EF	LSR	\$EF	; NL = NL/2

```

93EB-   A9 01      LDA   $$01      ; INITIALIZE L - INDEX
93ED-   85 09      STA   $09
93EF-   A9 00      LDA   $$00
93F1-   85 FA      STA   $FA
93F3-   A5 EF      LDA   $EF
93F5-   85 FB      STA   $FB
93F7-   A5 09      LDA   $09
93F9-   38         SEC
93FA-   E9 01      SBC   $$01
93FC-   85 FE      STA   $FE
93FE-   85 E3      STA   $E3
9400-   A9 00      LDA   $$00
9402-   85 FD      STA   $FD
9404-   20 3C 95   JSR   $953C      ; NL * (SUBL - 1)
9407-   A6 1F      LDX   $1F
9409-   BD 00 91   LDA   $9100,X   ; GET SINE AND SAVE IT
940C-   85 19      STA   $19
940E-   BD 00 92   LDA   $9200,X
9411-   85 1A      STA   $1A
9413-   A5 1F      LDA   $1F
9415-   18         CLC
9416-   69 40      ADC   $$40
9418-   AA         TAX
9419-   BD 00 91   LDA   $9100,X   ; ** CORR ERROR ORIG LDX
941C-   85 1B      STA   $1B      ; GET COSINE AND SAVE IT
941E-   BD 00 92   LDA   $9200,X
9421-   85 1C      STA   $1C
9423-   A5 08      LDA   $08      ; ILOC * 2 * (SUBJ -1) + SUBL -1
9425-   38         SEC
9426-   E9 01      SBC   $$01
9428-   0A         ASL
9429-   85 FB      STA   $FB
942B-   A5 ED      LDA   $ED
942D-   85 FE      STA   $FE
942F-   A9 00      LDA   $$00
9431-   85 FA      STA   $FA
9433-   85 FD      STA   $FD
9435-   20 3C 95   JSR   $953C
9438-   A5 1F      LDA   $1F
943A-   18         CLC
943B-   65 E3      ADC   $E3
943D-   AA         TAX
943E-   65 ED      ADC   $ED      ; PUT IT IN X
9440-   A8         TAY
9441-   A5 1B      LDA   $1B      ; PUT (X + ILOC) IN Y.  X & Y
9443-   85 FD      STA   $FD      ; NOW CONTAIN TRANSFORM PAIR
9445-   A5 1C      LDA   $1C      ; ADDRESSES.
9447-   85 FE      STA   $FE
9449-   B9 00 40   LDA   $4000,Y
944C-   85 FA      STA   $FA
944E-   B9 00 20   LDA   $2000,Y
9451-   85 FB      STA   $FB
9453-   20 3C 95   JSR   $953C
9456-   A5 19      LDA   $19
9458-   85 FD      STA   $FD
945A-   A5 1A      LDA   $1A
945C-   85 FE      STA   $FE
945E-   B9 00 8F   LDA   $8F00,Y
9461-   85 FA      STA   $FA
9463-   B9 00 90   LDA   $9000,Y

```

```

9466- 85 FB      STA  $FB
9468- 20 44 95   JSR  $9544 ; CALCULATE REAL
946B- 20 10 95   JSR  $9510 ; = WR * RE (Y) + WI * IM (Y)
946E- A5 1D      LDA  $1D
9470- 85 EB      STA  $EB
9472- A5 1E      LDA  $1E
9474- 85 EC      STA  $EC
9476- A5 1B      LDA  $1B
9478- 85 FD      STA  $FD
947A- A5 1C      LDA  $1C
947C- 85 FE      STA  $FE
947E- B9 00 8F   LDA  $8F00,Y
9481- 85 FA      STA  $FA
9483- B9 00 90   LDA  $9000,Y
9486- 85 FB      STA  $FB
9488- 20 3C 95   JSR  $953C
948B- B9 00 40   LDA  $4000,Y
948E- 85 FA      STA  $FA
9490- B9 00 20   LDA  $2000,Y
9493- 85 FB      STA  $FB
9495- A5 1A      LDA  $1A
9497- 49 FF      EOR  #$FF
9499- 18         CLC
949A- 69 01      ADC  #$01
949C- 85 FE      STA  $FE
949E- A5 19      LDA  $19
94A0- 49 FF      EOR  #$FF
94A2- 69 00      ADC  #$00
94A4- 85 FD      STA  $FD
94A6- 20 44 95   JSR  $9544 ; CALCULATE IMAG
94A9- 20 10 95   JSR  $9510 ; = WR * IM (Y) - WI * RE (Y)
94AC- 38         SEC
94AD- BD 00 20   LDA  $2000,X ; RE (Y) = RE (X) - REAL
94B0- E5 EC      SBC  $EC
94B2- 99 00 20   STA  $2000,Y
94B5- BD 00 40   LDA  $4000,X
94B8- E5 EB      SBC  $EB
94BA- 99 00 40   STA  $4000,Y
94BD- 38         SEC
94BE- BD 00 90   LDA  $9000,X
94C1- E5 1E      SBC  $1E
94C3- 99 00 90   STA  $9000,Y
94C6- BD 00 8F   LDA  $8F00,X
94C9- E5 1D      SBC  $1D
94CB- 99 00 8F   STA  $8F00,Y
94CE- 18         CLC
94CF- BD 00 20   LDA  $2000,X ; RE (X) = RE (X) + REAL
94D2- 65 EC      ADC  $EC
94D4- 9D 00 20   STA  $2000,X
94D7- BD 00 40   LDA  $4000,X
94DA- 65 EB      ADC  $EB
94DC- 9D 00 40   STA  $4000,X
94DF- 18         CLC
94E0- BD 00 90   LDA  $9000,X ; IM (X) = IM (X) + IMAG
94E3- 65 1E      ADC  $1E
94E5- 9D 00 90   STA  $9000,X
94E8- BD 00 8F   LDA  $8F00,X
94EB- 65 1D      ADC  $1D
94ED- 9D 00 8F   STA  $8F00,X
94F0- E6 09      INC  $09

```



```
94F2-   A5 ED       LDA   $ED
94F4-   C5 09       CMP   $09
94F6-   90 03       BCC   $94FB
94F8-   4C EF 93   JMP   $93EF   ; CONTINUE L - LOOP
94FB-   E6 08       INC   $08
94FD-   A5 EE       LDA   $EE
94FF-   C5 08       CMP   $08
9501-   90 03       BCC   $9506
9503-   4C EB 93   JMP   $93EB   ; CONTINUE J - LOOP
9506-   06 ED       ASL   $ED   ; ADJUST PARAMETERS FOR NEXT
9508-   46 EE       LSR   $EE   ; PASS
950A-   F0 03       BEQ   $950F
950C-   4C E5 93   JMP   $93E5   ; DO NEXT PASS
950F-   60           RTS          ; DONE
```

SINE TABLE

9100-	00	00	00	00	00	00	00	00
9108-	00	00	00	00	00	00	00	00
9110-	00	00	00	00	00	00	00	00
9118-	00	00	00	00	00	00	00	00
9120-	00	00	00	00	00	00	00	00
9128-	00	00	00	00	00	00	00	00
9130-	00	00	00	00	00	00	00	00
9138-	00	00	00	00	00	00	01	01
9140-	01	01	01	00	00	00	00	00
9148-	00	00	00	00	00	00	00	00
9150-	00	00	00	00	00	00	00	00
9158-	00	00	00	00	00	00	00	00
9160-	00	00	00	00	00	00	00	00
9168-	00	00	00	00	00	00	00	00
9170-	00	00	00	00	00	00	00	00
9178-	00	00	00	00	00	00	00	00
9180-	00	FF	FF	FF	FF	FF	FF	FF
9188-	FF	FF	FF	FF	FF	FF	FF	FF
9190-	FF	FF	FF	FF	FF	FF	FF	FF
9198-	FF	FF	FF	FF	FF	FF	FF	FF
91A0-	FF	FF	FF	FF	FF	FF	FF	FF
91A8-	FF	FF	FF	FF	FF	FF	FF	FF
91B0-	FF	FF	FF	FF	FF	FF	FF	FF
91B8-	FF	FF	FF	FF	FF	FF	FF	FF
91C0-	FF	FF	FF	FF	FF	FF	FF	FF
91C8-	FF	FF	FF	FF	FF	FF	FF	FF
91D0-	FF	FF	FF	FF	FF	FF	FF	FF
91D8-	FF	FF	FF	FF	FF	FF	FF	FF
91E0-	FF	FF	FF	FF	FF	FF	FF	FF
91E8-	FF	FF	FF	FF	FF	FF	FF	FF
91F0-	FF	FF	FF	FF	FF	FF	FF	FF
91F8-	FF	FF	FF	FF	FF	FF	FF	FF
9200-	00	06	0D	13	19	1F	26	2C
9208-	32	38	3E	44	4A	50	56	5C
9210-	62	68	6D	73	79	7E	84	89
9218-	8E	93	98	9D	A2	A7	AC	B1
9220-	B5	B9	BE	C2	C6	CA	CE	D1
9228-	D5	D8	DC	DF	E2	E5	E7	EA
9230-	ED	EF	F1	F3	F5	F7	F8	FA
9238-	FB	FC	FD	FE	FF	FF	00	00
9240-	00	00	00	FF	FF	FE	FD	FC
9248-	FB	FA	F8	F7	F5	F3	F1	EF
9250-	ED	EA	E7	E5	E2	DF	DC	D8
9258-	D5	D1	CE	CA	C6	C2	BE	B9
9260-	B5	B1	AC	A7	A2	9D	98	93
9268-	8E	89	84	7E	79	73	6D	68
9270-	62	5C	56	50	4A	44	3E	38
9278-	32	2C	26	1F	19	13	0D	06
9280-	00	FA	F3	ED	E7	E1	DA	D4
9288-	CE	C8	C2	BC	B6	B0	AA	A4
9290-	9E	98	93	8D	87	82	7C	77
9298-	72	6D	67	62	5E	59	54	4F
92A0-	4B	47	42	3E	3A	36	32	2F
92A8-	2B	28	24	21	1E	1B	19	16
92B0-	13	11	0F	0D	0B	09	08	06
92B8-	05	04	03	02	01	01	00	00
92C0-	00	00	00	01	01	02	03	04
92C8-	05	06	08	09	0B	0D	0F	11
92D0-	13	16	19	1B	1E	21	24	28
92D8-	2B	2F	32	36	3A	3E	42	47
92E0-	4B	4F	54	59	5E	63	68	6D
92E8-	72	77	7C	82	87	8D	93	98
92F0-	9E	A4	AA	B0	B6	BC	C2	C8
92F8-	CE	D4	DA	E1	E7	ED	F3	FA

PROGRAM LISTING FOR SPECTROGRAPH

```

10 TEXT : HOME :D$ = CHR$ (4)
20 INPUT "FILE TO BE PLOTTED? ";F$
50 F3 = 32
80 PR# 5
90 PRINT ";; IOD 100 HUA 0,110 D 0,1410 1900,1410 1900,110 0,110 U "
95 IN# 5: INPUT C$: IN# 0
100 PRINT " 500,-15 S13 TIME (SEC * 10) "; CHR$ (95)
110 PRINT " 1430,0 S12 ";F$; CHR$ (95)
120 FOR I = 10 TO 0 STEP - 1
130 IN# 5: INPUT C$: IN# 0
140 TM = INT (1800 * (I / 10))
150 PRINT TM;" ,55 S12 ";I; CHR$ (95)
160 PRINT TM;" ,100 D ";TM;" ,110 U
170 NEXT I
180 PRINT " -100,283 S43 FREQUENCY (HZ*.01) "; CHR$ (95)
185 GOSUB 440
250 PRINT ";; IOD 100 HA 0,110 AD "
251 IN# 5: INPUT C$: IN# 0
252 PR# 0
254 CALL 1002
255 PRINT D$;"BLOAD FFT. ";F$;" ,D2,A$4000"
257 PR# 5
260 P = 16384
270 FOR J = 0 TO F3 - 1
280 Z = 1300 / 127
290 PRINT " D "
300 FOR I = 2 TO 127
310 X = INT (Z * I)
320 Y = INT ( PEEK (P + I) / 3 + .5) + Y1
330 PRINT " ";Y,X;" "
360 NEXT I
370 PRINT " U "
380 Y1 = INT ((J + 1) * 1800 / (F3 - 1))
390 PRINT " ";Y1;" ,0 "
400 P = P + 128
405 IN# 5: INPUT C$: IN# 0
410 NEXT J
420 PR# 0: END
430 REM ***** SET UP X-AXIS
440 N1 = 1300 / 8: PR# 5
450 FOR I = 8 TO 0 STEP - 1
460 I2 = INT (110 + I * N1)
470 PRINT " -75, ";I2 - 15;" S12 "; STR$ (5 * I); CHR$ (95)
480 PRINT "-10, ";I2;" D 0, ";I2;" U"
485 IN# 5: INPUT C$: IN# 0
490 NEXT I
500 IN# 5: INPUT C$: IN# 0
505 FOR I = 1 TO 12000: NEXT I
510 RETURN

```